

DESIGN OF SINGLE PHASE INVERTER AND ACTIVE AND REACTIVE
POWER CONTROL OF UNBALANCED POWER DISTRIBUTION GRID

by

Shashank Sriram Subramaniam

A thesis submitted to the faculty of
The University of North Carolina at Charlotte
in partial fulfillment of the requirements
for the degree of Master of Science in
Electrical Engineering

Charlotte

2018

Approved by:

Dr. Sukumar Kamalasan

Dr. Robert W. Cox

Dr. Abasifreke Ebong

ABSTRACT

SHASHANK SRIRAM SUBRAMANIAM. Design of Single Phase Inverter and Active and Reactive Power Control of Unbalanced Power Distribution Grid. (Under the direction of DR. SUKUMAR KAMALASADAN)

This thesis presents a new d-q based control of single phase grid connected inverters. The inverters are capable of delivering active and reactive power based on the reference set points and/or demand from the load. Also, an on-grid and off-grid control strategy for the single phase inverter has been proposed, that can seamlessly transition from from an "on-grid" state to the "off-grid" state and vice-versa. In this context, a Synchronous Frame PLL has been developed that can help the controller to retain a frequency set point in both the on-grid and off-grid states. Further, a methodology has been proposed for inverter re-synchronization with the grid.

In order to support unbalance power distribution grid, a methodology has been designed for single phase load management that takes into account of the size of the inverter and the local load balance required at each phase where the inverter is connected. Both active and reactive power balance are simultaneously introduced with this architecture. As some load changes may be too large for the inverter to supply, an Apparent power limiter is also proposed, such that the active and reactive power reference remains within the operating capacity of the inverter. Finally, a simple droop control model has been proposed for the single phase inverter that can work in grid connected mode. The approach supports active power sharing between inverters by measuring the change in frequency and voltage.

ACKNOWLEDGEMENTS

I would like to express my sincere gratitude to my advisor, Dr. Sukumar Kamalasan who provided me with an opportunity to be a part of a wonderful research team and supported me in every stage of my thesis.

This thesis would be impossible to complete without the aid and assistance of my parents, my teachers and my friends. I would like to thank my parents and friends for their support and the constant encouragement they have provided. I would like to thank Robin Bisht, Aniket Joshi, Jakir Hossain, Abhilash Thakallapelli, Muhammad Ahmed, Arun Suresh, Biswajit and many others, for being a moral support throughout this ordeal.

My parents are the only reason I am here, I work hard knowing that even when I lose hope, they are still on my side, cheering for me.

To my teachers who have made me the person who I am and without whom I would not be here today.

I would like to thank my friends who have supported me through every step in my life.

DEDICATION

To my:

My Grandmothers: Meenakshi Krishnamoorthy, Shanta Moorthy.

My Grandfathers: Krishnamoorthy, G.N. Moorthy.

My Parents: Lakshmi Subramaniam, S.K. Subramaniam.

To my Family and all my Friends.

TABLE OF CONTENTS

APPENDIX	ix
LIST OF FIGURES	x
CHAPTER 1: INTRODUCTION	1
1.1. Need for Solar Energy Generators	2
1.1.1. Advantages of using PV generation	3
1.1.2. Components of Grid Tie PV Farms and Energy Storage	6
1.2. Single Phase Inverters and Three Phase Inverters	7
1.2.1. Single Phase Inverter Topology	7
1.3. Operation of Multiple Single Phase Inverters	10
1.3.1. Current Research on Single Phase Inverter Control Methodology	10
1.4. Motivation for This Thesis	11
1.4.1. Problems Faced by the Grid Today	11
1.4.2. Solving the Dispatchability Problem	12
1.4.3. Solving the Increased Cost in Scaling up the System	12
1.4.4. Solving the Voltage Support Issue	13
1.5. Contributions of this Thesis	13
1.6. Organization of Thesis	14
1.7. Summary	15

CHAPTER 2: DESIGN & IMPLEMENTATION OF PV FARM & BATTERY ENERGY STORAGE SYSTEM AT THE DC BUS	17
2.1. Design of DC-DC Boost Converter	17
2.1.1. Mathematical Model of the Boost Converter	17
2.1.2. Control methodology	19
2.1.3. Test results of Boost converter	20
2.2. Design of PV farms	21
2.2.1. Selection of the PV farm	22
2.2.2. Control of PV Farm using MPPT	22
2.3. Implementation of the PV farm in MATLAB	24
2.3.1. Test of the PV system in a standalone case	26
2.4. Design of DC-DC boost converter	29
2.5. Implementation of the PV farm in MATLAB with Battery storage	30
2.5.1. Case 1: PV farm implementation on a sunny day	31
2.5.2. Case 2: PV farm implementation on a cloudy day	33
2.6. Summary	36
CHAPTER 3: SINGLE PHASE INVERTER CONTROL	37
3.1. Power Inverter	37
3.1.1. Pulse Width Modulation based control	38
3.1.2. Space Vector Pulse Width Modulation	40
3.2. Control Architectures of Single Phase Inverters	40
3.2.1. Stationary Reference Frame & Rotating Reference Frame	41

3.2.2.	Single Phase d-q control	44
3.3.	Implementation strategy	51
3.4.	Summary	52
CHAPTER 4: DESIGN OF PROPOSED GRID-TIE & OFF-GRID SINGLE PHASE INVERTER		54
4.1.	Control Implementation Strategy	55
4.1.1.	Single Loop Control Method	55
4.1.2.	Predictive Model	56
4.1.3.	Multi-control loop	56
4.2.	Controller design	56
4.2.1.	Grid Connected Mode	57
4.2.2.	Transition from on-grid to off-grid	58
4.2.3.	Off-grid Mode	60
4.2.4.	Synchronous Frame PLL	61
4.3.	Implementation and Test Results	63
4.3.1.	Architecture in MATLAB	63
4.3.2.	Results and Discussion	64
4.4.	Summary	73
CHAPTER 5: ACTIVE & REACTIVE POWER CONTROL FOR GRID CONNECTED SINGLE PHASE INVERTER		75
5.1.	Overview of the IEEE 13 bus system	75
5.1.1.	Modified IEEE 13 bus system	77
5.1.2.	Integration of PV-Energy storage system with the grid	81

	ix
5.2. Active Power Management with Single Phase Inverter	82
5.2.1. Case 1: Study done for a constant 2 kilowatt Load at Node 634	83
5.2.2. Case 2: Study done for Varying Active Power Load at Node 634	86
5.3. Reactive Power Management with Single Phase Inverter	88
5.3.1. Case 1: Study Done for Constant 2 kiloVAr Load at Node 634	89
5.3.2. Case 2: Study for a Varying Reactive Power Load at Node 634	92
5.4. Active and Reactive Power Support Simultaneously	94
5.5. Summary	98
CHAPTER 6: DROOP CONTROL OF SINGLE PHASE INVERTER	100
6.1. Droop Control Introduction	100
6.1.1. Droop Methodology	101
6.1.2. Droop in distribution systems	103
6.2. Simulation overview	105
6.3. Simulation results for Droop Control	107
6.3.1. Summary	113
CHAPTER 7: CONCLUSIONS AND FUTURE WORK	115
7.1. Conclusion	115
7.2. Future Work	116
REFERENCES	118

LIST OF FIGURES

FIGURE 1.1: United States energy production based on fuel[1]	2
FIGURE 1.2: Renewable Energy growth in the United States	4
FIGURE 1.3: Contribution of PV generation In USA, per Month[1]	4
FIGURE 1.4: Investment in Renewable Energy growth in the United States[2]	5
FIGURE 1.5: Typical Grid-Connected Inverter Architecture	6
FIGURE 1.6: A single phase full bridge inverter[3]	8
FIGURE 1.7: Flow of the thesis	15
FIGURE 2.1: Boost Converter Model	19
FIGURE 2.2: Boost converter's voltage comparison (a) Input voltage remains constant at 54.7V (b) Output voltage graph has some transients when load is switched from 300 to 150 W	20
FIGURE 2.3: Boost converter's input vs output power comparison (a) Input Power is 330W and 180W (b) Output power is 300W and 150W	21
FIGURE 2.4: Flowchart of the Perturb and Observe algorithm	23
FIGURE 2.5: Irradiance Curve	25
FIGURE 2.6: Temperature Curve	25
FIGURE 2.7: Voltage output of the PV	27
FIGURE 2.8: Power output of the PV	27
FIGURE 2.9: Cascade control of the Boost converter	29
FIGURE 2.10: Voltage of the PV during a sunny day	31
FIGURE 2.11: DC Bus voltage maintained at 400V; (a) When PB functions alone, (b) When battery functions with PV	32

FIGURE 2.12: Power Sharing between PV and Battery	32
FIGURE 2.13: Voltage of the PV during a cloudy day	33
FIGURE 2.14: DC bus voltage during a cloudy day.	34
FIGURE 2.15: Power drawn by the load during a cloudy day	34
FIGURE 2.16: Battery and PV power during a cloudy day	35
FIGURE 3.1: Hysteresis Current Control PWM[4]	39
FIGURE 3.2: Hysteresis Current Control PWM[5]	40
FIGURE 3.3: Clarke's Transformation from Three Phase to 2 phase orthogonal plane	43
FIGURE 3.4: Typical Solar Cell with its components	43
FIGURE 3.5: Typical Solar Cell with its components	44
FIGURE 3.6: Single Phase inverter circuit	45
FIGURE 3.7: Real-Imaginary model of the single phase inverter	46
FIGURE 3.8: Single Phase inverter model in d-q domain	50
FIGURE 4.1: Single phase half-bridge inverter, with LC filter	55
FIGURE 4.2: Inverter control schematic for On-grid application	58
FIGURE 4.3: Grid connected and islanded mode reference management	59
FIGURE 4.4: Circuit Breaker Control	59
FIGURE 4.5: Inverter control schematic for off-grid application	60
FIGURE 4.6: Synchronous Frame PLL	62
FIGURE 4.7: Grid Connected Circuit Diagram	63
FIGURE 4.8: Active and reactive power reference while working in grid connected mode.	65

FIGURE 4.9: Active and reactive power reference while working in is- landed mode	66
FIGURE 4.10: Voltage at the output of the inverter in grid connected and islanded mode	66
FIGURE 4.11: Current at the output of the inverter in grid connected and islanded mode	67
FIGURE 4.12: Frequency sags when the prime-mover excitation was reduced	68
FIGURE 4.13: Frequency check performed and inverter grid frequency alignment	68
FIGURE 4.14: Active and reactive power output of inverter tracking the reference	69
FIGURE 4.15: Moment when synchronization is performed, the voltage is synchronized	70
FIGURE 4.16: Frequency spike seen when a fault is present at the grid side	71
FIGURE 4.17: Active and reactive power reference followed during the fault scenario	72
FIGURE 4.18: Active and reactive power reference followed even during fault scenario	73
FIGURE 5.1: IEEE 13 bus Distribution Network	76
FIGURE 5.2: IEEE 13 bus is modified to study the effect of a dynamic load on the bus voltage	78
FIGURE 5.3: Dynamic Power and Voltage profile at node 632; Lack of variation in voltage suggests that node 632 is a strong bus	79
FIGURE 5.4: Dynamic Power and Voltage profile at node 634; Significant variation in voltage suggests that node 634 is a weak bus	80
FIGURE 5.5: Inverter control methodology for interconnection with 13 bus system	81

FIGURE 5.6: Modified 13 bus system; With constant active power load connected to Node 634	83
FIGURE 5.7: Active Power Reference Generated for the Inverter	83
FIGURE 5.8: Comparison of power supplied by the inverter and the grid	84
FIGURE 5.9: Effect of active power compensation on the PCC Voltage For Phase A, B and C	85
FIGURE 5.10: Modified 13 bus system; Load Profile for Dynamic Load	86
FIGURE 5.11: Load Demand shared between the inverter and the grid	87
FIGURE 5.12: Active Power demand of the load in each phase increases to a different value, contributing to unbalanced voltage at PCC	87
FIGURE 5.13: Effect of Active Power Support on balancing the voltage at the PCC	88
FIGURE 5.14: Modified 13 bus system with constant 2kVAr load at Node 634; the power references provided to the inverter is also shown	89
FIGURE 5.15: Reactive power support provided by the inverter for constant load of 2kVAr.	90
FIGURE 5.16: Effect of reactive power support on the PCC Voltage for Phase A, B and C	91
FIGURE 5.17: Modified 13 bus system with variable reactive power load connected at Node 634	92
FIGURE 5.18: Reactive Power Demand shared between the inverter and the grid	93
FIGURE 5.19: Reactive Power demand in Each Phase	93
FIGURE 5.20: Effect of Reactive Power Support on the PCC Voltage	93
FIGURE 5.21: Three Phase Active and Reactive Power Demand	95
FIGURE 5.22: Power profile of the PV and the Battery	96

FIGURE 5.23: Inverter's Supply of Active and Reactive Power in each Phase	97
FIGURE 5.24: Voltage profile for all three phases at Node 634	98
FIGURE 6.1: Flow of Apparent power	102
FIGURE 6.2: Implementation of conventional droop control	105
FIGURE 6.3: Modified 13 bus system to perform active power sharing; there are multiple PV inverters connected to each phase	106
FIGURE 6.4: Inverter configuration in each phase, in Node 634	107
FIGURE 6.5: Droop control in Phase A between three inverters.	108
FIGURE 6.6: Droop control in Phase B between three inverters.	109
FIGURE 6.7: Droop control in Phase C between three inverters.	109
FIGURE 6.8: Active Power shared by the inverters and the grid	110
FIGURE 6.9: Voltage at Phase A, Phase B and Phase C, while performing Droop control	110
FIGURE 6.10: Frequency variation caused by the variation of the inverter Power output.	111
FIGURE 6.11: Substation Characteristics; Active and reactive power supplied by the substation and the voltages in each phase at the substation	113
FIGURE 1: Load flow results of IEEE 13 bus system	130
FIGURE 2: Load flow results of the modified IEEE 13 bus system	131

CHAPTER 1: INTRODUCTION

Energy is critical for human existence. When used efficiently, effectively and wisely, it can provide abundant growth to all communities on earth. For the past century, humanity has been influenced by the discovery and rampant use of fossil fuels. This spurt of growth has been at the cost of both the environment and a disregard for the supply of the fuel. As the cost of fossil fuel rises and the effects of climate change grows, a greater effort has been placed to understand and implement renewable energy systems, in the hope to solve the ever increasing global energy needs. Although energy is analyzed solely in terms of its availability and consumption, the true value of energy lies in its ability to assist the user in completing everyday tasks like cooking, lighting and transportation, while being available for use the following day[6]. Today, electricity is primary and most important part of energy generation. This is primarily because humanity has been able to develop electricity as a universal form of currency. We are capable of using electricity to keep us warm by the use of a device that can convert electricity to heat and keep our food cold, by the use of another device that can convert electric work into a coolant circulation system. This versatility and the fact that we can transport electrons over great distances by the use of a simple metallic wire, makes electricity the most important human invention. Governments are also cracking down on carbon emissions and generally encouraging engineers to develop negative carbon emission technologies. The future seems to be setting a stage for alternative fuel sources, to help humanity extract energy reliably, safely and consistently. The main push in renewable energy is from developed nations like United States, European Union, China and India, whose energy share in renewable technology is predicted to account up to 70% of global energy production[7].

1.1 Need for Solar Energy Generators

The United States and China have been the major players in research and development of renewable energy technology in the last decade[8]. Though the present political climate chooses to diminish the renewable energy gains the United States has made, the scientific community still considers the use of renewable energy technology as the focus in the forthcoming decades. As the amount of fossil fuels reduce and as the climate continues to worsen, the need for solar energy generators increases. The added advantage of this particular form of energy generation is that the solar energy is available everywhere. There is no spot on earth that there is a continuous lack of energy. This allows us to use photo-voltaic devices to capture the energy of the sun and use it to generate usable electricity[9].

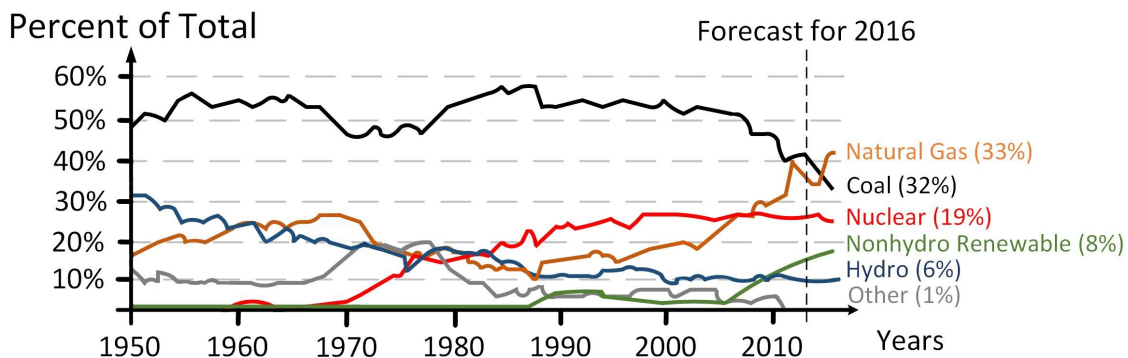


Figure 1.1: United States energy production based on fuel[1]

Fig 1.1 shows the United States energy production chart, which clearly shows the decline in coal. The increase in natural gas use is primarily a method to provide for immediate demand and is linked with short-term economic gains. This is very common in developing and under-developed nations. The renewable energy sources is on the rise along with Nuclear energy. Although these energy sources are "clean" for the environment, accidents with respect to nuclear power plants may be extremely dangerous for the environment. Of all the energy sources mentioned above, the cleanest is the Solar and Wind energy systems followed by hydro, due to its ability to block

water flow channels for fishes and other wildlife in the area. Further research needs to be performed on Renewable energy devices to identify any potential hazards and work towards mitigating them[10].

1.1.1 Advantages of using PV generation

Increasing demand for electrical energy in the ever growing world economy gives the concept of Hybrid Distributed Generation Systems (DG) a new meaning. Traditionally, energy was extracted from a material that was able to provide heat and light, by consuming combustible fuels. In modern times, on much larger scales, this same principle has been evolved to generate electricity. In large power plants, a fuel (such as coal or gas) is used to produce steam. The steam is pressurized and made to spin a turbine that develops the electric power through a mechanically coupled synchronous generator. Power plants like the one mentioned above are technologies that have been available for a hundred years. They have been refined and perfected through the decade. Although the power plants have proven to be robust and extremely reliable, they bring along environmental and sustainability concerns. These large power plants are also confined to the whereabouts of the fuel they use, as transportation of the fuel adds to the cost of generation. This implies that it is not feasible to develop power plants in remote areas and are far away from the raw materials needed for traditional power plants. The power plants of yesteryear were developed as a part of the lumped "Legacy" model for energy generation. As the presence of a threat drives innovation, so has the development of DER assisted the transition from fossil fueled generation plants to consumer-end solar power plants.

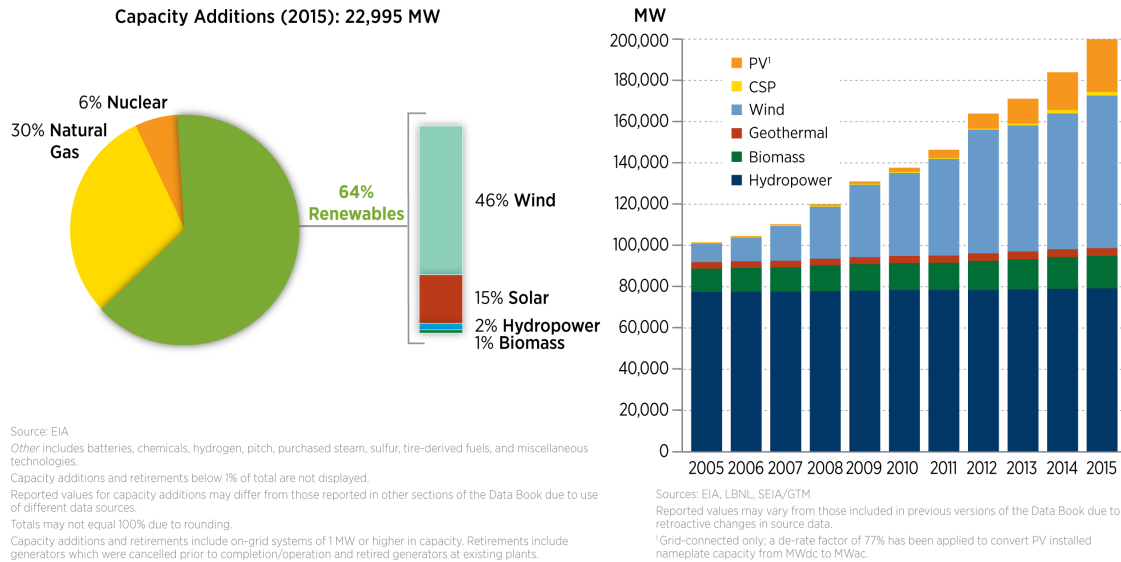


Figure 1.2: Renewable Energy growth in the United States

This is where the concept of DER or distributed energy resources comes in. DER are capable of utilizing renewable energy technology that is abundant in almost all corners of the globe and develop power in a distribution network. Electricity is generated primarily from solar and wind energy [11]. These resources are available in all corners of the globe and helps developed nations to reduce their carbon footprint, while developing nations use these resources to supply their peak demands.

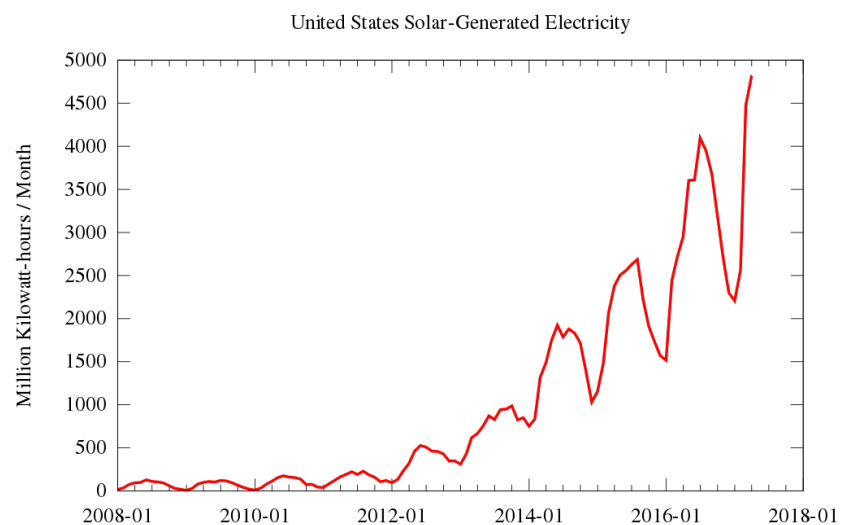
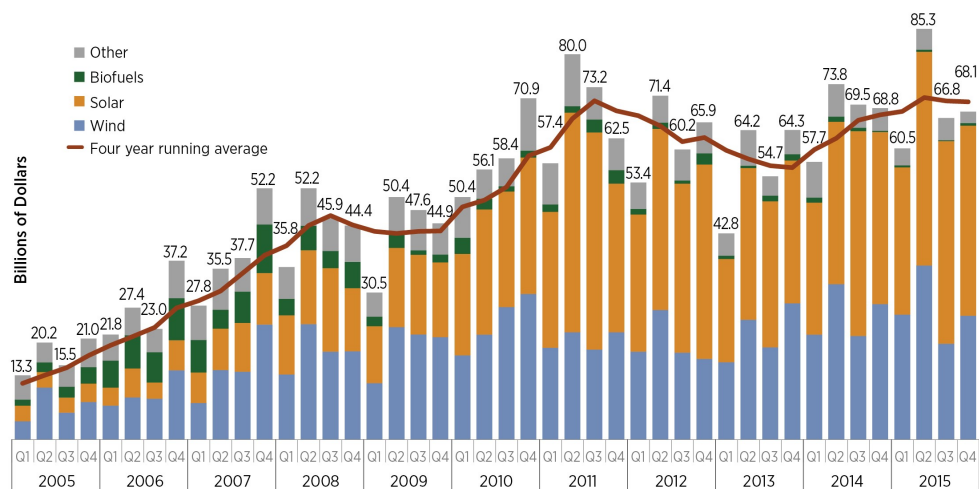


Figure 1.3: Contribution of PV generation In USA, per Month[1]

Investment in DER is steadily rising at the public and private sector. DERs have become crucial energy sources and a safe investment option in locations with cheap land value and high solar energy availability. There is a considerable increase in small scale business that is also employer of a large number of workers in various fields. This includes both skilled and unskilled workers, who are a part of a growing industry. Utility companies are major players in the emerging photo-voltaic market. The utilities use this non-dispatchable power for critical loads, to work in tandem with traditional generators.



Source: BNEF
 Reported values may vary from those included in previous versions of the Data Book due to retroactive changes in source data.
 Total values include estimates for undisclosed deals; includes corporate and government R&D and spending for digital energy and energy storage projects (not reported in quarterly statistics).

Figure 1.4: Investment in Renewable Energy growth in the United States[2]

Solar energy can effectively supplement electricity supply from an electricity transmission grid, such as when electricity demand peaks in the summer. As the size and generating capacity of a solar system are a function of the number of solar modules installed, applications of solar technology are readily scalable and versatile. Solar power production facilities can be installed at the customer site which reduces required investments in production and transportation infrastructure. Governmental

incentives for PV installation in the residential areas and at work, also is a key contribution to the fact that the PV systems are extremely appealing renewable energy generation options.

1.1.2 Components of Grid Tie PV Farms and Energy Storage

This section provides the in-depth description of the components of a PV grid tied inverter. The figure shows a "big picture" look at the system architecture used in this project.

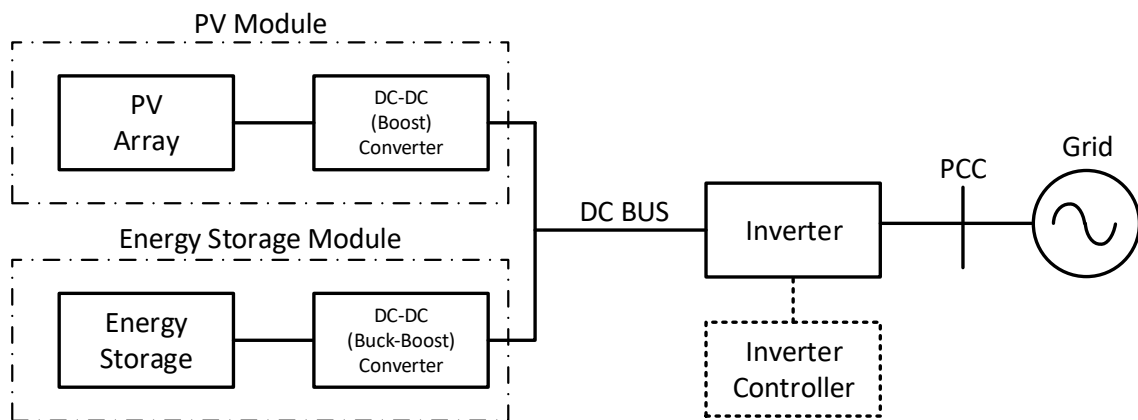


Figure 1.5: Typical Grid-Connected Inverter Architecture

A typical grid connected inverter consists of the following devices:

- Solar Array.
- DC-DC converter (Generally a boost converter for the PV system).
- Energy storage.
- DC-DC converter (Generally a bi-directional buck-boost converter for the energy storage system).
- Inverter.
- Inverter controller.

The PV Array and the DC-DC boost converter is a part of the PV module[12]. This module produces a DC power, whose power rating depends on the number of

cells that make up the PV array. As the number of cells in parallel increases, a higher current may be drawn and as the number of series cells increases, a higher voltage may be produced[13]. It is important to note that this power is not purely DC, due to fluctuations that are caused by the Maximum Power Point Tracking Algorithm, that is capable of extracting the optimal power to effectively use a particular dimension of the PV array [14]. Before working on AC power transfer, it is important to have a strong and robust DC source. The main objective of the DC side, should be to handle any fluctuation of the DC bus voltage[15]. PV is an intermittent voltage source, so it is common to attach a battery to support the PV system.

1.2 Single Phase Inverters and Three Phase Inverters

A single phase inverter is a two wire system that consists of solid state switches that can convert a DC signal to an AC signal. This equipment is very light and are rather cheap to purchase and install. These devices are connected to a PV array or a Battery to provide the DC input needed and they can be tied to the grid, or they can function in standalone mode. In most homes, single phase power is fed to the loads. So these single phase systems can be connected to the largest load in the home, to save on electricity bills, or they can be connected on a much smaller scale to a shed.

The three phase inverter is a 3 or 4 wire system that contains 3 live wires with a neutral/ ground wire. These are much larger systems and are available at large homes or businesses. These devices usually produce power at much smaller voltages. There are a larger number of switches in the network which will account for more switching losses and possible more harmonics, as the device gets older.

1.2.1 Single Phase Inverter Topology

The Single phase inverter consists of full bridge and half bridge typologies. The inverter is a commonly available in Switched Mode Power Supply (SMPS) and in renewable energy conversion topology The most commonly used form is the full bridge

topology for its ability to maintain a better output waveform, which is key in grid connection. The inverter consists of 2 switches in each branch, which keep switching the output states based on the Pulses provided to the individual switches. This signal is known as the Pulse Width modulated signal, as the signal is provided to the switches in the form of pulses.

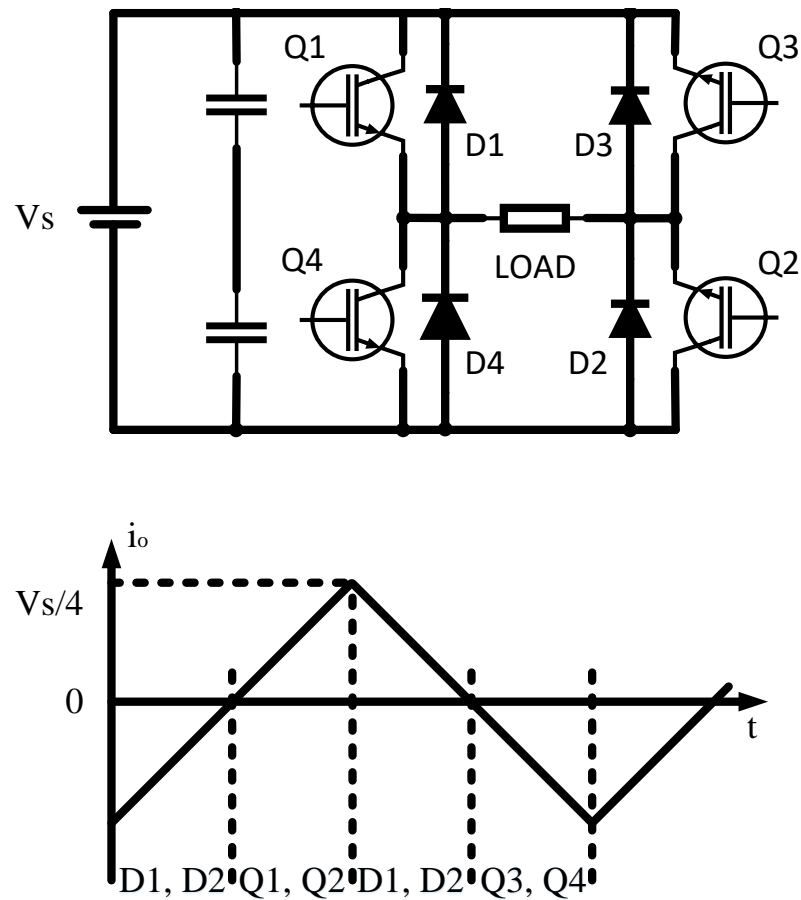


Figure 1.6: A single phase full bridge inverter[3]

The half bridge topology work the same way, but the transition is a little more abrupt as there is only 2 controlled switches and the other 2 switches are the anti-parallel diodes that conduct only when they are forward biased. It is a 'two-quadrant converter' because the load current can flow in both directions. The main drawback is that a positive and negative voltage needs to be fed to the output neutral, which is extremely expensive to implement in large systems.

Hence, most inverters available in the market are full-bridge instead of the half-bridge type. Power densities in excess of 50W per in³ are commonly available in some commercially available SMPS.

The figure 1.6 shows the single phase full bridge topology of the inverter. The transistors and diodes are represented as a single switch[16]. The diode is in the anti-parallel configuration, so that the leakage current does not harm the transistor[17]. The switches are operated such that the switches in the same branch are not closed simultaneously, to avoid short circuits[18]. The figure also shows the generation of the pseudo AC signal created by switching the transistors on and off. This inverter topology is called 'H-Bridge' inverter.

The next form of single phase inverter topology is called the buck-boost type where, it is suitable for standalone application and grid connected application[19]. The proposed topology is based on the buck-boost operation. The configuration consists of two DC-DC converters, they act as current source inverters. The power factor is at unity and THD is about 5% the output is about 300W[20].

Fly-back type chopper is designed such that the inductance is calculated based on the inductance of the transformer. The design of the inductance and the peak current are based on the control of switching times and the power output[21]. The inductor operates in DCM from the experimental setup. The experimental results show that there are some ripples due to switching frequency being low. There is some loss in the circuit, due to the transformer[22].

Z-Source inverter is applied to a PV system. two bidirectional current conducting and one unidirectional voltage blocking device like IGBT is used[23]. This type of device is useful for low power grid connected application. It needs more energy storage elements[24]. From the simulation results, both converters generated output current with acceptable THD and have the high efficiency at high loads. At low loads, the efficiency drops rapidly compared to the buck-boost converter[25]. Due to higher

circulating current in the Z-Source inverter[26].

1.3 Operation of Multiple Single Phase Inverters

Addition of multiple inverters to a single node of the grid causes the inverter is very common as the number of inverters increases in the distribution network. A concept called distributed energy resources allows for the fact that having multiple generation stations leads to a better opportunity for the energy to be generated closer to the load. This is also important when safety is taken into account as multiple independently controlled system is more secure as compared to a large system failure on synchronous generators.

Power sharing might be a key point to take into account when it comes to multiple generation systems in the distribution network. So it is important to devise a strategy that will allow multiple inverters to communicate with each other, only based on the changes in the voltage and current in the grid. The ability for inverters to share power between each other and also dispatch power to the local area when the grid is having a fault is also a very exciting prospect. This is the basic concept of droop which is explored in the later chapters of this thesis.

1.3.1 Current Research on Single Phase Inverter Control Methodology

There are various types of inverter typologies and various types of control techniques applied to them. The main type of control typologies studied in literature are.

- Linear regulator - it is a carrier based control with linear regulator with linear switching frequency operation, but they have poor performance tracking sinusoidal references. Steady state error when harmonics are present in the DC signal, with poor noise elimination, eliminate this type of controller's use in this thesis[27].
- Hysteresis control method guarantees a good peak current limiting capability,

but the high THD present at the output eliminates this type of controller in this thesis[28].

- Peak current control method grants current limiting capability, but the controller is inherently unstable, beyond a small operating range[29].
- d-q control mode is promising as it is capable of being implemented into circuit board easily and is relatively simple to design[30]. This also has no steady state error as the controller uses a PI control loop that eliminates any errors in the output.
- P/Q Control Strategy This strategy is used in grid connected system, where the inverter is regulated to ensure the correct output of active and reactive power[28]. The P/Q control strategy is a form of vector control strategy.

There has been a push in recent years to allow the islanding operation of the inverter, so that the power can be fed to the local load regardless of the health of the power system. There is also a push to create a micro-grid where inverters share power in the local area and supply the grid when they are connected to the main power network.

1.4 Motivation for This Thesis

The main motivation for this research work is to develop a single phase inverter controller design that can be used to manage active and reactive power of the unbalanced distribution grid. Also, the capability of multiple such single phase inverters to collectively share and manage the power is investigated. For this, research work is motivated by the fact that droop control topology is capable of stabilizing the PCC voltage and also provide to the loads based on the requirement of the load.

1.4.1 Problems Faced by the Grid Today

The issues faced by traditional inverters are as follows:

- Non Dispatch-ability of the PV power.
- Scaling up cost is too high.

- Unable to support voltage, sometimes adding to the problems.

1.4.2 Solving the Dispatchability Problem

Usual inverters present today contain PV panels connected to the grid. But these devices produce non-dispatchable power. In case that the inverter produces more power than the requirement of the local load and the grid, the controller disconnects the PV panels from the inverter and lets the power that is produced by the PV to go to waste. This shows us that the technology has not caught up with the inverter models that are present in the market. Adding batteries to the PV inverter systems, allows the PV systems to charge the batteries when the load does not require the power. This also allows the battery to store the charge that can be dispatched later. The battery backup also allows the operation of the inverter in off-grid mode. As the traditional systems have higher penetration of PV systems, there is more cause for concern with regards to the "Duck" curve. This problem may be mitigated when the power is capable of being dispatched.

1.4.3 Solving the Increased Cost in Scaling up the System

The traditional PV systems do not have batteries connected to the system, due to the bulk or the cost. The reasoning for that is that batteries are heavy or the type of battery that they use is expensive, considering the size of the battery. This need for large battery is eliminated, as the size of the battery in the system presented in this thesis is limited to that of a few Lead-acid batteries which are capable of supplying the local load for about an hour when it is fully charged. This system can be scaled up by connecting multiple batteries in series or parallel, depending on the voltage and current needed based on the user's demand. This scale-up cost is not as high as traditional battery backup systems.

The inverter was also developed with the capability of islanding when the grid is offline, which lets the inverter to operate as an uninterrupted power supply. This

change is performed in a seamless manner, with the ability to disconnect and reconnect to the grid, without introducing harmful voltage and current spikes. This ability makes the inverter crucial in places where the power lines get damaged by the unusual weather. The islanding capability is also useful for consumers in developing nations where power supply is unreliable.

1.4.4 Solving the Voltage Support Issue

As the number of inverters increase in the traditional distribution system, there is an added problem when the voltage fluctuates. As most inverters follow the grid reference, it is highly likely that the inverter picks up this deviation from the nominal value and operates beyond the capability of its individual components. This damages the inverters and the life is reduced considerably, the ability to leave the grid in case of a spike or support the grid by supplying reactive power to mitigate this problem, allows the inverter to support the grid and not work against it.

Additional of additional DC bus elements like the ultra-capacitor will also aid the inverter in performing reactive power and voltage support to the grid for high-frequency transients in the grid.

1.5 Contributions of this Thesis

The contributions of this thesis is summarized by the following points.

- Developed a single phase PV and Battery, DC system, that can maintain a constant output voltage, despite the variations in irradiance.
- Developed d-q control for single phase inverter, to supply active and reactive power, based on the per-unit reference provided.
- Developed a single phase inverter system that can function in the on-grid and off-grid modes of operation and perform seamless islanding and grid connection.
- Developed a method of providing active and reactive power support for a large

power system.

- Developed a method of providing voltage and frequency support at the PCC on a large system.

1.6 Organization of Thesis

- The first chapter discusses the need for solar energy generators and the advantages of using solar energy compared to other renewable sources along with a brief introduction to the grid connected PV farms, and the single phase and three phase inverter topology of a traditional full bridge inverter. This chapter also highlights the contribution of the organization of the thesis.
- The second chapter discusses the DC bus, the components of the DC bus, the PV and MPPT control, the battery and charge control and the implementation framework of the overall architecture.
- The Third chapter discusses the proposed control schemes of the inverter, the present research on the controllers and the introduction to stationary and rotating reference frame analysis of the inverter.
- The fourth chapter introduces the d-q controller and describes the active and reactive power control of the inverter in the grid connected and off-grid modes. A seamless transfer between the grid connected and off grid mode is also proposed.
- The fifth chapter discusses the methodology for active and reactive power management of single phase loads and thus the unbalance power distribution grid.
- The sixth chapter discusses the droop control methodology for active power management of single phase loads that can be used to share multiple inverters and chapter seven concludes the work.

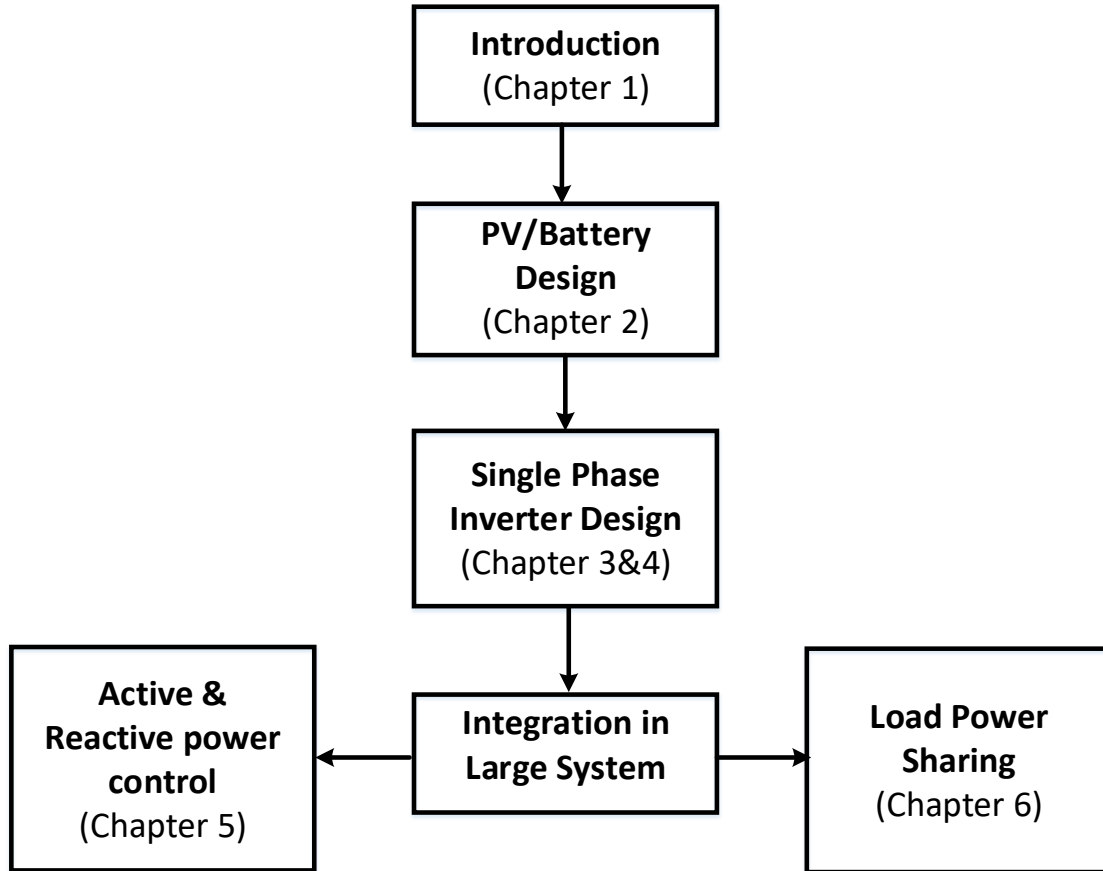


Figure 1.7: Flow of the thesis

The organizational sketch is illustrated in figure 1.7 which shows the basic flow of the thesis. The chapters discuss individual components mentioned in the flow-chart.

1.7 Summary

In the first chapter the following topics were explored in detail:

- The reasons why renewable energy technology is on the rise.
- The economics of operating distributed power generators, why it is better than conventional legacy generation method.
- The problems with the inverter technology today and the issues, like the duck curve, that may be alleviated by the use of better controls and power system management.

- The contributions of the thesis were highlighted. Along with the organization of the thesis.

CHAPTER 2: DESIGN & IMPLEMENTATION OF PV FARM & BATTERY ENERGY STORAGE SYSTEM AT THE DC BUS

The key elements of a PV generation system is the PV Array, the DC-DC converters and an energy storage elements, most likely a battery. All these elements are connected to what is called the DC-Bus. The energy generated by the PV system is fed to the DC bus. A battery works in tandem, to maintain the DC bus voltage constant. The battery is also capable of supplying power, when the PV irradiance is low. This chapter discusses the basic elements of single phase PV farm and battery system at the DC level and the design and implementation framework of the PV/Battery integrated DC system.

2.1 Design of DC-DC Boost Converter

The boost converters in this system is responsible to maintain the PV MPPT and also to prevent overcharging of the battery. The DC-DC converter connected to the battery is also responsible to maintain the DC bus voltage constant at 400V. The output of the DC-DC converter is controlled by the charging and discharging cycles of the passive components.

2.1.1 Mathematical Model of the Boost Converter

To create a stable model of the boost converter, a mathematical model must be created. The model must be such that it accurately represents the dynamics of the input, the process of energy conversion and the desired output. A mathematical analysis is performed to develop an accurate model for the DC-DC converters needed as a part of the DC bus.

$$\frac{d\bar{i}_l}{dt} = \frac{\bar{v}_{in}}{L} - d' \frac{\bar{v}_o}{L} \quad (2.1)$$

$$\frac{d\bar{v}_o}{L} = \frac{\bar{v}_o}{RC} + d' \frac{\bar{i}_l}{C} \quad (2.2)$$

Where, $d'=(1-d)$ Considering small perturbation in V_{in},d,V_{out} and i_l

$$\bar{V}_{in} = V_{in} + \tilde{V}_{in} \quad (2.3)$$

$$\bar{i}_l = i_l + \tilde{i}_l \quad (2.4)$$

$$\bar{V}_o = V_o + \tilde{V}_o \quad (2.5)$$

$$d = D + d \quad (2.6)$$

Substituting the above values, we get:

$$\frac{d\tilde{i}_l}{dt} = \frac{\tilde{v}_{in}}{L} - \frac{D'}{L} \tilde{v}_o + \frac{V_o}{L} \tilde{d} \quad (2.7)$$

$$\frac{d\tilde{V}_o}{dt} = -\frac{\tilde{v}_o}{RC} - \frac{D'}{C} \tilde{i}_l - \frac{i_l}{C} \tilde{d} \quad (2.8)$$

After performing Laplace transform and re-arranging the equations, we get:

$$\frac{\tilde{v}_o}{\tilde{d}} = -\frac{s \frac{i_l}{C} + v_o \frac{D'}{LC}}{s^2 + \frac{s}{RC} + \frac{D'^2}{LC}} \quad (2.9)$$

The duty ratio equation of the dc-dc boost converter is given by the equation below.

$$D = 1 - \frac{V_{in}}{V_{out}} \quad (2.10)$$

The rating of the PV voltage at MPP is shown to be 54.7 V. So the duty value is 0.865. This Duty ratio only works for a steady state of operation, if the input varies (which it does), the duty ratio would need to be updated for the variation in the input.

2.1.2 Control methodology

The control methodology for boost converters is based on variation of duty ratio along with the selection of the correct capacitive and inductive components. This is key as the method in which power is delivered from the DC-DC converter depends on the storage of energy in the passive elements in the system. MATLAB simulation's DC voltage source is an ideal source, hence the voltage source is capable of supplying any amount of current, without dropping the voltage. This means that the overall simulation will be more useful when the PV module is connected to the boost converter, to simulate actual dynamics.

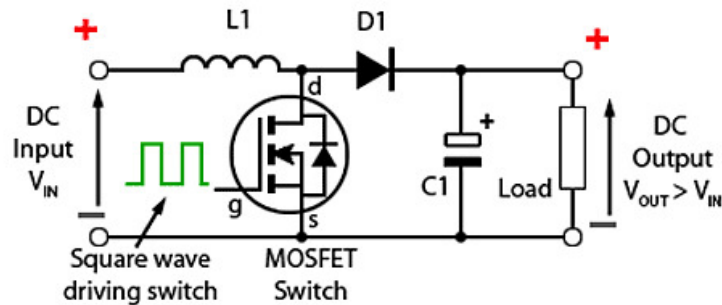


Figure 2.1: Boost Converter Model

The boost converter model is represented in figure 2.1. The values for the passive elements used for the boost design is shown in the table below. The calculations of the DC-DC converter power stage is done in Appendix A

Components of the Boost converter		
Sr. No.	Parameters	Value
1.	V_{in}	57.4V
2.	V_{out}	400V
3.	Inductor (L)	0.53 H
5.	Output Capacitance (C)	$400e^{-6}$ F

2.1.3 Test results of Boost converter

The test results of the boost converter consists of the input voltage and the output voltage comparison, the input power and output power comparison, when the power requirement from the load is changed from 300W to 150W.

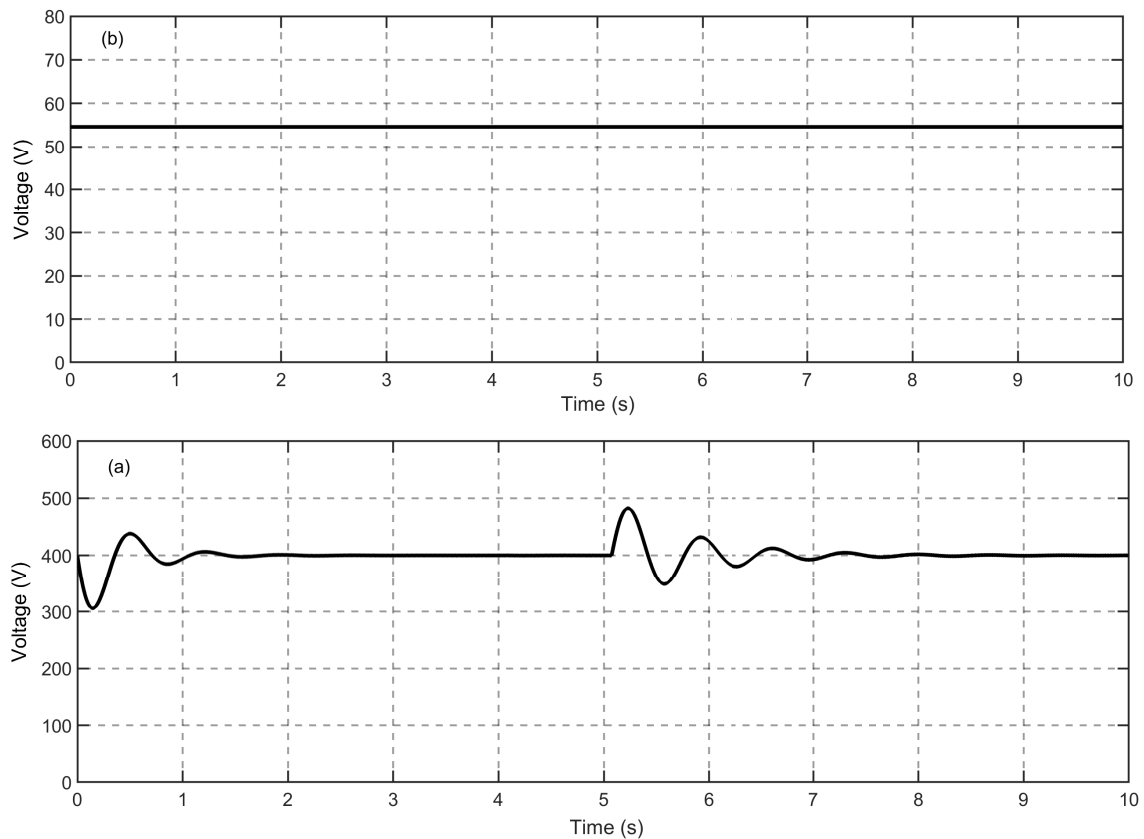


Figure 2.2: Boost converter's voltage comparison (a) Input voltage remains constant at 54.7V (b) Output voltage graph has some transients when load is switched from 300 to 150 W

In the practical scenario, the input voltage would fluctuate as the current demanded from the load changes. The wave-forms are useful to identify if the control design of the Boost converter is able to maintain the output voltage at a steady 400V. Figure 2.3 compares the input and output voltage, which confirms the calculations made for the DC-DC boost converter.

The input voltage and the output voltages are compared in figure 2.2. When the

load changes from 300W to 150W, the output sees some transients, but the output is brought back to the operating point.

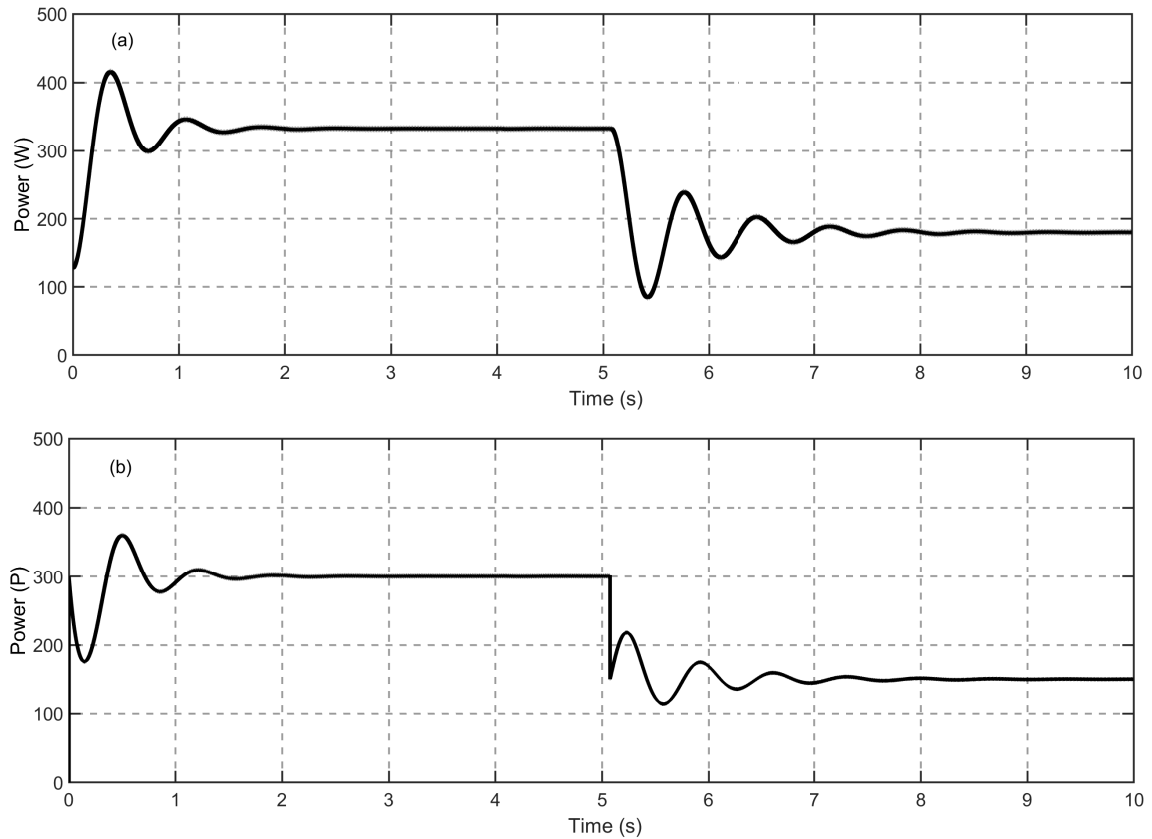


Figure 2.3: Boost converter's input vs output power comparison (a) Input Power is 330W and 180W (b) Output power is 300W and 150W

A loss of 30W is observed. Which is an efficiency of 90 %, when the input and the output power is compared. The efficiency can be made higher by reducing the parasitic components in the system.

2.2 Design of PV farms

After the development of the boost converter, it is important to connect the DC-DC converter to the PV farm. Unlike voltage sources like batteries, the PV systems needs to be running on maximum load at all times, to achieve better utilization efficiency. The section deals with the selection of the size of the PV module, the Maximum Power Point Tracking and study on the PV-Battery system.

2.2.1 Selection of the PV farm

PV systems are classified based on the power rating into 3 types:

- Small Scale Systems - Typically on rooftops with a rating lower than ten kilowatts.
- Medium Scale Systems - Typically ranging from ten kilowatts to tens of kilowatts.
- Large Scale Systems - Typically used by the utility. With power capacity up to a few Megawatts.

The thesis focuses on the development of the PV system for use in the individual domestic dwelling application. Hence the focus would be on the small scale system. These are typically systems that can be used to provide power necessary for a small number of units in the house, should the grid power fail.

2.2.2 Control of PV Farm using MPPT

The simulation software of choice was MATLAB, due the wide variety of electrical components and the simple interface.

To optimally utilize a solar panel, of a particular size, the power that is produces must be at its maximum at all times[31]. This is tough to maintain as the semiconductor material that constitutes a solar panel, also changes its characteristics based on the temperature and the irradiance, which tends to fluctuate throughout the day. Hence it becomes difficult to constantly monitor and sustain a steady maximum power. So, every PV panel manufacturer provides a V vs. I and P vs. V curve for a particular temperature and irradiance level, so that a Maximum Power Point tracker can keep the output power of the PV at a Maximum point, at all operating conditions.

The two main issues with PV generator system are as follows:

- The conversion efficiency of PV power generation is very low (around 40%), especially under low irradiation conditions.

- The amount of electric power generated by the PV cell varies continuously with respect to time.
- The solar cell V vs. I characteristics is non-linear and varies with respect to irradiance and temperature.

Figure 2.4 shows the flow chart that describes the perturb and observe algorithm used to perform MPPT.

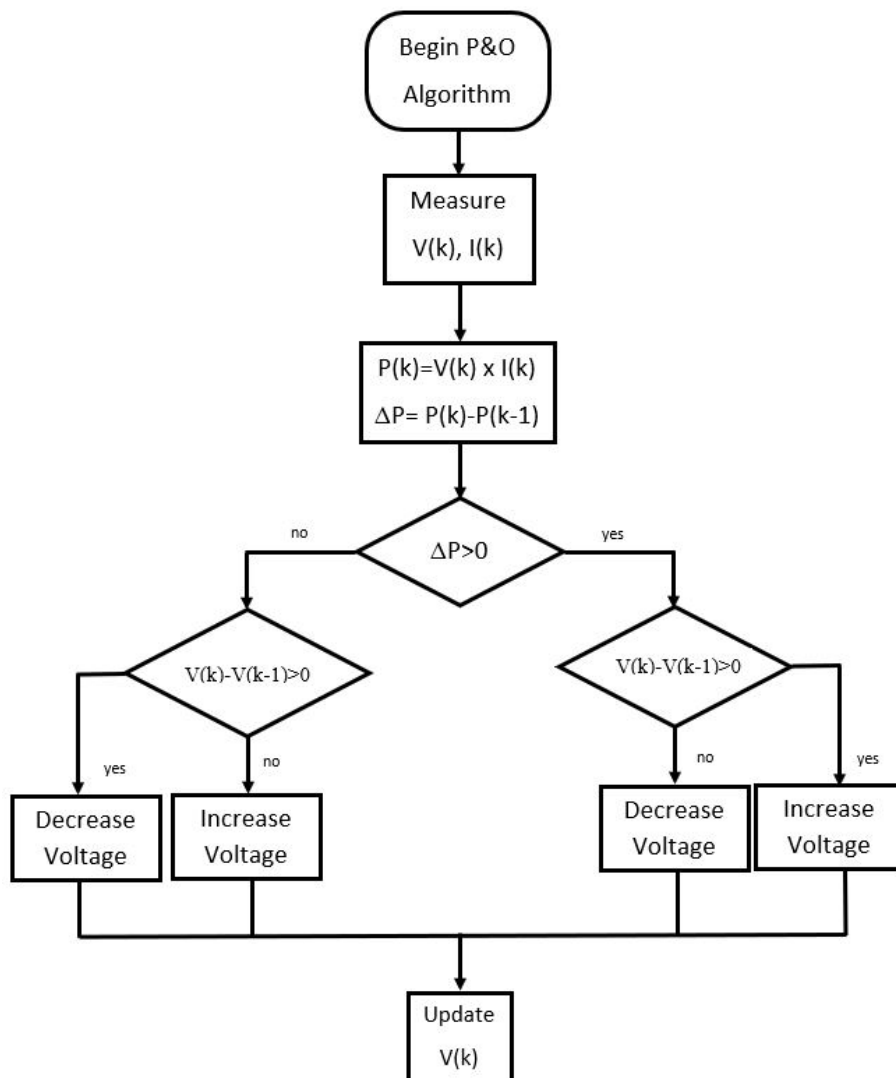


Figure 2.4: Flowchart of the Perturb and Observe algorithm

All of these issues may be mitigated using a Maximum Power Point Tracking

(MPPT) control scheme. The MPP cannot be easily found analytically, but can be located either through numerical models, or by search algorithms. The MPPT algorithm must be able to find the knee point of the V vs. I curve, by observing the Thevenin equivalent resistance of the cell, and extract the maximum power from the cell. Maximum power is transferred from the solar panel, when the impedance of the load is optimized with the source impedance. Thus, this control circuit must be connected to a converter circuit, that is capable of extracting the power from the cell, by the variation of the converter's duty cycle. The most common MPPT algorithm is the perturb and observe method. But there are many other control schemes that perform MPPT.

The DC-DC boost converter for the PV system is a crucial aspect of the PV system. It is responsible to regulate the voltage and also in implementing MPPT. A boost converter is a DC-DC power converter that steps up voltage (while stepping down current) from its input (supply) to its output (load).

2.3 Implementation of the PV farm in MATLAB

The figure 1.9 shows the MATLAB implementation of the PV and the boost converter. The PV used in this simulation is based on the MATLAB default model, figure 1.10 shows the internal components of the PV array. It must be noted that the simulation time is 48 seconds, the simulation time is selected such that 0 seconds represents 12 a.m at day 1 while 48 seconds represents 12 p.m at Day 2.

Notice, that the only inputs of this model is the temperature and the irradiance profile. This is provided through a signal generator block. The signal generator block provides this input. The irradiance profile is simulated such that every two second of the simulation represents 1 hour of the day.

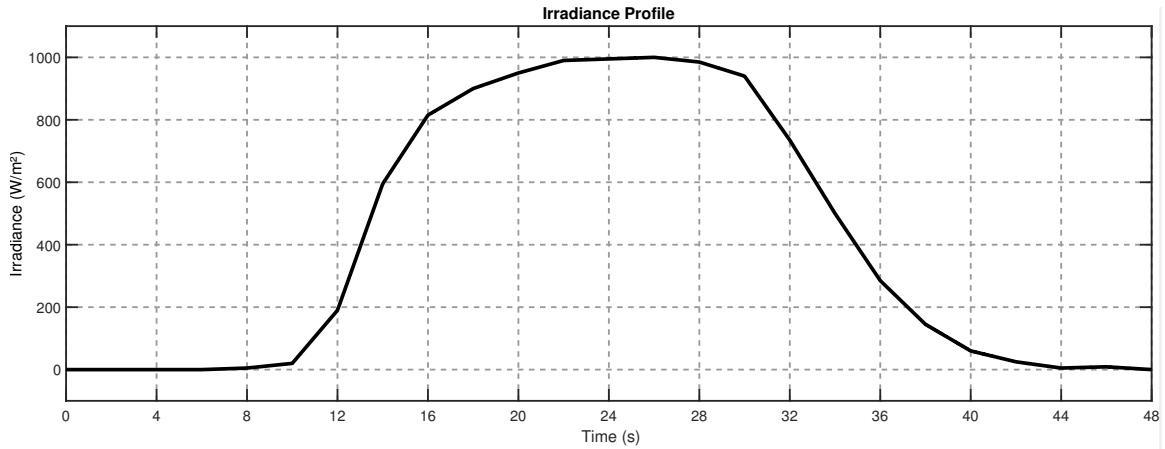


Figure 2.5: Irradiance Curve

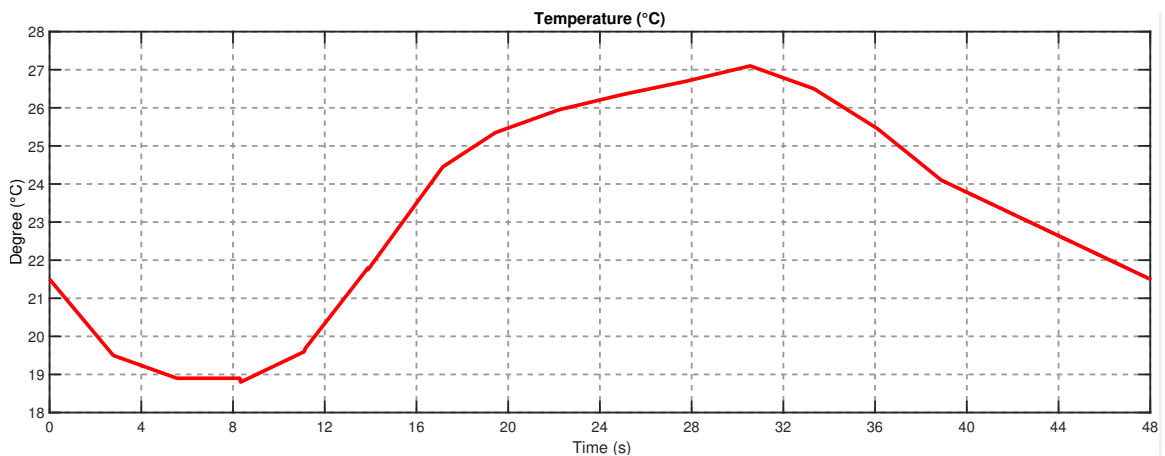


Figure 2.6: Temperature Curve

The day to day simulation would be able to reveal if the controller is robust enough to maintain the Maximum Power Point. A simulation with the daily PV profile or the cloudy day profile will show us whether the MPPT can maintain the peak voltage at a constant value or if it fails in supplying enough power to the DC bus.

The key take away is that the maximum voltage supplied by this PV module is 64.2 V and a maximum current of 5.96 Amps. The maximum voltage at MPP is 54.7V with an amperage of 5.58 Amps. The DC-DC converter that will be discussed later will require these values for controlling the DC output. So the DC-DC converter is designed based on the MPP Voltage as its input value.

The irradiance profile provided to the solar array follows the traditional understanding of the peak amount of sunlight present in a day. So, an average day gets about 12 hours of sunlight. Considering the fact that the average sunlight available in 1 year is 4422 hours. Now, the sunlight is at its peak between 10 a.m. and 4 p.m. on average. The temperature is at its highest at 3 p.m. and reduces gradually after that. The highest(maximum) temperature occurs when heat gain due to incoming solar radiation, and heat loss due to outgoing terrestrial radiation balance this occurs some time after midday. These graphs are shown in Figure 2.5 and 2.6.

Components of the Boost converter		
Sr. No.	Parameters	Value
1.	V_{in}	57.4V
2.	V_{out}	400V
3.	$P_{out} = P_{in}$	350W
4.	Inductor (L)	0.5381 H
5.	Input Capacitance (C_1)	$100e^{-6}$ F
6.	Output Capacitance (C_2)	$4.0464e^{-4}$ F

Note that the temperature and irradiance are averages and do not account of cloudy and warm/cold days. But this simulation will however allow to test whether our controller is capable of following set point and deliver smooth DC power to the load.

These values were all developed based on the mathematical model introduced in the beginning of this chapter. A MATLAB code has been developed such that the calculation of the components of the DC-DC converter is a lot easier.

2.3.1 Test of the PV system in a standalone case

The Stand-alone case allows us to analyze the performance of the PV and the Boost converter when a variable irradiance and temperature profile is provided to the PV.

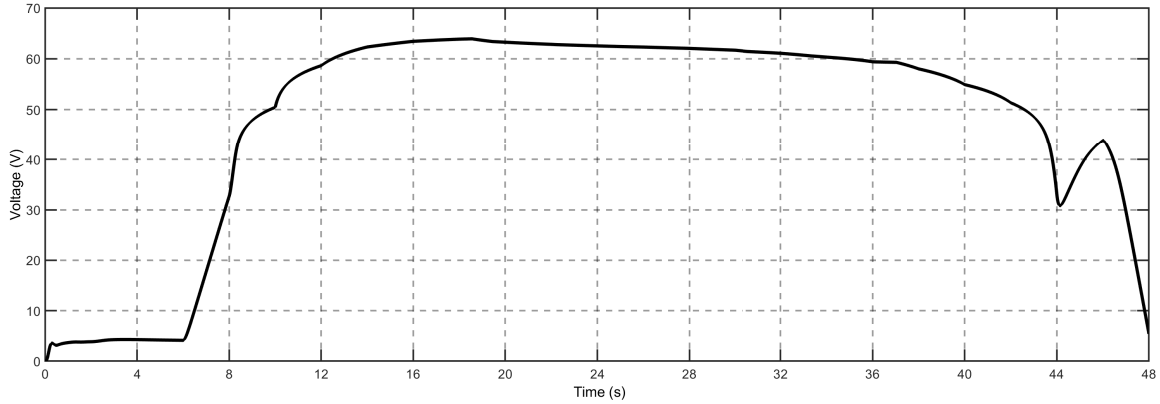


Figure 2.7: Voltage output of the PV

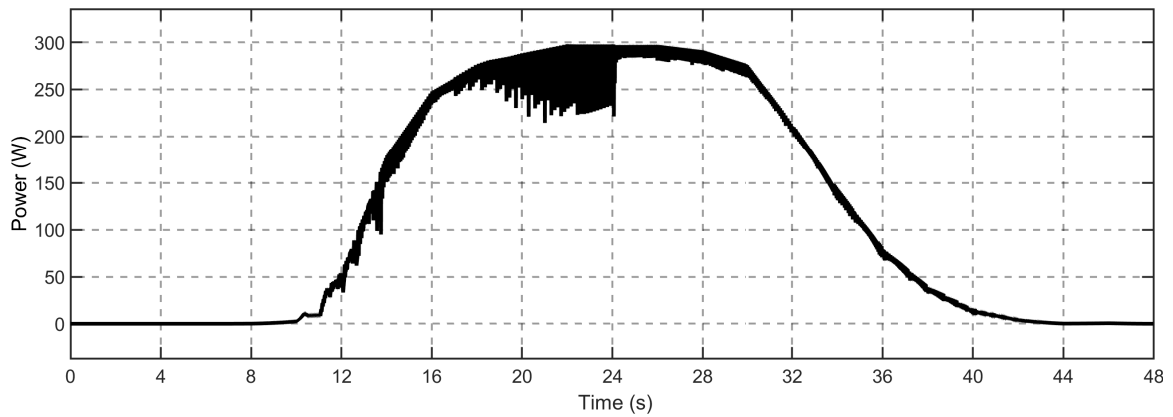


Figure 2.8: Power output of the PV

The PV standalone system was connected to two switching loads, the first one is rated at 150W and the second one is rated at 300W. The reason that the first half of the graph wobbles a lot due to the fact that the inverter performs better at higher loading.

2.3.1.1 Design of Energy storage system

Although renewable energy sources are progressing to take over the majority of the energy production around the world, the perks of clean energy comes with a major disadvantage, i.e. intermittent supply of energy. Be it solar or wind, the renewable energy sources suffer from irregular generation outputs due to the way they are extracted from nature. In case of Photo-voltaics, temperature, irradiation and

inclination of the PV arrays towards sun change the output and make the generation variable in nature. For PV to be considered as a standalone generating source, it needs to solve the problem of intermittence. This generates the need of energy storage devices which can store the surplus power and dispatch it when PV needs support during intermittence. If we consider the load demands, there are fast and slow changing loads. In case of fast changing loads transient power changes needs to be supplied by the source. For this requirement high density power devices can work well, which can supply high amounts of power in a short period of time. For such applications energy storage devices like ultra-capacitors are suitable as they have one of the highest power density levels. These storage devices are known as 'short term storage'.

But most common type of load is the slow changing type of loads, which need energy storage device with a higher energy density like batteries that are capable of storing energy for a longer period than the ultra-capacitor, but it has a slower response in comparison with the Ultra-capacitors. That however, is not an issue when it comes to supplying power to the load.

Battery is a device which converts chemical energy into electrical energy. Like in a PV array, the battery comprises of cells connected in series and parallel combination to get the desired voltage and current at its output. Each cell consists of a positive and negative electrode and an electrolytic solution which serves as a medium to transfer charge between to electrodes. On completing the external circuit, the electron flow through the path generates electric current. Li-Ion, Nickel-Cadmium, Nickel-Metal-Hydride and Lead-Acid battery are the most commonly used batteries in the industry. Among these varieties, Li- Ion batteries are the most suitable for applications related to grid storage and distributed generating auxiliary sources. Lower weight, higher energy density, longer life cycle and no memory effects make Li-Ion based battery technology stand out among others. Especially in the case of distributed and portable

generations like that of standalone PV.

2.4 Design of DC-DC boost converter

To design the DC-DC boost converter for the battery system, a detailed analysis needs to be done for the battery. This DC-DC converter must be capable of maintaining the output voltage constant. The DC-DC converter should also prevent the battery from overcharging and try to reduce any over current into the battery.

The discharge model of the battery shows that when the battery is completely discharged, the current flowing out of the circuit will be zero and so the voltage will be close to zero.

The mathematical equation is represented as follows:

$$V_{Bat} = E_0 - K \frac{Q}{Q - it} it - Ri + Ae^{-B \int idt} - K \frac{Q}{Q - it} i^* \quad (2.11)$$

The DC-DC converter is used to regulate the output of the battery. It is a class of switched-mode power supply (SMPS) containing at least two semiconductors (a diode and a transistor) and at least one energy storage element, a capacitor, inductor, or both. To reduce voltage ripple, filters made of capacitors (sometimes in combination with inductors) are normally added to the converter's output and input as load-side and supply-side filters.

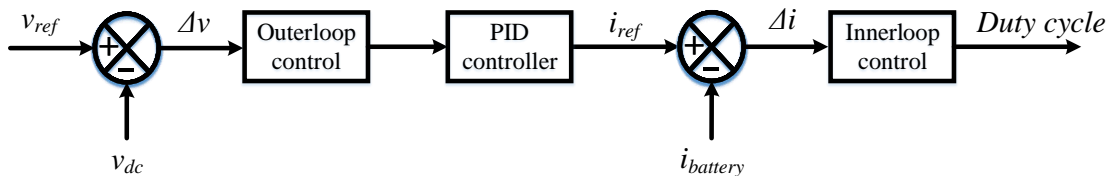


Figure 2.9: Cascade control of the Boost converter

This converter is quite different in the battery side, because the battery needs to supply and absorb power, based on its charge[32]. So, a bi-directional buck boost

converter needs to be used. The primary objective of the controller, of this bidirectional buck-boost converter, must be to maintain the DC link voltage at 400V[33]. The second objective must be to limit the changing of the battery beyond the allowed capacity. Thus, a cascade controller must be designed to perform both these operations. This is modeled in MATLAB, in conjunction with the default model of the battery.

The P and I values for the PI controller used in the outer-loop is about 1.3 and 0.89 respectively. The inner-loop controller's PI values are about 0.56 and 0.35 respectively. Now the final output of the cascade controller is the duty cycle and that is provided to the DC-DC converter.

Components of the Battery system		
Sr. No.	Parameters	Value
1.	Nominal Voltage	200V
2.	Nominal Capacity	1.125Ah
3.	$P_{out} = P_{in}$	350W
4.	Inductor (L)	5.556 H
5.	Input Capacitance (C_1)	$0.17e^{-6}$ F
6.	Output Capacitance (C_2)	$43.94e^{-6}$ F

2.5 Implementation of the PV farm in MATLAB with Battery storage

To test the DC link, a simulation has been developed such that the DC bus is connected to a load, that changed based on the reference provided. The load has 2 resistances, connected to a switch. The switch is programmed to switch the load once at 24 seconds and continues to run at the new set-point. Note that there is no voltage source is present at the DC link. So the battery would only discharge and no charging cycle can be seen.

The voltage that is generated by the PV is shown in figure 1.15. Here, the switching

frequency for the PV MPPT controller is 20kHz. This objective of this controller is just to supply MPPT.

2.5.1 Case 1: PV farm implementation on a sunny day

The best case scenario for PV operation is when the irradiance is constant when the sun is at its highest point in the sky and there is no cloud to interrupt the performance of the PV.

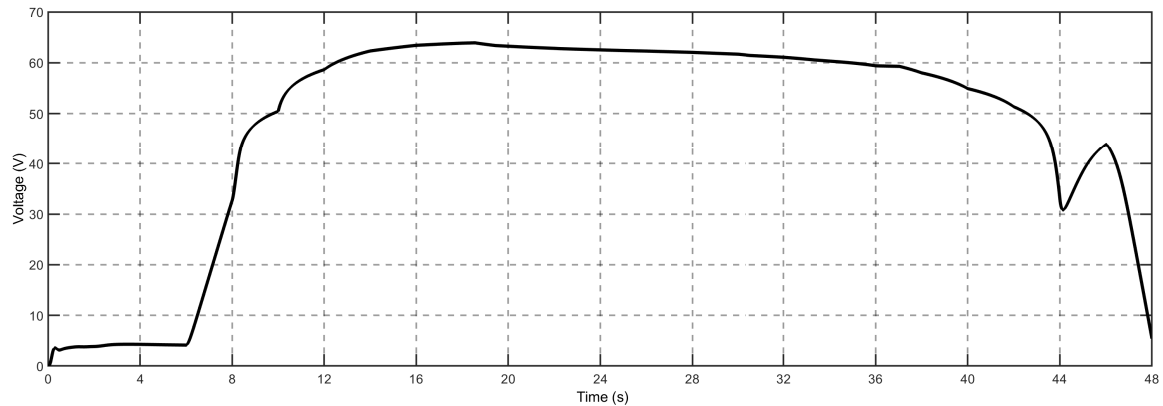


Figure 2.10: Voltage of the PV during a sunny day

The output voltage of the PV should be maintained at a constant value of 400V, with the battery assisting the PV system. It can be seen that the battery is able to maintain the voltage at 400V, with a comparison of when the battery supports the PV and when the PV functions alone.

It is clear that the voltage source or a higher battery capacity, is capable of maintaining the voltage constant and is able to supply the load when it is beyond the capacity of the battery. This is a great base point to add an inverter and convert it to AC power. The higher capacity battery will also assist the inverter in supplying more active power. But this would mean that the size of the system would increase. It is important to note, that in creasing the size of the battery system would not be as expensive as increasing the PV capacity, adding additional lead-acid battery as modelled in this system would greatly affect the power output, while remaining economical.

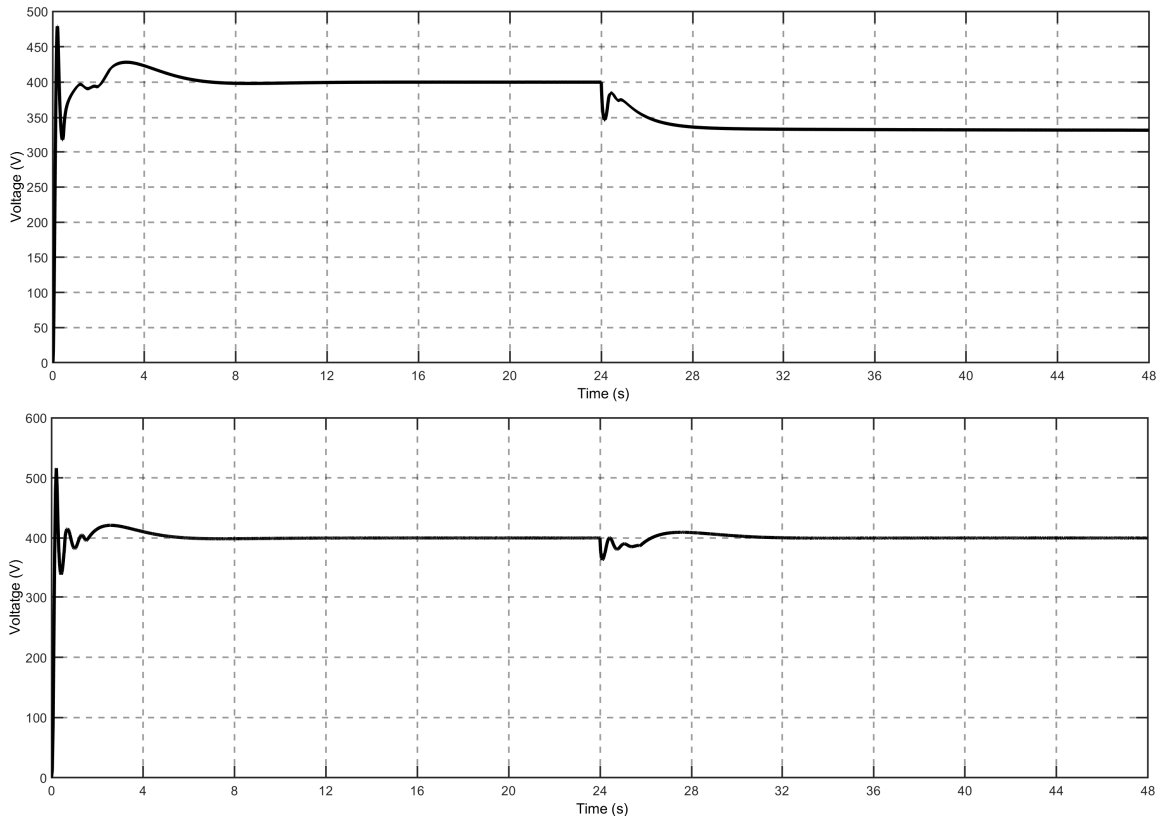


Figure 2.11: DC Bus voltage maintained at 400V; (a) When PB functions alone, (b) When battery functions with PV

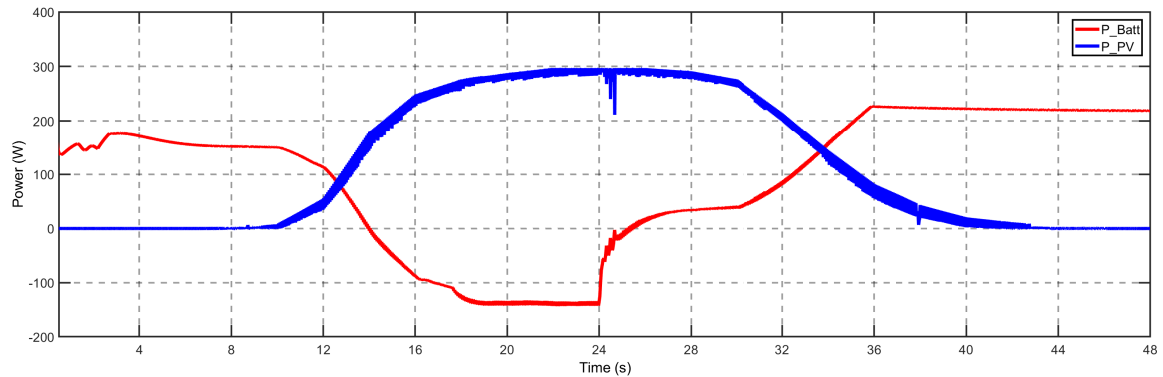


Figure 2.12: Power Sharing between PV and Battery

Based on the figure 2.14, it can be noted that the power is shared between the PV and the battery in a sustainable manner. The voltage is also maintained at a constant value. The results of the simulations match the design for this system.

2.5.2 Case 2: PV farm implementation on a cloudy day

The worst case of operation for a PV farm is when the sky is cloudy. The voltage output of the PV varies drastically. This causes problems downstream, where the DC-DC boost converter is not able to maintain the output voltage. Another issue would be the spikes seen on the voltage due to the rapid discharge of the battery, during the PV's intermittent operation.

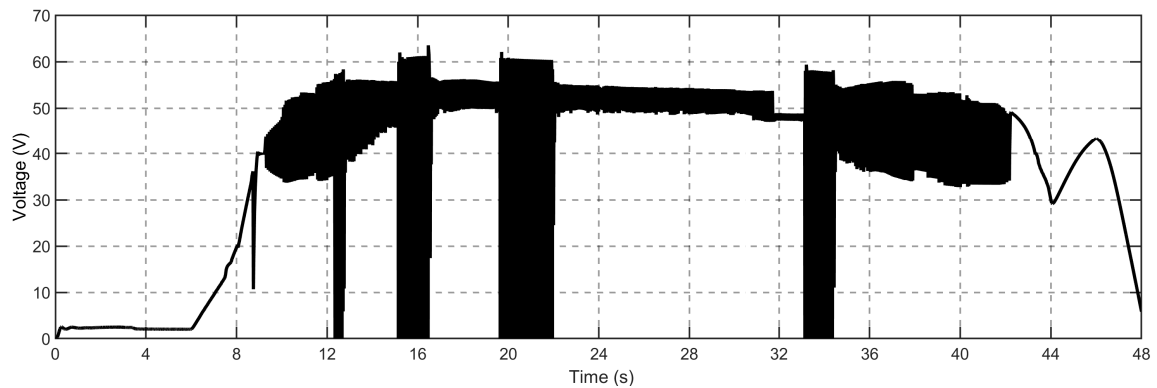


Figure 2.13: Voltage of the PV during a cloudy day

The voltage is intermittent when a cloud passes over the sky, covering the sun. The PV voltage fluctuations must be stabilized by the MPPT and Battery, such that the output remains constant. This can be seen, by measuring the DC-Bus voltage. The voltage profile of the PV array on a cloudy day is shown in figure 2.13. The voltage suddenly drops and rises back to operational capacity which is a challenge to control for the DC-DC converter. But the capacitor at the input is capable of stabilizing the voltage to some extent.

The output voltage of the DC-DC converter connected to the PV module is shown in figure 2.14. The fluctuations are very short-lived and it can be concluded that the voltage control of the DC-bus is quite stable and is maintained at 400V. Note that the fluctuations in the voltage would also reflect on the power supplied to the load. The size of the input and output capacitance may be increased to provide better filtering, but this would also increase the bulk of the system, while also negatively contributing

to the voltage conversion process, developed for the DC-DC converter.

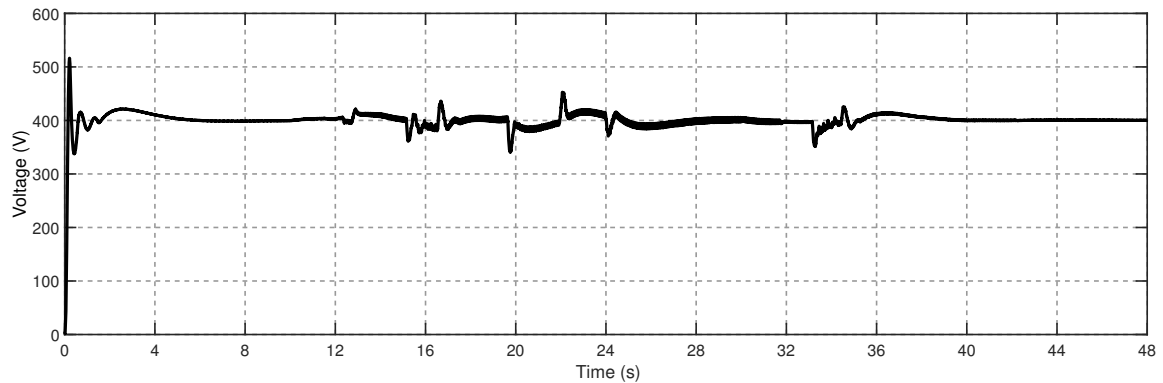


Figure 2.14: DC bus voltage during a cloudy day.

The DC-bus is connected to a varying load, such that the load's demand increases from 150 W to 300W. This would be able to test the performance of the entire DC-bus system. The goal here is to maintain the DC bus voltage constant, while supplying the power demanded by the load. An analysis on the power sharing performed by the PV and the battery is also crucial in understanding the performance of the DC system. Figure 2.15 shows the power being drawn by the load and the step change from 150W to 300W performed during this simulation. Figure 2.16 shows the intermittent nature of the PV voltage when the irradiance profile is intermittent.

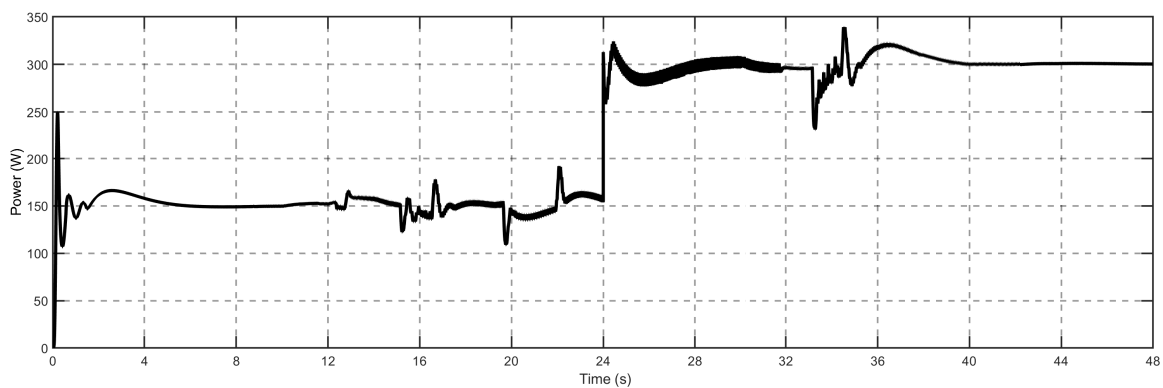


Figure 2.15: Power drawn by the load during a cloudy day

The power output on a cloudy day is shown in Figure 2.15, here the power demand from the load is changed from 150W to 300W. It can be seen that the power is

delivered in a consistent manner, with some transients introduced when the PV power changes, as it was present in the DC bus voltage.

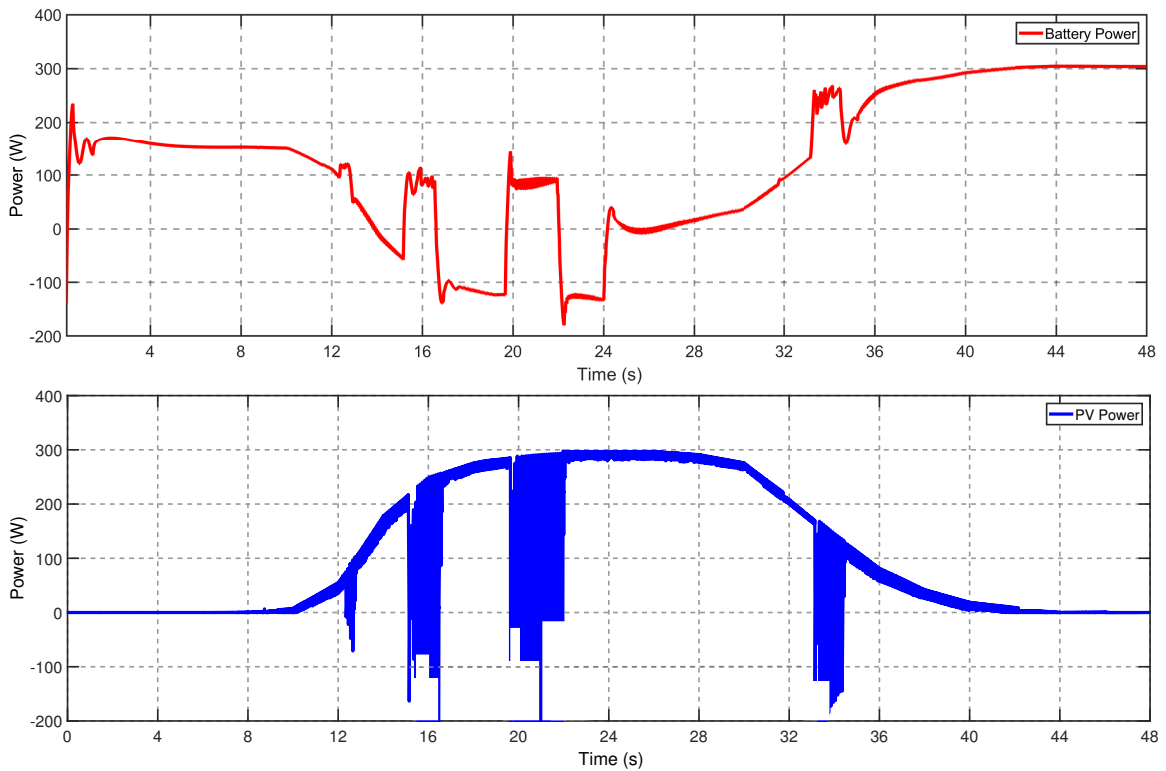


Figure 2.16: Battery and PV power during a cloudy day

This would not be an issue in practical systems as the speed of response of the battery would be quite fast. Power sharing between the battery and PV would show that the battery would supply the power needed to keep the voltage at the DC bus constant, when the PV experiences intermittent irradiance. The PV and battery power is shown in figure 2.18.

All the analysis presented in sections 2.1.3, 2.5.1 and 2.5.2 show that the PV-battery system functions as it was intended. The DC-DC converter also works according to the design. These results validate the function of the DC-bus and the components connected upstream. The next step would be in developing an inverter system that can be connected to the DC-Bus.

2.6 Summary

- The chapter mainly discusses the design and development of a DC energy system that consists of PV farm and Battery. A controller is developed for the battery and PV module such that the voltage is constant and any load within the size can be shared between the PV and Battery.
- The chapter also discusses the design and implementation of the DC-DC converter.
- A single phase PV system connected to the input of the DC-DC converter with an MPPT algorithm has also been designed to extract the maximum power from the PV arrays.
- A battery system provides connected to the DC-bus provides bi-directional control to ensure that the output voltage is maintained at a constant value.
- Also analysis has been performed on the design of the controller so that the battery current can be limited.

In the next chapter a framework for d-q control of single phase inverter is discussed.

CHAPTER 3: SINGLE PHASE INVERTER CONTROL

This chapter discusses various types of inverters in brief and the control strategies for these inverters. A discussion on the theory of stationary and rotating reference frame is also presented. Then a method for single phase inverter control based on stationary and rotating reference frame is discussed. The mathematical model of the inverter is developed in stationary and rotating reference frame. Overall goal is to provide a mathematical framework that can be used to design the proposed single phase inverter control.

3.1 Power Inverter

An inverter is a power electronic device that converts power from the Direct Current form to the Alternating Current form at the required frequency and voltage. The main applications for inverters include DC source conversion, uninterrupted power supplies, electric motor speed control, solar inverters, induction heating, HVDC power transmission, Electroshock weapons and grid-tie power inverters[34]. This thesis deals with the grid connection of PV inverters, with energy storage system attached at the DC bus.

The key point to be noted about inverter is that, in DG systems, the inverter is used to interface a renewable energy source to the grid. This is mainly due to the manner in which energy is produced from renewable energy. The inverter may need to operate in both grid connected or islanded mode. In grid connected mode, the inverter supplies active and reactive power to the local loads, and supplies the surplus to the grid[35]. This power that is transferred to the grid is managed by managing the output current.

An inverter is mainly classified into 2 types:

1. Voltage Source Inverters (VSI) - The voltage source inverter has stiff DC source voltage that is the DC voltage at the input of the inverter is maintained at a constant value.
2. Current Source Inverters (CSI) - A current source inverter is supplied with a variable current from a DC source, hence CSIs have a high input impedance. The resulting current waves are not influenced by the load.

The switching devices consists of a semiconductor switch and an anti-parallel diode. As and when the switching frequency is increased, we get a wave on the inverter output closer to a sine wave, but the trade off is switching losses and this is an important part of the design process, and bi-directional switches especially need to have lower losses. MOSFETs and IGBTs are usually used in inverters due to their ruggedness in high power applications.

3.1.1 Pulse Width Modulation based control

As mentioned before, inverters operate on PWM switching. The most common types of PWM are either uni- or bipolar; uni-polar is better than bipolar switching due to the fact that the ripple content is lesser. In bipolar switching the upper and lower stitches in the same leg operate complementary to each other and all switches operate at the same time, whereas in uni-polar the upper two switches do not work simultaneously. This also has the effect of lower chances of a fault caused by the short circuit between 2 inverter legs.

Although the aforementioned PWM switching is common, a few other switching schemes have been developed such as the hysteresis-band current control PWM, sinusoidal pulse width modulation and space-vector pulse width modulation. Hysteresis-band current control PWM employ variable switching frequency strategy in which carrier frequency varies with the output waveform[36]. The hysteresis current con-

trol limits the load current by following a fixed reference band. The current is then kept in check by switching the transistors, so as to keep the output current within that band. The output voltage is similar to that of the Bipolar PWM. As one might imagine, this provides a great and simple control over the output current. But there are major flaws in this system, mainly the fact that the current limit is dependent on the load, which might vary drastically and also that the switching of current in such a fashion causes a large amount of harmonics in the system, which is not optimal. The load current harmonic ripple leads to a wide range of variable frequency, causing a wider noise band. This can be mitigated by complex active filters, which are quite expensive in practical use.

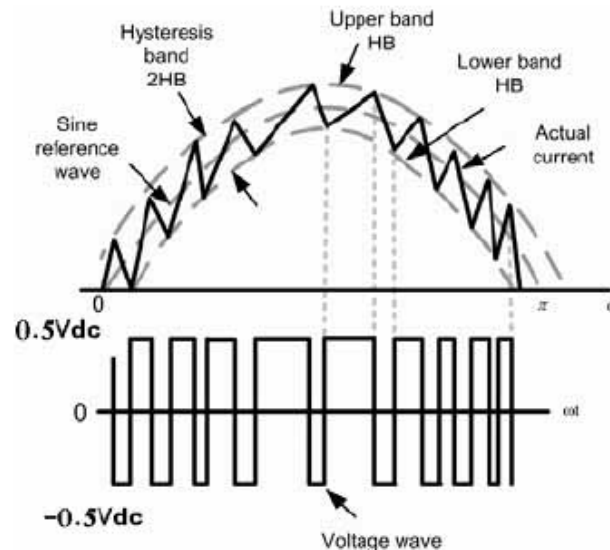


Figure 3.1: Hysteresis Current Control PWM[4]

Sinusoidal PWM compares a reference signal with a triangular wave carrier signal. The modulation index depends on the ratio of the peak of the modulating sinusoidal wave and the peak of the carrier wave. Ideally this tends to have a value between 0 and 1. This type of PWM is useful in keeping the size of the filter small while also producing better output quality.

Synchronous Vector PWM has overwhelmed SVPWM in 3 phase inverter control systems. This has a better utilization of the DC link voltage. Capable of producing

higher output voltage, with less THD, with the ability to implement it easily in digital systems. The main goal is to control the voltage at the output of the switches, which may be $+V_{dc}$, 0 or $-V_{dc}$. The goal is to create an AC output from appropriate control of the switching sequence.

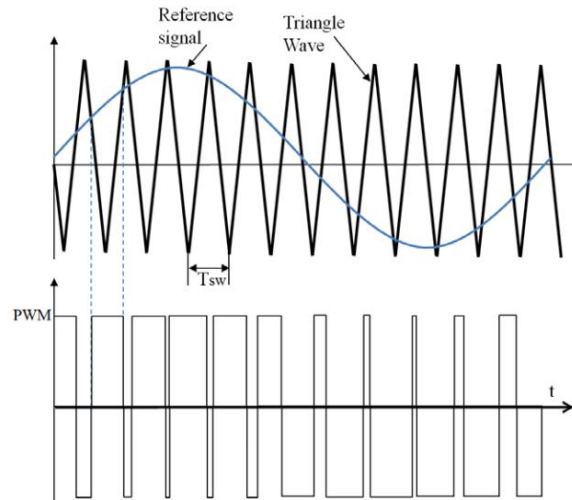


Figure 3.2: Hysteresis Current Control PWM[5]

3.1.2 Space Vector Pulse Width Modulation

This type of PWM was developed for 3 phase systems. The three phase time varying components are represented in 2 orthogonal time invariant quantities. This is done by representing the voltage vector projected on a 2 dimensional reference frame[37]. So the volt-second product is developed using discrete switching states.

3.2 Control Architectures of Single Phase Inverters

Many control techniques have been developed for single phase inverters, mainly to control the output voltage, and providing a good dynamic response with zero steady state error.

- Hysteresis control, also known as tolerance band control, utilizes the inverter output current as a feedback mechanism to limit the current in a hysteresis band. The inverter's legs switch on and off based on the current reference

touching the limits of the band, which limits the peak current. This type of control is ineffective because the variation of the frequency of the PWM and the high amount of peak-peak ripple is to be controlled all the time and therefore we often notice a high THD where this controller is used. Although, the efficiency of this control can be increased by optimizing the hysteresis band with respect to its load parameters, but there is a trade off with a high variation of PWM switching frequency.

- Synchronous reference frame controller, is an important controller scheme for our research as the current error compensation design has been proposed for this study[38]. Regulated vectors are rotated into the synchronous reference frame to that of the fundamental output frequency. We can say that the DQ control methodology is derived from this type of control.
- DQ reference frame controller, in three phase systems this controller is utilized for zero steady state errors. Converting the inverter current output to their respective d components and q components and evaluating the error signal from the references (either dc-link voltage or reactive power or dq components of the grid side voltage) we use PI controllers to generate the reference signal for the pulse width modulation[39]. In literature, these methods have been successfully implemented on grid tied inverters.

The work done as a part of this thesis deals with the third type of control, the DQ control of single phase inverter.

3.2.1 Stationary Reference Frame & Rotating Reference Frame

Power inverters are generally classified as grid following inverter or a grid forming inverter. A grid forming inverter is programmed to maintain a particular operating voltage and frequency. This type of inverter is generally used in micro-grids, that are isolated from the main traditional grid. A grid following inverter, takes its reference

from the grid and matches its voltage and frequency as best as it can. These are the grid tie inverters. Hence, it is imperative that the grid references, provided to a grid tie inverter, is in a manner that is easy for the inverter control system to process and track accurately.

Due to the nature of an alternating grid reference signal, the control of the inverter tends to be complex. The grid has an added level of complexity in that it contains three phase signals that are phase shifted from one another. This makes it quite difficult for the controller to accurately track the grid references and consequently, difficult for a suitable grid-tied operation of the inverter[40].

However, there are certain mathematical tools that are capable of reducing the complexity of the reference, by transforming the three phase quantity into two dimensional reference quantities and also allow us in transforming the time varying quantities into time-invariant DC signals. One such tool is the Clarke's transformation that is capable of converting a balanced three phase into an orthogonal 2 phase reference space. Park transformation is commonly used in machine modelling, and is capable of eliminating the time varying parameter and convert the rotating 2 dimensional vector into stationary 2 dimensional vector.

Any three phase quantity can be converted into a two phase quantity using the equation below:

$$\begin{bmatrix} X_\alpha \\ X_\beta \end{bmatrix} = \begin{bmatrix} 1 & -\frac{1}{2} & -\frac{1}{2} \\ 0 & -\frac{\sqrt{3}}{2} & \frac{\sqrt{3}}{2} \end{bmatrix} \begin{bmatrix} A \\ B \\ C \end{bmatrix} \quad (3.1)$$

Where, A,B and C represent three-phase stationary-frame components and X_α and X_β represent the components projected onto the 2 stationary orthogonal axes. This is crucial as it eliminates the complex mathematics involved in three phase systems, the only problem is that the orthogonal axis is stationary. This means that the effects of the frequency in the three phase system will still affect the stationary frame terms.

Which means that the plane is stationary, but the vectors will rotate at an angular speed that is determined by the frequency of the three phase system.

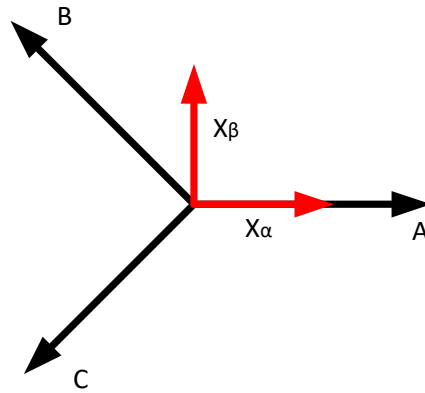


Figure 3.3: Clarke's Transformation from Three Phase to 2 phase orthogonal plane

To make the controls simpler, Park's transformation may be performed to develop d-q reference frame values, which are stationary.

$$\begin{bmatrix} X_d \\ X_q \end{bmatrix} = \begin{bmatrix} \cos \omega t & \sin \omega t \\ -\sin \omega t & \cos \omega t \end{bmatrix} \begin{bmatrix} X_\alpha \\ X_\beta \end{bmatrix} \quad (3.2)$$

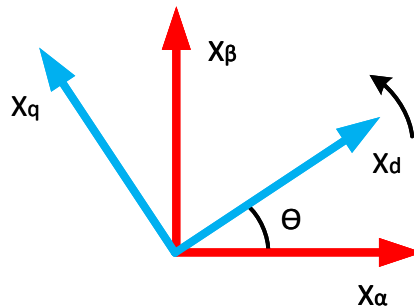


Figure 3.4: Typical Solar Cell with its components

The Park's transformation matrix is a orthogonal non-singular matrix. it represents the relationship between stationary and rotating reference frames. This can be pictured as though the entire plane is rotating with an angular velocity that is determined by the frequency of the three phase system, so the vectors appear to be

stationary, which eases our calculations at each time-step. So, using just 2 mathematical operations, the three phase system is converted to a rotating vector that helps us develop a digital controller that can monitor just 2 quantities and control the three phase output of the system.

3.2.2 Single Phase d-q control

The application of the transformation mentioned before, requires the use of a minimum of 2 phases. That's why the single phase system cannot have a direct implementation of the transformation of stationary to rotating reference frame. This can be mitigated by creating a virtual orthogonal phase for every state variable in the circuit[41]. This is shown in the following diagram below, as the voltage and current are being converted to the d-q domain, using the transformation blocks and the frequency[42].

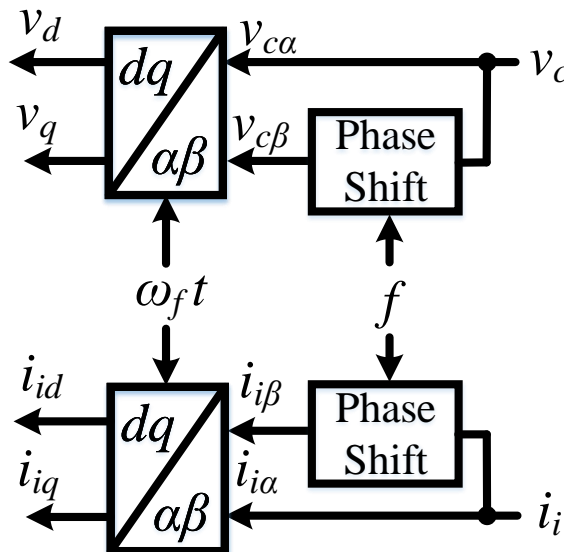


Figure 3.5: Typical Solar Cell with its components

This delay may be implemented in MATLAB using a customized delay block. This is useful as variations in the grid frequency must be ignored when providing the delay for the transformation.

Figure 3.6, depicts the single phase circuit scheme, this is useful when it comes

to building the initial mathematical model of the inverter. We may use this simple model for state space analysis of the system.

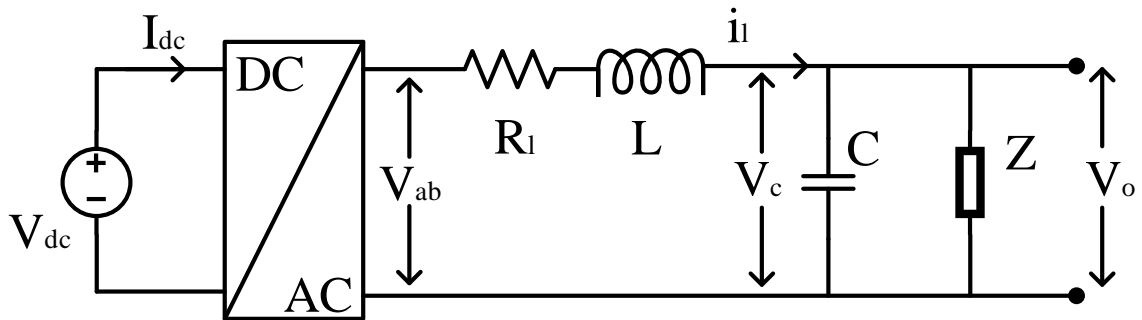


Figure 3.6: Single Phase inverter circuit

$$L \frac{di_l}{dt} + R_l i_l = V_{ab} - V_o \quad (3.3)$$

Where, $V_{ab} = \delta V_{dc}$ and,

$$i_l = C \frac{dv_c}{dt} + \frac{V_o}{Z} \quad (3.4)$$

Here, δ is the duty cycle, Z is the load impedance. A single phase inverter average circuit model was developed, by splitting the inverter model into 2 virtual circuit as depicted. The virtual circuit has the exact same values as the real components, but they does not physically exist. This circuit is primarily present for modelling. The only difference is that all the components are delayed by a factor of 0.25, meaning that the virtual circuit lags behind the real circuit by 90 degrees. This can now be fed to the Parks transformation to perform the rotating reference frame transformation, which will assist us in developing the inverter control [43]. The model used to develop the single phase inverter model in the rotating reference frame is shown in figure 3.7.

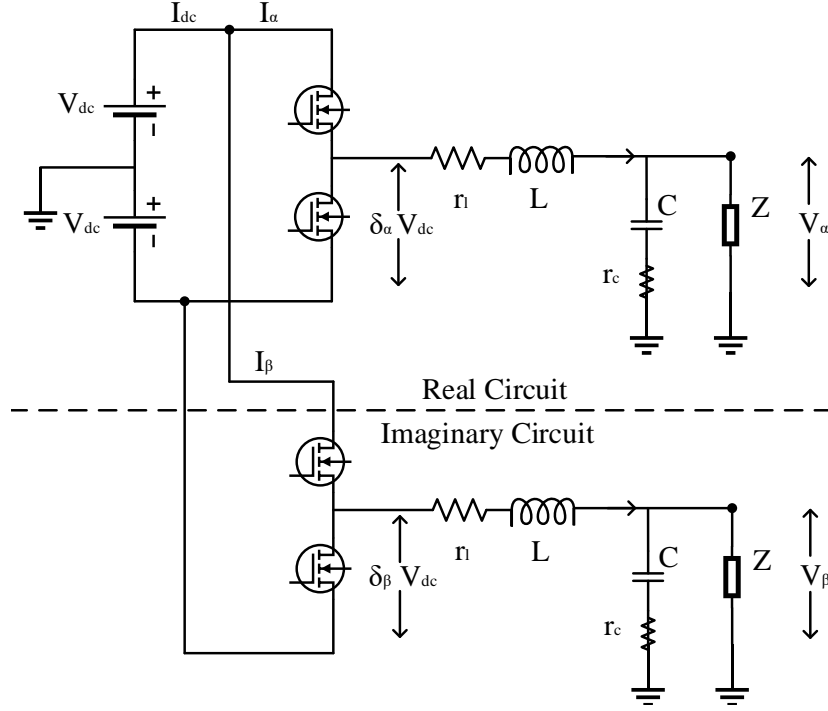


Figure 3.7: Real-Imaginary model of the single phase inverter

$$L \frac{dI_{\alpha}}{dt} + r_l I_{\alpha} = V_{dc} \delta_{\alpha} - V_{\alpha} \quad (3.5)$$

$$L \frac{dI_{\beta}}{dt} + r_l I_{\beta} = V_{dc} \delta_{\beta} - V_{\beta} \quad (3.6)$$

$$I_{\alpha} = C \frac{dv_{\alpha c}}{dt} + \frac{V_{\alpha}}{Z} \quad (3.7)$$

$$I_{\beta} = C \frac{dv_{\beta c}}{dt} + \frac{V_{\beta}}{Z} \quad (3.8)$$

Where, v_{α} is the real output voltage, v_{β} is the imaginary output voltage, I_{α} is the real inductor current, I_{β} is the imaginary inductor current. The $V_{dc} \delta_{\alpha}$ term can be averaged out in the equation 3.5 and 3.6, such that "u" represents the inverter average sinusoidal duty ratio. Applying the average state variables to the switching model of the single phase inverter, based on the real and the imaginary circuits.

Now, The equation 3.5 to 3.8 may be written as:

$$L \frac{dI_\alpha}{dt} + r_l I_\alpha = u_\alpha - V_\alpha \quad (3.9)$$

$$L \frac{dI_\beta}{dt} + r_l I_\beta = u_\beta - V_\beta \quad (3.10)$$

$$I_\alpha = C \frac{dv_{\alpha c}}{dt} + \frac{V_\alpha}{Z} \quad (3.11)$$

$$I_\beta = C \frac{dv_{\beta c}}{dt} + \frac{V_\beta}{Z} \quad (3.12)$$

Here, $v_{\alpha c}$ and $v_{\beta c}$ are the real and imaginary capacitor voltage.

$$V_\alpha = v_{\alpha c} + C \frac{dv_{\alpha c}}{dt} r_c \quad (3.13)$$

$$V_\beta = v_{\beta c} + C \frac{dv_{\beta c}}{dt} r_c \quad (3.14)$$

Combining them, we get

$$L \frac{dI_\alpha}{dt} + r_l I_\alpha = u_\alpha - [v_{\alpha c} + C \frac{dv_{\alpha c}}{dt} r_c] \quad (3.15)$$

$$L \frac{dI_\beta}{dt} + r_l I_\beta = u_\beta - [v_{\beta c} + C \frac{dv_{\beta c}}{dt} r_c] \quad (3.16)$$

$$I_\alpha = C \frac{dv_{\alpha c}}{dt} + \frac{1}{Z} [v_{\alpha c} + C \frac{dv_{\alpha c}}{dt} r_c] \quad (3.17)$$

$$I_\beta = C \frac{dv_{\beta c}}{dt} + \frac{1}{Z} [v_{\beta c} + C \frac{dv_{\beta c}}{dt} r_c] \quad (3.18)$$

The state space average model of the single phase inverter in real and imaginary stationary reference frame is given below.

$$\frac{d}{dt} \begin{bmatrix} I_\alpha \\ I_\beta \end{bmatrix} = \begin{bmatrix} u_\alpha \\ u_\beta \end{bmatrix} \frac{1}{L} - \begin{bmatrix} I_\alpha \\ I_\beta \end{bmatrix} \frac{1}{L} \left[r_L + \frac{Z r_c}{Z + r_c} \right] - \begin{bmatrix} V_\alpha \\ V_\beta \end{bmatrix} \left[\frac{1}{L} - \frac{r_c}{L(Z + r_c)} \right] \quad (3.19)$$

$$\frac{d}{dt} \begin{bmatrix} v_{\alpha c} \\ v_{\beta c} \end{bmatrix} = \begin{bmatrix} i_{\alpha} \\ i_{\beta} \end{bmatrix} \frac{Z}{C(Z + r_c)} - \begin{bmatrix} V_{\alpha c} \\ V_{\beta c} \end{bmatrix} \frac{1}{C(Z + r_c)} \quad (3.20)$$

The figure depicts the schematic diagram that represents the mathematical expression that has been derived from the state space model.

Once we derive the equation 3.19 and 3.20 from the real and imaginary model of the inverter. The d-q model of the inverter may be developed by performing the operations in the transformation matrix of Parks transform.

$$\begin{bmatrix} X_d \\ X_q \end{bmatrix} = T \begin{bmatrix} X_{\alpha} \\ X_{\beta} \end{bmatrix} \quad (3.21)$$

$$\begin{bmatrix} X_{\alpha} \\ X_{\beta} \end{bmatrix} = T^{-1} \begin{bmatrix} X_d \\ X_q \end{bmatrix} \quad (3.22)$$

Where T is the transformation matrix,

$$T = \begin{bmatrix} \cos \omega t & \sin \omega t \\ -\sin \omega t & \cos \omega t \end{bmatrix} \quad (3.23)$$

$$T^{-1} = \begin{bmatrix} \cos \omega t & -\sin \omega t \\ \sin \omega t & \cos \omega t \end{bmatrix} \quad (3.24)$$

Now, equation 3.19 and 3.20 can be converted to the following

$$\frac{d}{dt} (T^{-1} \begin{bmatrix} I_d \\ I_q \end{bmatrix}) = T^{-1} \begin{bmatrix} u_d \\ u_q \end{bmatrix} \frac{1}{L} - T^{-1} \begin{bmatrix} I_d \\ I_q \end{bmatrix} \left(\frac{r_L}{L} + \frac{r_c}{1 + \frac{r_c}{Z}} \right) - T^{-1} \begin{bmatrix} V_d \\ V_q \end{bmatrix} \left(\frac{1}{L} + \frac{r_c}{1 + \frac{r_c}{Z}} \right) \quad (3.25)$$

$$\frac{d}{dt} (T^{-1} \begin{bmatrix} v_{dc} \\ v_{qc} \end{bmatrix}) = T^{-1} \begin{bmatrix} I_d \\ I_q \end{bmatrix} \frac{1}{C(1 + \frac{r_c}{Z})} - T^{-1} \begin{bmatrix} V_{dc} \\ V_{qc} \end{bmatrix} \left(\frac{1}{ZC(1 + \frac{r_c}{Z})} \right) \quad (3.26)$$

By applying the differentiation operation across the transformation matrix we get:

$$\frac{d}{dt}T^{-1} = \begin{bmatrix} -\omega \sin \omega t & -\omega \cos \omega t \\ \omega \cos \omega t & -\omega \sin \omega t \end{bmatrix} \quad (3.27)$$

So,

$$T \frac{d}{dt}T^{-1} = \omega \begin{bmatrix} -\cos \omega t \sin \omega t + \sin \omega t \cos \omega t & -(\cos \omega t)^2 - (\sin \omega t)^2 \\ (\cos \omega t)^2 + (\sin \omega t)^2 & -\cos \omega t \sin \omega t + \sin \omega t \cos \omega t \end{bmatrix} \quad (3.28)$$

Now,

$$T \frac{d}{dt}T^{-1} = \omega \begin{bmatrix} 0 & -1 \\ 1 & 0 \end{bmatrix} = \begin{bmatrix} 0 & -\omega \\ \omega & 0 \end{bmatrix} \quad (3.29)$$

$$\frac{d}{dt} \begin{bmatrix} I_d \\ I_q \end{bmatrix} = \begin{bmatrix} u_d \\ u_q \end{bmatrix} \frac{1}{L} + \begin{bmatrix} 0 & -\omega \\ \omega & 0 \end{bmatrix} \begin{bmatrix} I_d \\ I_q \end{bmatrix} - \begin{bmatrix} I_d \\ I_q \end{bmatrix} \left(\frac{r_L}{L} + \frac{r_c}{L(1 + \frac{r_c}{Z})} \right) - \begin{bmatrix} V_d \\ V_q \end{bmatrix} \left(\frac{1}{L} + \frac{r_c}{LZ(1 + \frac{r_c}{Z})} \right) \quad (3.30)$$

$$\frac{d}{dt} \begin{bmatrix} v_{dc} \\ v_{qc} \end{bmatrix} = \begin{bmatrix} I_d \\ I_q \end{bmatrix} \frac{1}{C(1 + \frac{r_c}{Z})} + \begin{bmatrix} 0 & -\omega \\ \omega & 0 \end{bmatrix} \begin{bmatrix} V_{dc} \\ V_{qc} \end{bmatrix} - \begin{bmatrix} V_{dc} \\ V_{qc} \end{bmatrix} \left(\frac{r_L}{CZ(1 + \frac{r_c}{Z})} \right) \quad (3.31)$$

By neglecting the r_l and r_c , we get,

$$\frac{d}{dt} \begin{bmatrix} I_d \\ I_q \end{bmatrix} = \frac{1}{L} \begin{bmatrix} u_d \\ u_q \end{bmatrix} + \begin{bmatrix} 0 & -\omega \\ \omega & 0 \end{bmatrix} \begin{bmatrix} I_d \\ I_q \end{bmatrix} - \frac{1}{L} \begin{bmatrix} V_d \\ V_q \end{bmatrix} \quad (3.32)$$

$$\frac{d}{dt} \begin{bmatrix} V_d \\ V_q \end{bmatrix} = \frac{1}{C} \begin{bmatrix} I_d \\ I_q \end{bmatrix} + \begin{bmatrix} 0 & -\omega \\ \omega & 0 \end{bmatrix} \begin{bmatrix} V_d \\ V_q \end{bmatrix} - \frac{1}{CZ} \begin{bmatrix} V_d \\ V_q \end{bmatrix} \quad (3.33)$$

Notice that there is a cross coupling terms in both the above equations. This is depicted in the figure. As noted, the d-q parameters are DC, meaning that they are constant, time-invariant in nature. So the inverter's steady state operation is also

time invariant. The continuous time state space equations for the inverter in the dq domain is written as

$$u_d = L \frac{di_d}{dt} - \omega L i_q + r_i i_d + v_d \quad (3.34)$$

$$u_q = L \frac{di_q}{dt} - \omega L i_d + r_i i_q + v_q \quad (3.35)$$

The coupling term is derived from the inverter modelling in the synchronous rotating reference frame. Here, u_d and u_q are the inverter output voltage components in the d-q domain respectively. The references I_{dref} and I_{qref} are acquired from the outer-loop control. The outer-loop control is based on v_{dc} control. The proposed control strategy is intended to maintain maximum power flow between inverter's front-end and the inverter supplying the grid. This is achieved by using a feed-forward controller to control the dc link voltage by generating an appropriate d-axis reference current I_{dref} . This is generated by measuring the difference between the V_{dcref} and the measured V_{dc} , fed through a PI controller.

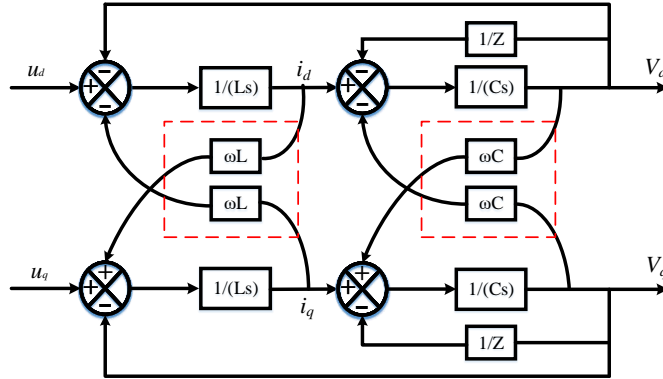


Figure 3.8: Single Phase inverter model in d-q domain

The feed forward controller is shown in the block diagram. The inner-loop control is based on the active power control.

In the rotating reference frame, the value of v_q becomes zero when the inverter is

synchronized with the grid [44]. Then P and Q can be obtained by:

$$P = \frac{1}{2}(v_d i_d + v_q i_q) = \frac{1}{2}(v_d i_d) \quad (3.36)$$

$$Q = \frac{1}{2}(v_d i_q + v_q i_d) = \frac{1}{2}(v_d i_q) \quad (3.37)$$

To transfer maximum power to the grid, the d axis current and the active power command is shown below, along with the q axis current or active power command is obtained as follows:

$$i_{dref} = \frac{2P}{v_d} = \frac{2P_{max}}{v_d} \quad (3.38)$$

$$i_{qref} = \frac{2Q}{v_d} \quad (3.39)$$

3.3 Implementation strategy

The single phase inverter and the grid are modelled in synchronous reference frame as 2 voltage sources. The continuous time state space equation in d-q reference frame is given as follows:

$$u_d(t) = L \frac{di_d(t)}{dt} - \omega L i_q(t) + R i_d(t) + e_d(t) \quad (3.40)$$

$$u_q(t) = L \frac{di_q(t)}{dt} - \omega L i_d(t) + R i_q(t) + e_q(t) \quad (3.41)$$

Here, $u_d(t)$ and $u_q(t)$ are the control signals in the d and q reference frame while e_d and e_q are the grid voltages. R is the equivalent line resistance and L is the equivalent line inductance. To model the closed loop system, the grid tie mode is represented by the following equations:

$$u_{d,k} = L \frac{i_{d,k} - i_{d,k-1}}{T_s} - \omega L \frac{i_{q,k} - i_{q,k-1}}{2} + R \frac{i_{d,k} - i_{d,k-1}}{2} + e_{d,k-1} \quad (3.42)$$

$$u_{q,k} = L \frac{i_{q,k} - i_{q,k-1}}{T_s} - \omega L \frac{i_{d,k} - i_{d,k-1}}{2} + R \frac{i_{q,k} - i_{q,k-1}}{2} + e_{q,k-1} \quad (3.43)$$

The steady state error can be seen as the sum of all the previous errors. Which is logical as the steady state error is the addition of all the small errors in the system.

$$u_{d,k+1} = \left[\frac{L}{T_s} + \frac{R}{2}\right](i_{d,k}^* - i_{d,k}) - \omega L \left(\frac{i_{q,k} + i_{q,k-1}}{2}\right) + Ri_{d,k} + e_{d,k} \quad (3.44)$$

$$u_{q,k+1} = \left[\frac{L}{T_s} + \frac{R}{2}\right](i_{q,k}^* - i_{q,k}) - \omega L \left(\frac{i_{d,k} + i_{d,k-1}}{2}\right) + Ri_{q,k} + e_{q,k} \quad (3.45)$$

We can represent the $i_{d,k}$ and $i_{q,k}$ terms as a summation of all the previous terms. Then, we have

$$u_{d,k+1} = K_p \left\{ (i_{d,k}^* - i_{d,k}) + \frac{1}{T_i} \sum_{m=1}^{k-1} [i_{d,k}^*(m) - i_d(m)] \right\} - K_c \frac{(i_{q,k} + i_{q,k-1})}{2} + e_{d,k} \quad (3.46)$$

$$u_{q,k+1} = K_p \left\{ (i_{q,k}^* - i_{q,k}) + \frac{1}{T_i} \sum_{m=0}^{k-1} [i_{q,k}^*(m) - i_q(m)] \right\} - K_c \frac{(i_{d,k} + i_{d,k-1})}{2} + e_{q,k} \quad (3.47)$$

So, the k_p and k_c terms are the constant terms used in the simulation as a part of the PI controller.

$$k_p = \frac{L}{T_s} + \frac{R}{2} \quad (3.48)$$

$$k_c = \omega L \quad (3.49)$$

$$T_i = \frac{R}{\frac{L}{T_s} + \frac{R}{2}} \quad (3.50)$$

Using all the data from our model, we realize that the k_p , T_i and k_c values are in the range of 0.02138,1 and 0.02 respectively.

3.4 Summary

- In this chapter a mathematical framework is presented for the design of a single phase inverter, with a comparison between Voltage source and current source inverters.
- Also, the pulse-width modulation technique is introduced, with a brief analysis

of the SVPWM technique. The various control architectures of the single phase inverter is also introduced.

- Then the mathematics behind the concept of stationary and rotating reference frame is introduced, with the development of the Synchronous Frame PLL.
- Further, a mathematical model of the single phase inverter is developed in the d-q rotating reference frame domain.

In the next chapter, a new controller design for the active and reactive power control of single phase inverter is designed.

CHAPTER 4: DESIGN OF PROPOSED GRID-TIE & OFF-GRID SINGLE PHASE INVERTER

In the previous chapter the method used to generate the d and q axis references from the grid is discussed. Also inverter's d-q model is derived such that it can be controlled with active and reactive power set points. As mentioned in the previous chapters, the objective of the proposed modelling strategy for the single phase inverter is to facilitate the use of the synchronous rotating reference frame based control of active and reactive power. This allows the transformation of signal components at the fundamental frequency to DC quantities, allowing a simple PI controller to be used in feedback loops in order to achieve stable operation of the system [45].

This chapter describes the design of the controllers and the selection of the parameters. Using state space approach. This allows us to determine the transfer function of the system, which in turn help us understand the dynamics and the stability of the system [46]. For ease in calculation, we may assume that the DC link voltage is constant for one switching cycle. This is true, as the DC link capacitor maintains the DC link voltage close to a constant value. The single-phase half-bridge inverter is shown in the figure, where the parasitic resistance have been neglected. The switching strategy is based on the power stage topology [47].

The single phase inverter transfer function is as follows:

$$G(s) = \frac{V_o}{\delta} = \frac{v_{dc}}{1 + (\frac{L}{Z})s + (LC)s^2} \quad (4.1)$$

The plant represents a traditional second-order low-pass transfer function with the following parameters:

$$\omega_0 = \frac{1}{\sqrt{LC}} \quad (4.2)$$

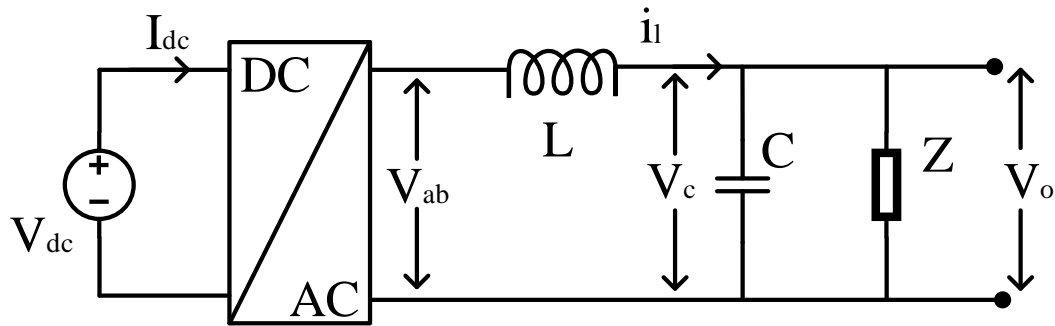


Figure 4.1: Single phase half-bridge inverter, with LC filter

$$Q = Z\sqrt{C/L} \quad (4.3)$$

$$\zeta = \frac{1}{2Z}\sqrt{\frac{L}{C}} \quad (4.4)$$

When the system has no load, the Z tends to infinity, so the Q tends to infinity. So our aim should be to damp this undamped system, in the no load and full load operation. This can be done by limiting the voltage and current output of the inverter.

4.1 Control Implementation Strategy

Many control methods have been developed for inverters, all aimed to control the output voltage with zero steady state error at the fundamental frequency. In this section a few of the control methods have been highlighted.

4.1.1 Single Loop Control Method

This method uses a single feedback loop to regulate the output voltage of the inverter, ignoring the time-varying signals that the inverter generates. The output voltage of the inverter is compared with a reference sinusoidal signal, whose error is supplied to a controller [48]. This does not provide good voltage regulation and more often fails under highly nonlinear loads, which is a key drawback as the power grid mainly contains non-linear loads.

4.1.2 Predictive Model

This is much harder to implement, but is capable of providing the best results. The only issue with this approach would be the fact that the user would need to know the load characteristics in advance, which will greatly improve the ability of the controller to function. In most grid scenario, it is difficult to get an accurate reading of the user data, in real-time.

4.1.3 Multi-control loop

Better performance is generated by using a multi-loop control system. Here, both the output current and voltage have feedback loops. The error of the voltage is fed to the current loop. This results in a better performance of the inverter. This kind of inverter is able to stabilize the voltage and current, and when a active and reactive power set-point is used to create the current control signal, it is capable of performing active and reactive power control as well.

Due to the ease of implementation and the control capability, this type of control is chosen as the desired control methodology for the thesis.

4.2 Controller design

Like the DC-DC converter, in the DC bus, a multi-loop controller needs to be designed, such that the voltage and current control is performed.

Subsequently, this reference is provided to the inner-loop controller that works on developing the v_d and v_q reference for the inverter. The reason for the multiple loops is Outer-loop performs P and Q control. The ratio of $\frac{P_{ref}}{V_d}$ gives us the current reference of I_{dref} . This is then compared to the actual current output of the inverter. Then the inner loop performs the current control [49, 50].

Note that a cross coupling term is present, where the measured current is multiplied by the reactance at the output of the inverter. This will stabilize the current that will be supplied to the grid. This control strategy works well, because the voltage

regulation is done by the grid. When the inverter is off grid, a set point is provided based on the load value. This is a constant, so the inverter will only serve this load. There is no reference provided by the grid, so the load will demand the power and the inverter will comply [51].

But, it is necessary to understand that in grid connected mode, the inverter will perform current control. When the grid is off, the inverter will begin working on controlling the output voltage. So, we can merge both these scenarios to perform on and off grid operation of the inverter. This thesis also presents a Synchronous frame PLL that is capable of taking the grid on and off grid, based on the quality of power at the grid.

4.2.1 Grid Connected Mode

This mode is the basic form of operation thought out grid connected inverters. Here the basic function of the inverter is to provide quality power at the same phase and the frequency as the grid at the point of common coupling. When the grid is healthy and is able to supply voltage at 1 p.u, the inverter will be operating in the healthy range. This means that the breaker connected at the PCC will be at the closed state [46]. The PI controller regulates the d-q grid currents according to the active and reactive power reference. As the decoupling is present on the controller side, we can alter the active and reactive power references individually and supply the power demanded by the local load.

The outer-loop performs voltage control as well as active and reactive decoupled control. The current reference is provided to the inner current control loop. The current control loop tries to limit the current based on the power rating of the inverter. The voltage regulation in the grid connected mode is done by the grid.

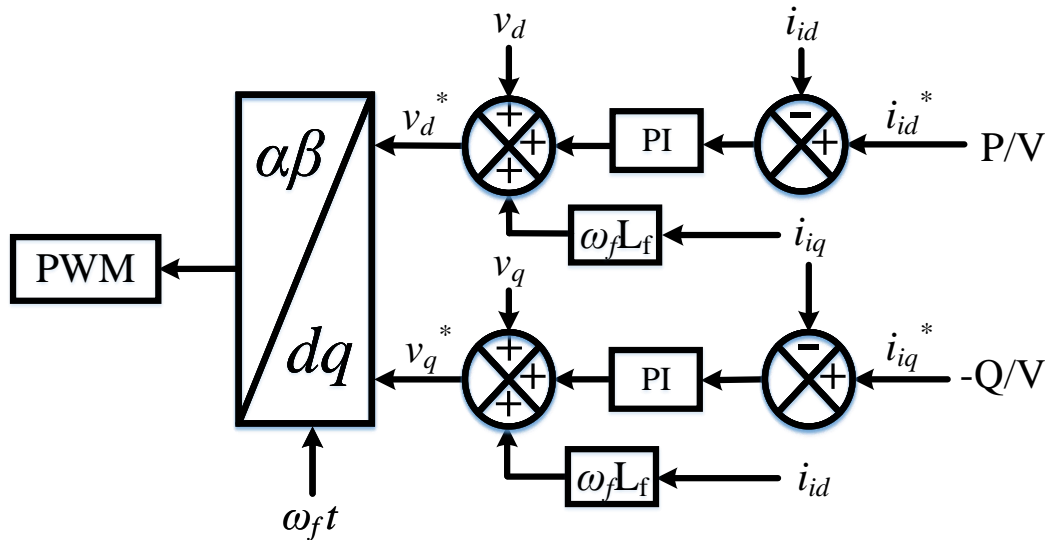


Figure 4.2: Inverter control schematic for On-grid application

The d-q components of the voltage is fed to the dq- $\alpha\beta$ transformer. The sinusoidal reference that is created is provided as the modulating signal for the PWM generator. These pulses are then fed over to the power inverter.

4.2.2 Transition from on-grid to off-grid

The transition from off-grid and on grid needs to take place seamlessly to maintain good power quality and improve the life-span of the inverters. When the frequency or voltage drops beyond a threshold point, the circuit breaker at the output of the inverter will trip, causing the inverter to go into the off-grid mode. The off-grid mode is also known as "the islanding mode".

It is critical to maintain the output voltage when inverter is in the off-grid mode, as the inverter does not have any voltage reference as it did in the grid-connected mode. So a voltage control loop is added into the outer-loop of the inverter. The active and reactive power control is done by generating a power reference from the local load.

The PCC will become a point of measurement, to check if the grid is brought back to a healthy state. Until that point, the inverter gets its power reference from the

local load.

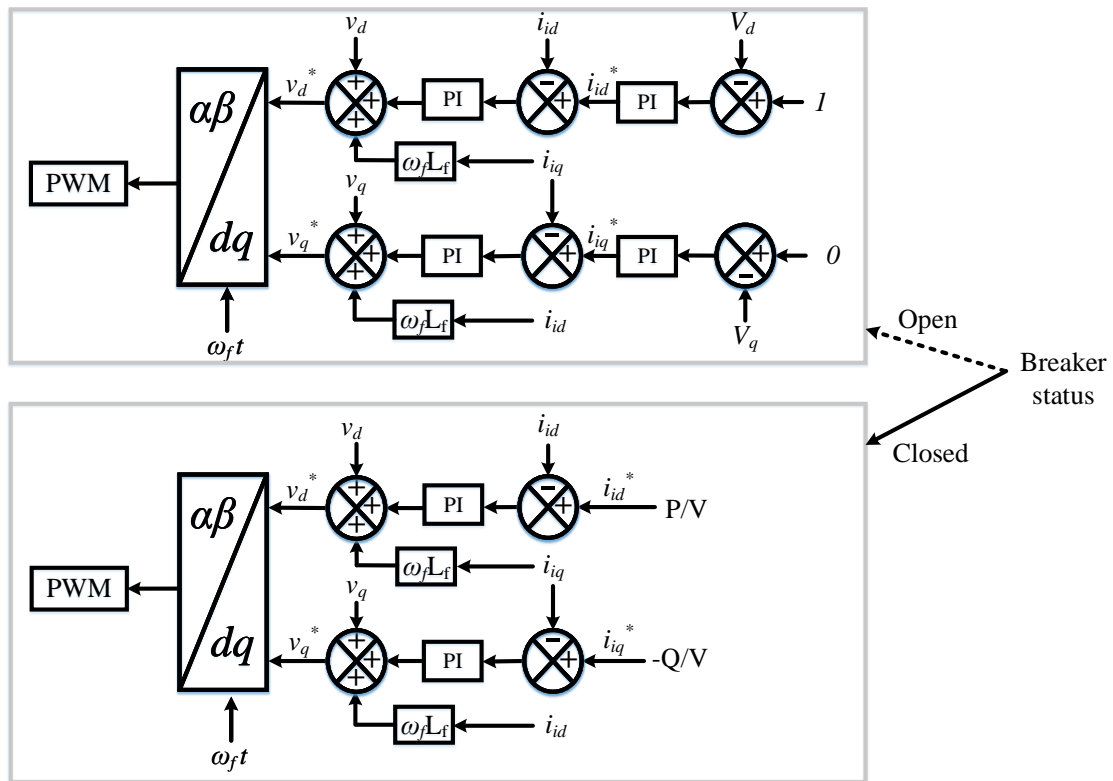


Figure 4.3: Grid connected and islanded mode reference management

Figure 4.3 shows how the controller is managed for on-grid and off-grid operation of the single phase inverter. When the breaker status is closed, it means that the inverter is in the on-grid mode of operation, while the breaker status in open state means that the inverter is in the off-grid state.

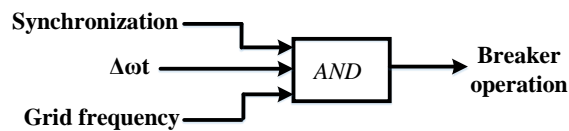


Figure 4.4: Circuit Breaker Control

Figure 4.4 shows the breaker operation, if all the three conditions in the input are satisfied, then the breaker operates, closing the circuit. The synchronization status is a check performed to see if the output voltage of the inverter is equal to the voltage

at the PCC. The $\Delta\omega t$ parameter checks if the inverter voltage and the grid voltage are in phase. This is critical as any change in phase will cause circulating currents. The grid frequency check is performed to see if the inverter and grid frequency match. when the grid frequency is in the limit, the $\Delta\omega$ terms are in limit (the difference in the frequency of inverter and grid is low) and synchronization (grid voltage is equal to the inverter voltage) status is high, the breaker will operate.

4.2.3 Off-grid Mode

Some critical loads require higher quality of power as compared to the power supplied to the residential neighborhoods. When the grid deviates from the normal operation, it can cause havoc among critical loads and also poses a safety hazard. Although protection devices are available to stop any kind of instability in the system, a backup source of power is always preferred. Hence the inverter system has been developed such that it is capable of disconnecting from the grid in case of fault at the grid side. Active power reference is directly fed from the local load.

$$\Delta(\omega t) = (\omega t)_{\text{grid}} - (\omega t)_{\text{PCC}} \quad (4.5)$$

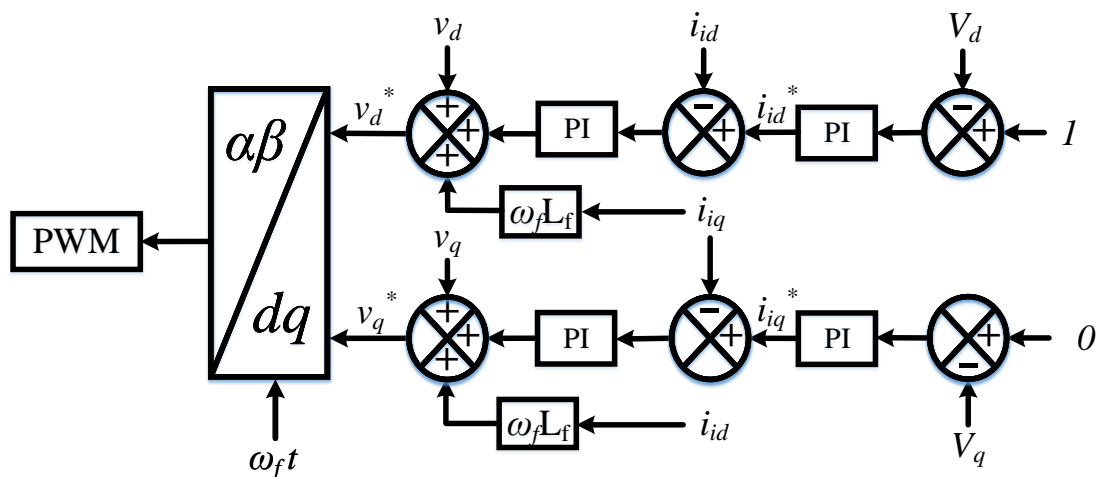


Figure 4.5: Inverter control schematic for off-grid application

When the fault is removed, the inverter needs to be synchronized to the grid to avoid large circulating currents. To perform synchronization, the inverter must check if the voltage and frequency of the grid, matches the inverter output. $\Delta\omega t$ decides whether the frequency is within the bounds of the operation of the inverter operation. Equation 4.5 shows the equation used to check whether the frequency is within the limit to reconnect to the grid[52].

The breaker status will instruct the PLL to change the reference from the off-grid to on-grid values. A PLL has been designed for the sole purpose to keeping track of the frequency and also in managing the switching references. When the inverter transitions from the grid connected to off grid mode, the power reference changes from the grid reference to the local load's reference.

4.2.4 Synchronous Frame PLL

A PLL is a feedback control system. It automatically matches the phase of the locally generated signal with the phase of the input signal. The main task of the PLL in grid connected systems is to match the frequencies of the inverter output to the grid value. This is done to maintain unity power factor.

The typical components of a PLL are as follows:

- Phase detector (PD): Measures the deference between the input and the output signal, and generates a voltage based on that difference.
- Low pass filter: Blocks all the higher frequency signal and extracts the DC components that arise from the PD.
- The DC component is then amplified and passed to the VCO, which could be a PI controller to generate the frequency of the output signal.

If the output of the PLL matches the input, the PD is eventually driven to zero[47]. SF-PLL is commonly used in three-phase systems. The instantaneous phase angle θ is detected by synchronizing the PLL's rotating reference frame to the grid voltage

vector[53]. The PI controller sets the d or q axis reference voltage V_d or V_q to zero. This results in the reference being locked to the grid voltage vector and the phase angle. The grid frequency f and voltage amplitude V_m can be obtained as well. During the stable operation of the grid, PLL include high bandwidth and accurate detection of amplitude and phase of the grid voltage vector. However, it does not mean that the PLL will not operate when there are harmonics present in the grid[54]. The bandwidth can be reduced to accommodate the distortion caused by high order harmonics, the trade-off being the reduction in the speed of response[55].

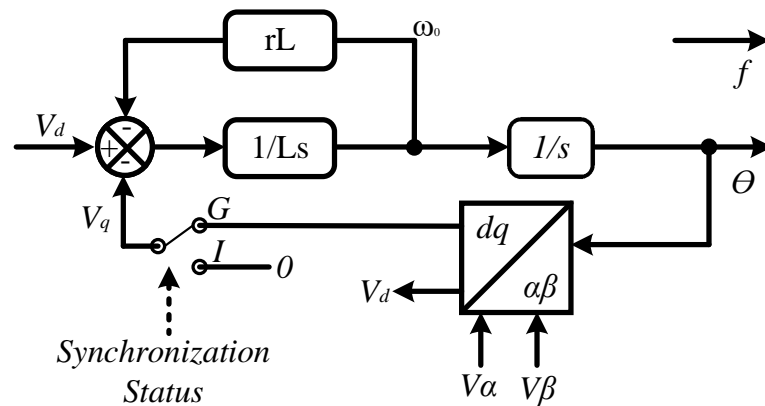


Figure 4.6: Synchronous Frame PLL

Figure 4.6 depicts the implementation of the SFPLL. The concept is to be able to detect and synchronize with the grid while acting quickly to lock the inverter output with the output of the grid[56]. Depending on the synchronization status, the PLL will work either in the grid connected mode (G) or the islanded mode (I) as shown in Fig. 4.6. Synchronization status is a voltage and frequency limit verification, it is high when the grid voltage and frequency is within the limits of interconnection and low when they are beyond the limits (fault condition)[57]. In the islanded mode, we use a constant q axis voltage of 0, while at the grid connected we use a q axis voltage synchronized to the grid[58, 59].

4.3 Implementation and Test Results

This section talks about the various components used in the simulation and how the topics in the previous sections and chapters tie in together to perform the simulation of the single phase grid tie inverter operating in both the grid tie and off grid mode, capable of supplying active and reactive power to the local load[58].

4.3.1 Architecture in MATLAB

A full-bridge inverter is connected to the DC bus that is created in chapter 2. The inverter was developed based on the modelling done in chapter 3. To simulate the effects of voltage and frequency transients in the grid, the inverter is connected to Phase A of a synchronous machine, through a transformer. The synchronous machine is connected to a load and a load-flow bus.

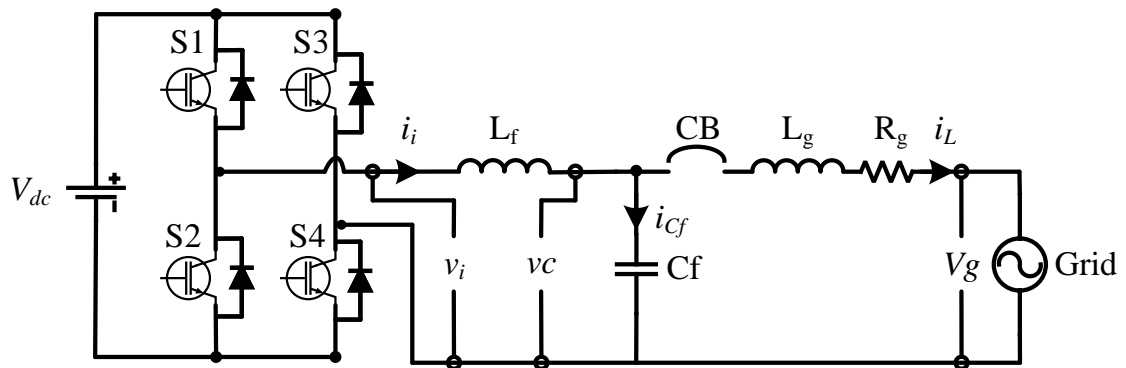


Figure 4.7: Grid Connected Circuit Diagram

The MATLAB circuit consists of a synchronous machine that generates 13800 V. That is supplied to a variable load, with the reference. That is connected in parallel to a transformer that steps down the 13800V to the distribution voltage of 400V (ph-ph).

The machine was initialized using load-flow option in MATLAB, that tells the user about the initial value required for machine to operate within the control limits. The transformer is then connected to the circuit breaker, to perform on grid to off-grid

operation, that is then connected to the local load, which is connected to the inverter. The only input that the inverter receives is the per-unit, sinusoidal reference, which will be compared to a triangular signal, to generate the output voltage.

Note that the voltage is 230V (line-ground), the power is 350W, so the per unit current is 1.52 A.

A sag and reduction in frequency was simulated by reducing the mechanical power supplied to the generator. In another case, a three phase fault was applied to the system. When a sag/swell of above 0.95 to 1.05 p.u. is experienced or frequency changes from 49.5 to 50.5, the inverter enters the off grid mode of operation.

When the voltage and frequency are within limits, the inverter checks the $\Delta\omega$ value is below 3 radians. This is considered within the range of operation of unity power factor.

4.3.2 Results and Discussion

This chapter discusses the results of the simulation of the single phase grid connected inverter with the PV Battery system, while functioning on grid connected and off grid mode.

4.3.2.1 Case 1 : Active and Reactive Power Reference Tracking

The active and reactive power is controlled by the inner current control loop, in both the on-grid and off-grid mode. The active and reactive power is determined by the load requirement, as the current output of the inverter is dictated by the load. However, the voltage reference used to generate the active and reactive power reference for the inverter is changed from the measured voltage to a constant voltage of 0 and 1 per unit for the q and d components respectively. Hence, the $\Delta\omega$ value is always equal to zero, and the frequency is generated to be 50 Hz and the angular frequency at its base value is 314 rad/sec.

The inner loop control regulates the d-q axis current components according to the

active and reactive power reference provided by the outer loop. The output of the current control loop is compared to the voltage of the grid, in order to produce better dynamic response. In the grid connected mode the voltage regulation occurs because of the grid. This would not be possible in the off-grid case, so a constant signal of the voltage set-point must be provided to the outer loop control.

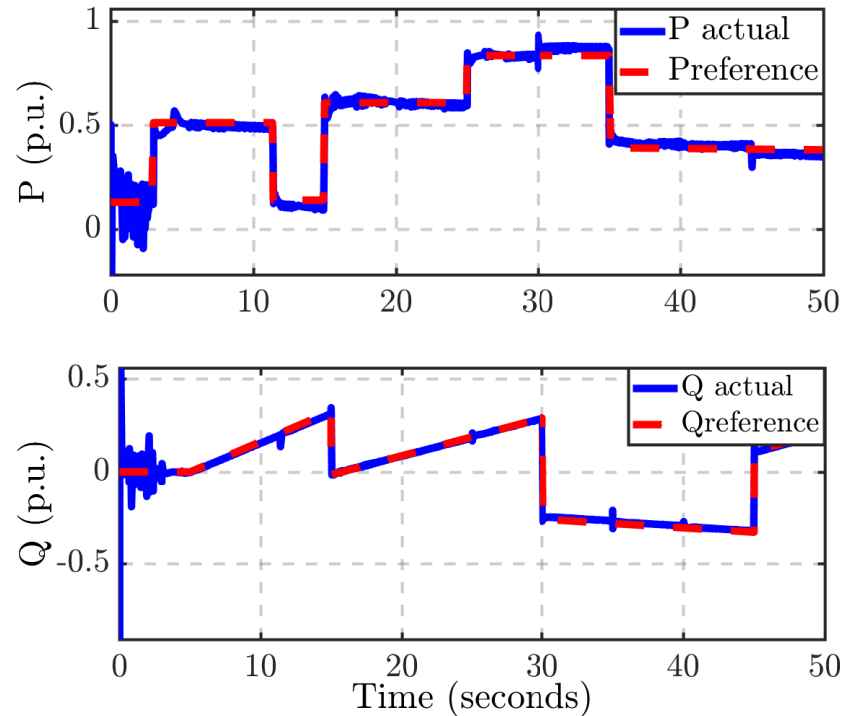


Figure 4.8: Active and reactive power reference while working in grid connected mode.

To evaluate the controller, the first step would be to verify that the inverter is capable of working in grid connected and off grid mode, independently. This would prove to be a good starting point for analyzing the operation in the transition conditions.

Figure 4.8 shows the inverter delivering active and reactive power in the grid connected mode. The stable transfer of power indicates that the controller performs well, in the grid-connected mode. The inverter is capable of supplying a stable amount of voltage and current for step changes in the active and reactive power. The operation of the inverter is stable in the ramp power. Although there are transients initially, the inverter is still able to track the active and reactive power references.

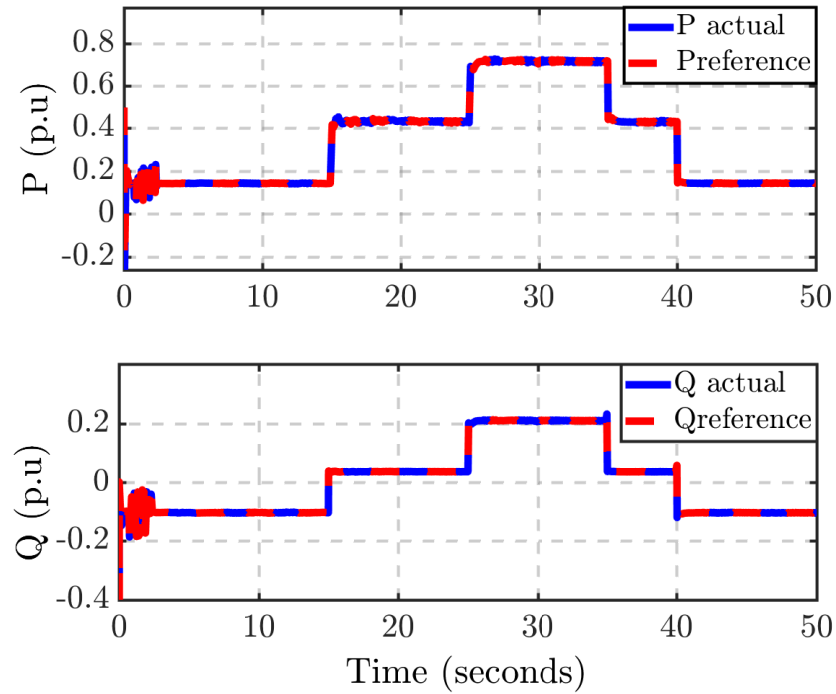


Figure 4.9: Active and reactive power reference while working in islanded mode

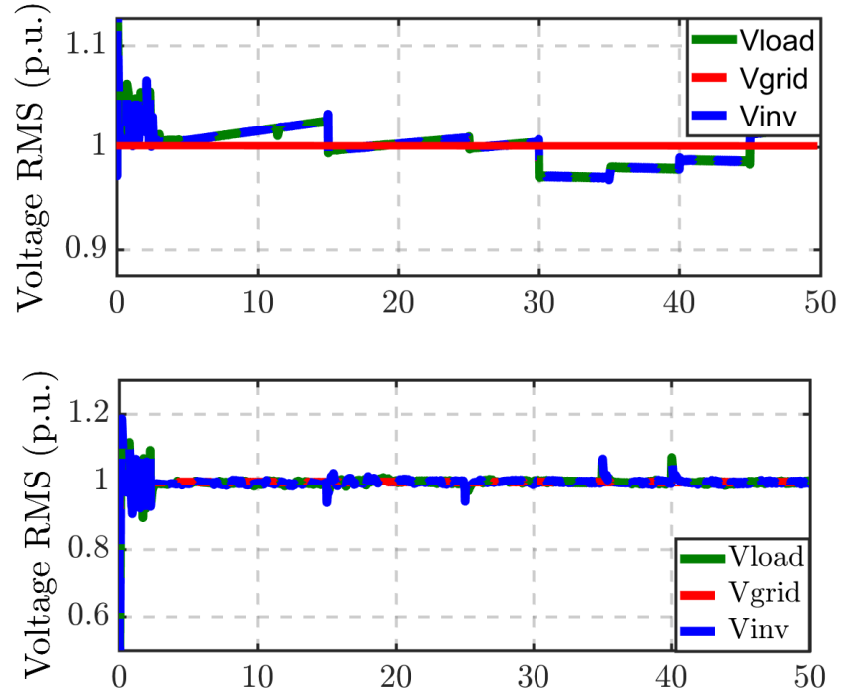


Figure 4.10: Voltage at the output of the inverter in grid connected and islanded mode

Figure 4.9 shows that the inverter is able to supply the active and reactive power in the off-grid mode. The inverter is able to track step changes in the load reference. The power outputs of the inverter seem to be stable.

Figure 4.10 shows the output voltage is stable in both the grid-connected and off-grid cases. In grid connected mode the inverter's output follows the changes in the voltage as required by the load.

Figure 4.11 shows that the inverter is able to deliver the current output needed to supply the load. Here, I_d and I_q are the d axis and q axis components of the current. They control the active and reactive power respectively. The graphs show that the inverter operates in the on-grid and off-grid state, while delivering active and reactive power to the local load. The voltage output is also stable in both the grid connected and off-grid modes.

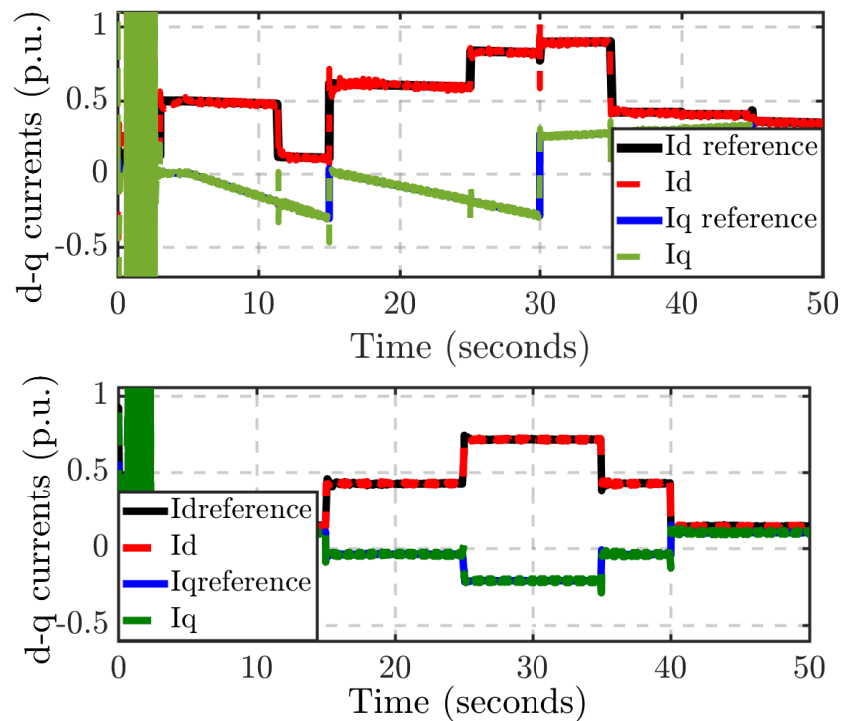


Figure 4.11: Current at the output of the inverter in grid connected and islanded mode

4.3.2.2 Case 2: Analysis during Sag case

To check if the breaker is able to sense abnormal operation of the grid, the first evaluation that needs to be performed is to check if the inverter enters islanded mode, if the frequency changes dramatically.

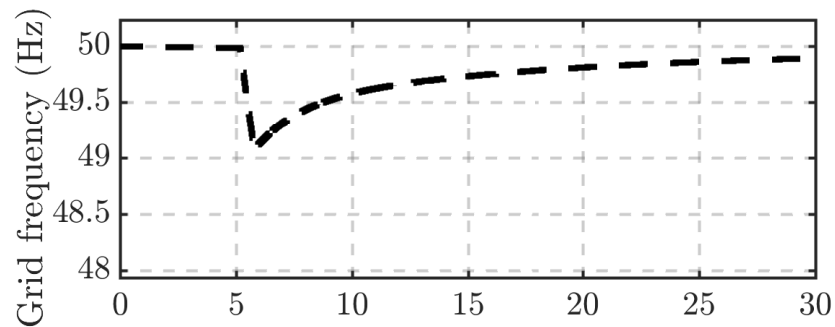


Figure 4.12: Frequency sags when the prime-mover excitation was reduced

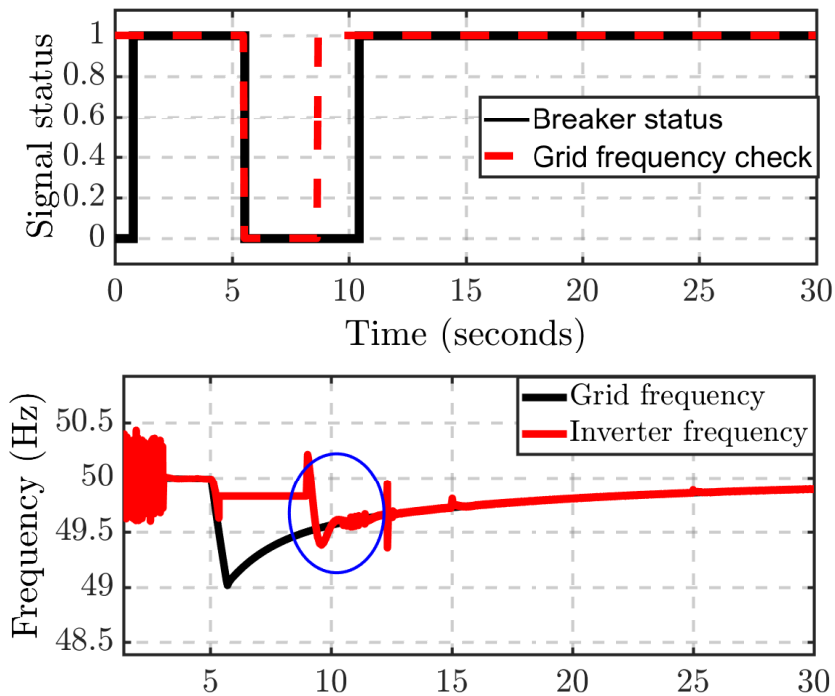


Figure 4.13: Frequency check performed and inverter grid frequency alignment

A frequency sag was created by reducing the prime mover excitation value from 1 pu to 0.8 pu. This created a frequency below the lower limit for our inverter circuit,

hence letting the circuit breaker to trip and lead the inverter into islanded mode of operation. So as discussed before, the PLL and controller get different voltage values, and they are tasked to maintain the operation of the inverter and the grid in a stable condition and is able to track the references without any errors.

Figure 4.12 shows the sag in frequency created when the mechanical excitation for the synchronous machine is reduced. After about eight and a half seconds, the frequency is normalized. The inverter detects the change in frequency and thus goes offline. When the inverter realizes that the grid frequency is normal, the inverter connected back online.

Figure 4.13, shows the re-connection of the inverter at around 8 second mark. There are a few spikes in the frequency, but this frequency spike is still within the operating range of the inverter. Performing this test of the inverter by introducing a voltage spike and a surge, allows for a more rounded approach to analyze the performance of the inverter.

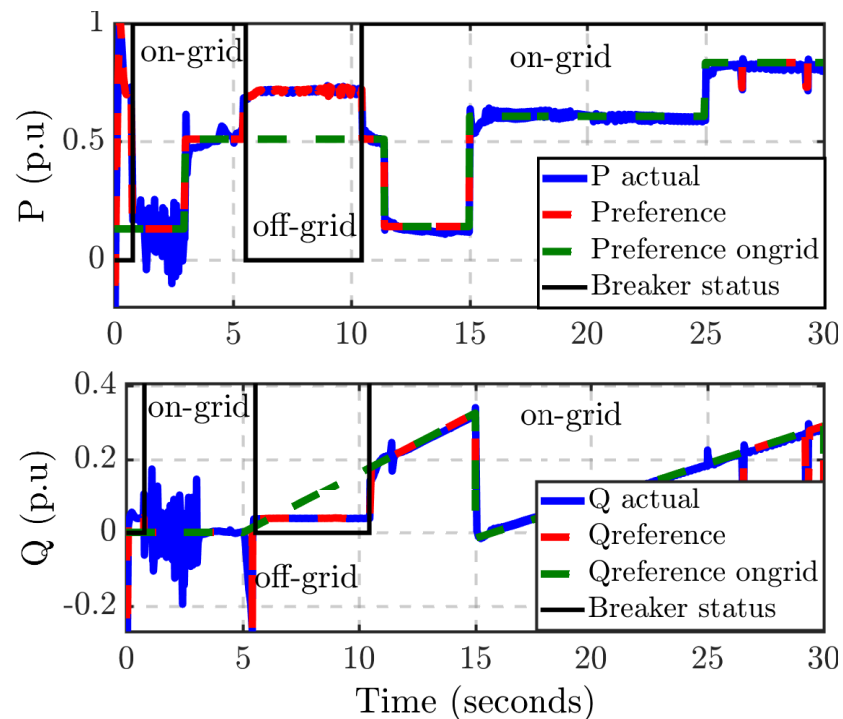


Figure 4.14: Active and reactive power output of inverter tracking the reference

Breaker status 0 means that the breaker is open, while the breaker status 1 means that it is closed. Note that the frequency gets aligned to the grid at around 8.5 seconds. The reason that the breaker operates much later is due to the fact that the $\Delta\omega$ condition is not satisfied and the synchronization doesn't take place.

The Power reference also works as expected. The inverter is able to follow the local load reference when the inverter is on or off grid. When the inverter is on-grid, a reference curve is provided such that the active and reactive power is supplied to the grid. When the inverter is off-grid, the reference is changed to match the local load references. This is the same case with the reactive power. The tracking seems to be functioning without large spikes. The re-synchronization with the grid also works fine. The following graphs show that the inverter is performing as it was designed. The synchronization and de-synchronization also take place without any large power quality concerns.

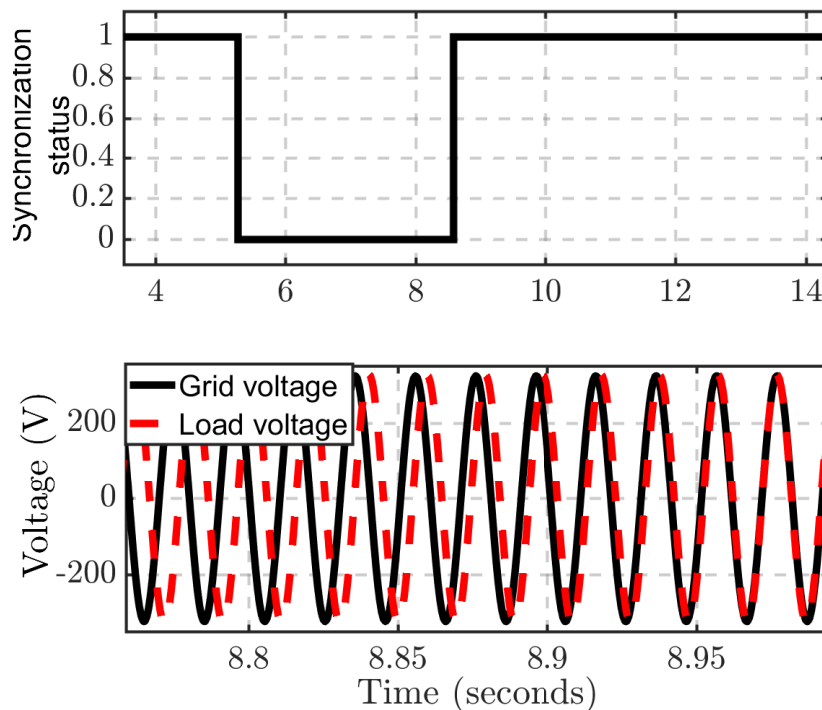


Figure 4.15: Moment when synchronization is performed, the voltage is synchronized

Note that Figure 4.15 is conclusive evidence that the connection is taking place

seamlessly, meaning that there are no spikes seen on the voltage during the time when the inverter reconnects to the grid. This allows the inverter to perform with the highest power quality. The seamless transfer action is also very critical for the health of the switching devices in the inverter.

4.3.2.3 Case 3: Analysis during fault condition

In this case, the grid is subjected to a fault scenario, such that the voltage drops dramatically, but the frequency spikes. This is detected by the inverter and the inverter goes to the off-grid mode. When the inverter senses that the grid is performing optimally, the inverter begins to synchronize with the grid.

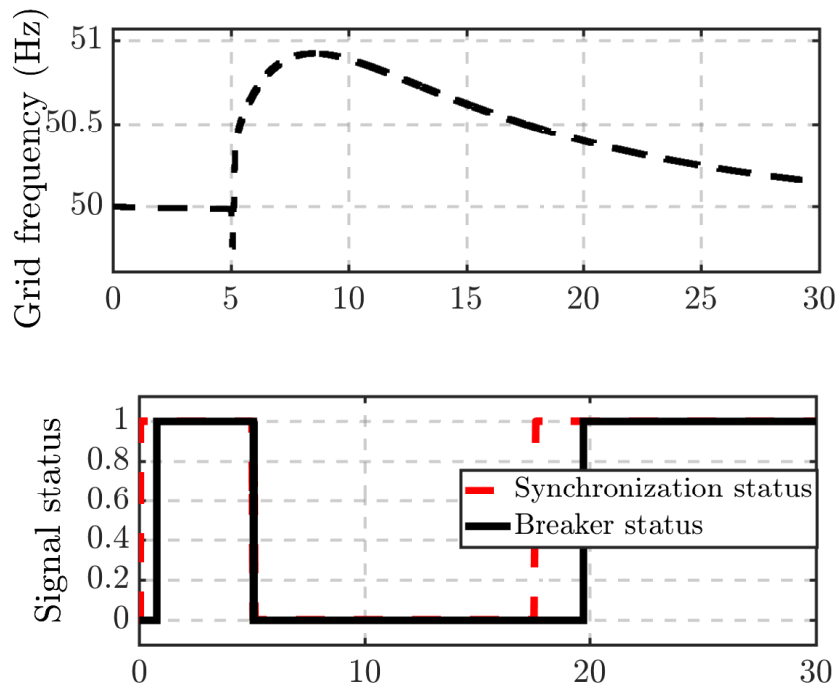


Figure 4.16: Frequency spike seen when a fault is present at the grid side

Figure 4.16 shows the spike in frequency when the fault takes place. The breaker status indicates that the inverter goes offline. When the voltage and frequency comes back to normal, as shown by the synchronization status, the breaker reconnects to the grid. It is important for the inverter to be disconnected from the grid in case of

faults, as the fault at the terminal of the inverter would definitely kill the switches and possibly cause a fire hazard. The ability to go off-grid while being also to maintain power output is really useful as uninterrupted power supply is realized.

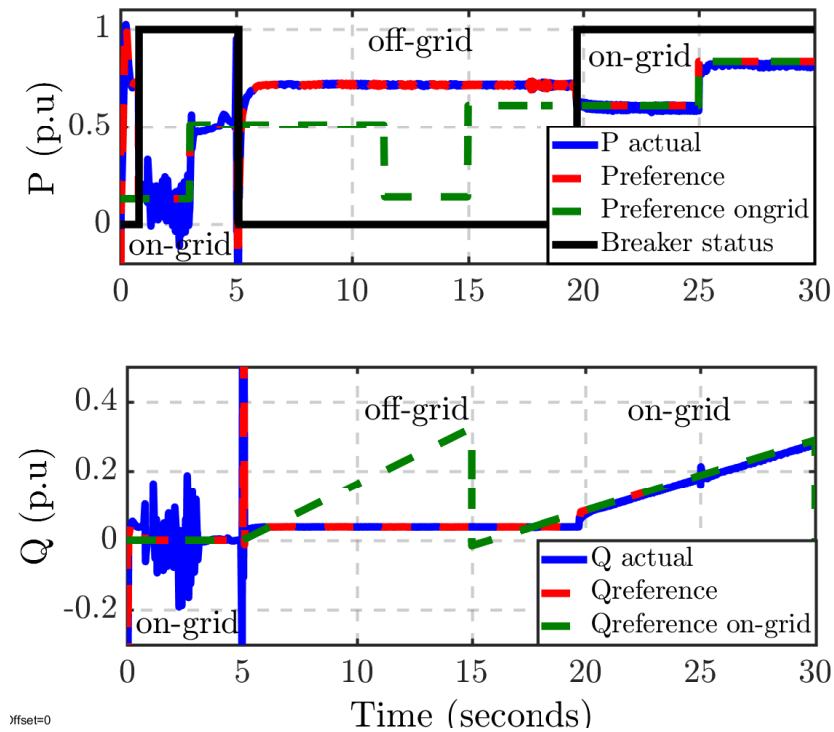


Figure 4.17: Active and reactive power reference followed during the fault scenario

Figure 4.17 shows the inverter following the active and reactive power reference provided by the local load during the fault scenario. When the fault is removed, the inverter connects to the grid and the normal grid tie operation is reached. Without seeing spikes in voltage or the current. Figure 4.18 shows the seamless operation of the inverter reconnecting with the grid. With these results, we have proved that the d-q control logic works well, the SFPLL is capable of keeping track of the frequency and the seamless transfer from grid connected to off-grid mode is performed.

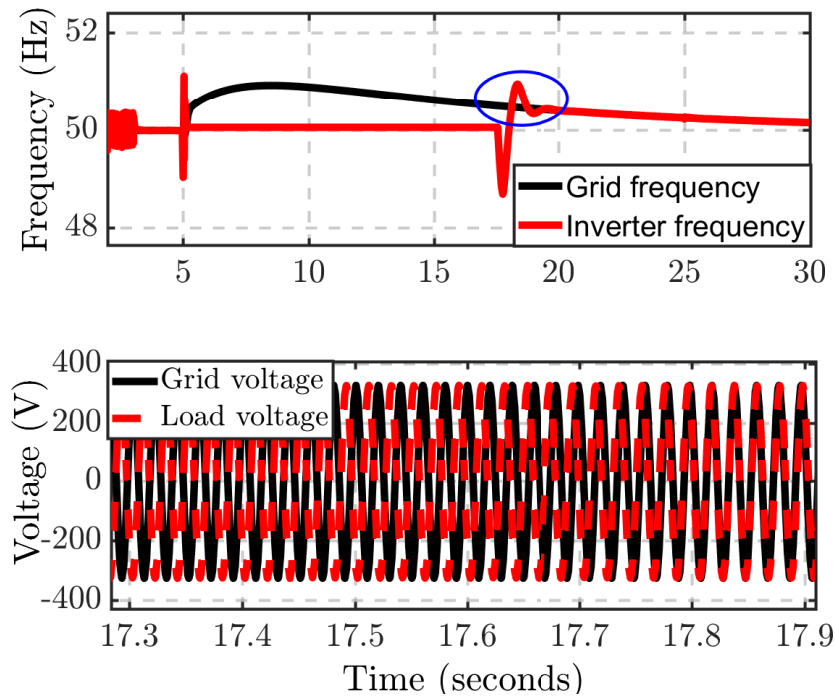


Figure 4.18: Active and reactive power reference followed even during fault scenario

Figure 4.15 and 4.18, shows that the grid connected and islanded modes of operation perform as intended. The Inverter is capable of following the references set by the load in both the grid connected and off grid modes, while keeping the voltage and the power delivery stable in both operating conditions.

4.4 Summary

In this chapter a new d-q control architecture is designed for a grid connected PV-battery system. Further a testing methodology of d-q control architecture is discussed for the proof-of-concept evaluation. The approach can provide tracking of the voltage and the power reference, in both the grid connected mode and the islanded mode. The inverter is also capable of transitioning from grid connected and off-grid mode, while maintaining the power references.

The seamless transfer capability is a new framework that allows a single control methodology for both on-grid and off-grid operation of the inverter. The approach

allows active power support during grid connected and off-grid mode which can be used as power source during blackout or to work as an uninterrupted power supply (UPS). The ability to transition from grid connected to off-grid mode will be useful for consumers in developing nations, where continuous supply of power from the grid is not available.

In the next chapter, a method is discussed for using this architecture to support active and reactive power simultaneously on an unbalance power distribution grid.

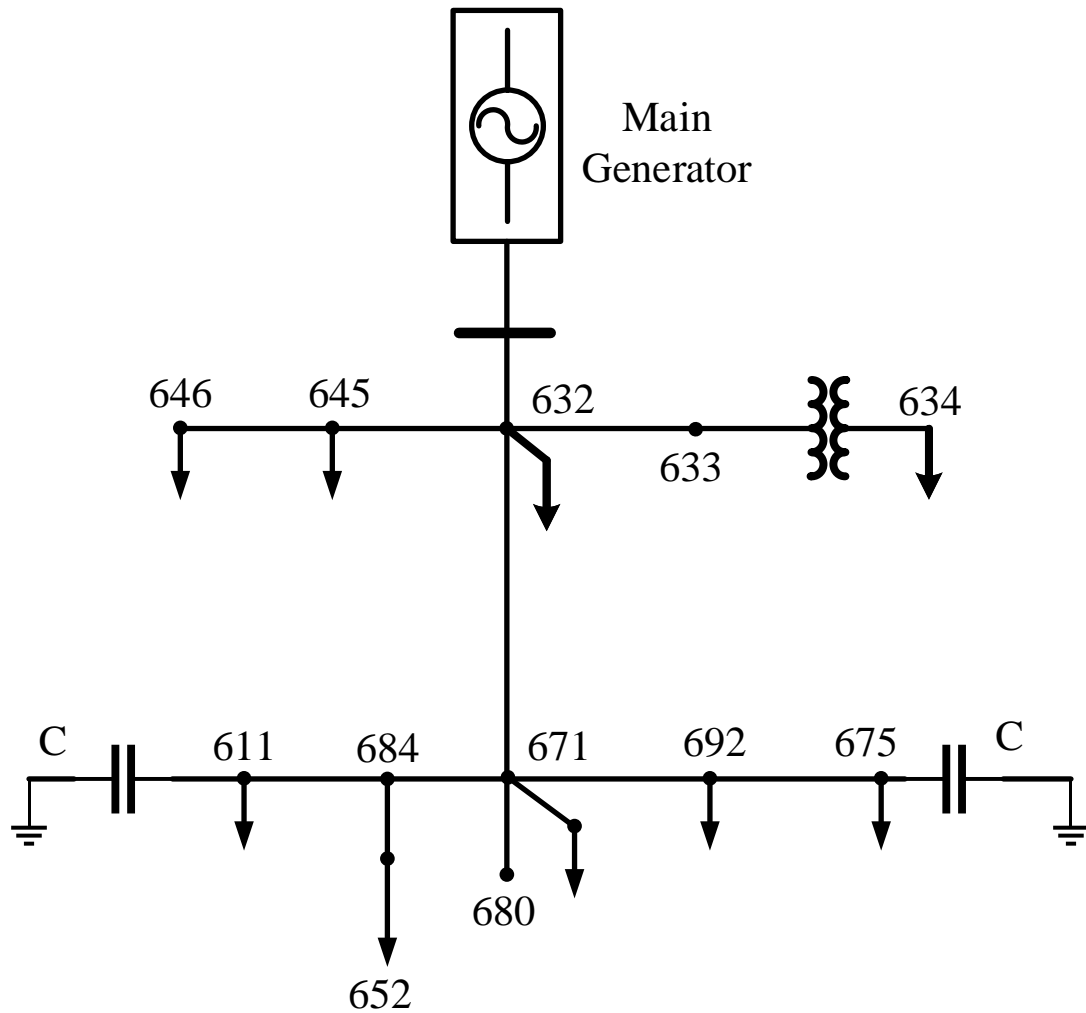
CHAPTER 5: ACTIVE & REACTIVE POWER CONTROL FOR GRID CONNECTED SINGLE PHASE INVERTER

In this chapter, active and reactive power control of grid connected unbalanced power distribution system is designed and presented. The IEEE 13 bus system is chosen to perform active and reactive power control in grid connected mode. The system is a distribution network with the rated power of the source at around 3MW. The chapter highlights the performance of the inverter in a large network and the ability to control to voltage at the point of common coupling by providing active and reactive power support at the weak bus.

5.1 Overview of the IEEE 13 bus system

The 13 bus system contains various loads, that require a certain amount of active and reactive power from the grid. This will mean that the voltages and the angles are dependent on the load's requirement on that bus. The best method to analyze the grid is to run a load flow. The load flow should reveal the weak and strong bus in the power system. There are nine loads connected to the system the values are mentioned in the table. The Figure 5.1 shows the one line diagram that contains the loads. There are nine loads connected to the grid. The load values are represented in the table. The maximum load connected to the system is the 485kW load connected to node 675. The peak load value in the system is about 3 MW. The active and reactive power drawn by the system, affects the voltage at the nodes. The resultant voltage analysis is called the power flow. The results of the unmodified 13 bus system is mentioned in Appendix A. For the ease in understanding the graphs in this chapter, the three phase quantities would be represented by the following colors as it is in the table. "Red" represents the Phase A quantity, "Green" represents the Phase B

quantity and "Blue" represents the Phase C quantity.



Node	Load Model	Ph-1	Ph-1	Ph-2	Ph-2	Ph-3	Ph-3
		kW	kVAr	kW	kVAr	kW	kVAr
634	Y-PQ	160	110	120	90	120	90
645	Y-PQ	0	0	170	125	0	0
646	D-Z	0	0	230	132	0	0
652	Y-Z	128	86	0	0	0	0
671	D-PQ	385	220	385	220	385	220
675	Y-PQ	485	190	68	60	290	212
692	D-I	0	0	0	0	170	151
611	Y-I	0	0	0	0	170	80
TOTAL		1158	606	973	627	1135	753

Figure 5.1: IEEE 13 bus Distribution Network

The total load connected to the system is 3.MW. There is additional power drop in

the transmission impedance. There is also an additional distributed load connected to the node numbered 632. The analysis presented in the appendix shows the power flow results. The load flow reveals the weak and strong buses in the system[60]. We can identify a weak and a strong bus, by the voltage and the amount of angle change is there, from normalcy. The study can also be done by placing a variable load and observing the change in the voltage at that particular node.

Hence, the IEEE 13 bus system needs to be modified to perform study on dynamics of the system and add the inverter.

5.1.1 Modified IEEE 13 bus system

The modified 13 bus system consists of variable loads connected to various points in the thirteen bus system. This updated system would be better suited to simulate the effects of variable loads in actual system.

The modified 13 bus system has been developed individually to perform different analysis. various modified 13 bus systems have been shown in each of the sections in this chapter.

5.1.1.1 Study of Weak and Strong bus

The first modification made to the 13 bus system is the replacement of 2 of the three phase loads in the IEEE 13 bus system. The constant load connected to node 632 and node 634 have been replaced with dynamic loads. The variation in the voltage due to the change in the load profile would assist us in identifying the weak and strong bus in the system.

The variable loads are fed with load curve data from an actual system. The load curve data from an actual system over a period of 15 hours. The 15 hour demand was compressed to a 48 second curve such that it can be simulated in MATLAB. The key point to take away is that the active and reactive power increases throughout the day, with maximum demand in the evening. From that point onward, the power

demand drops.

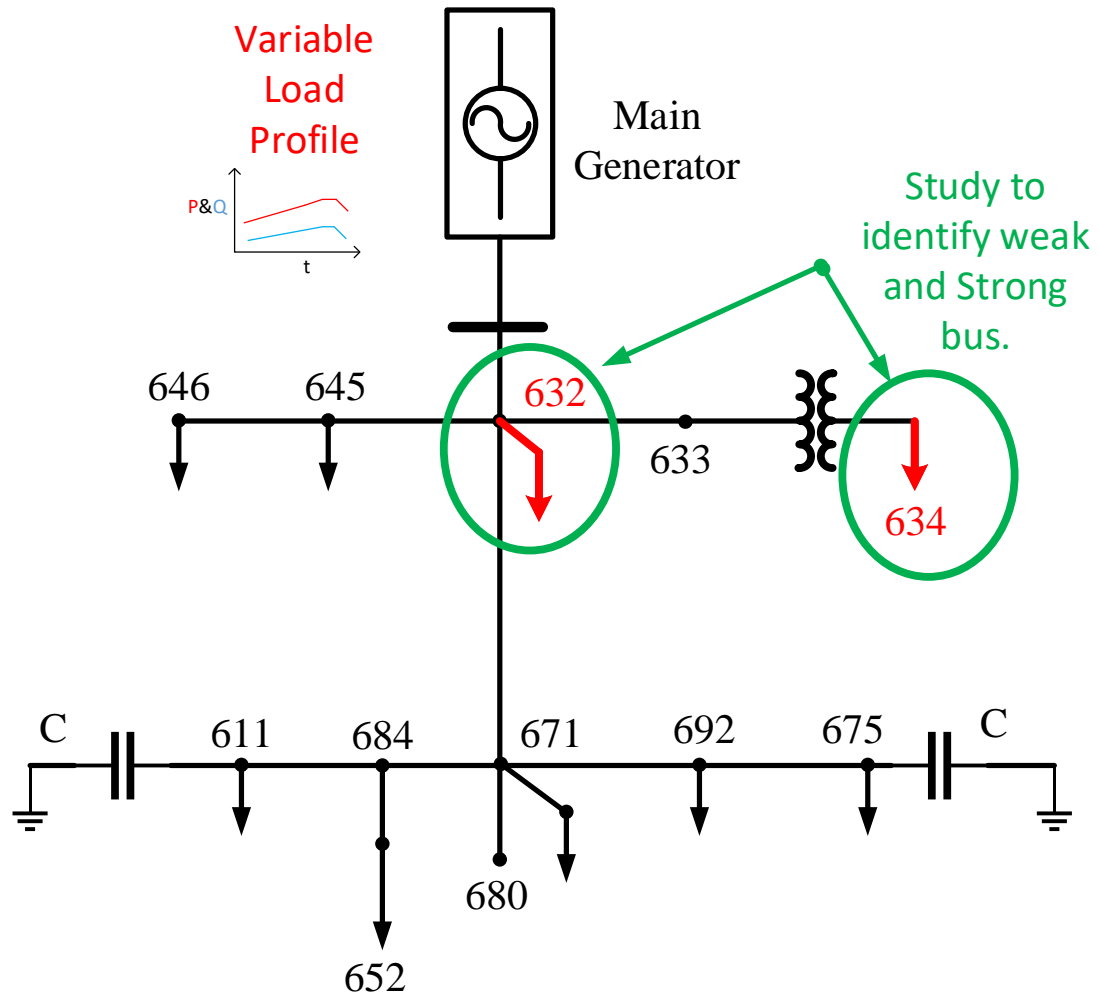


Figure 5.2: IEEE 13 bus is modified to study the effect of a dynamic load on the bus voltage

Figure 5.2 shows the modified IEEE 13 bus system for identification of weak and strong bus. The nodes numbered 632 and 634 are replaced with dynamic loads shown in the figure in red. The black arrows represent constant loads. The approximated load profile is shown in the top left corner of the figure. The voltage and dynamic load profile is observed for the two nodes. If the voltage variation is high, for change in the load profile, the bus is identified to be weak, but if the node voltage remains constant despite the change in load profile, the bus is said to be strong. The voltage

and power curves are presented as a part of this study and identification of the weak bus is performed, with explanation for the conclusion.

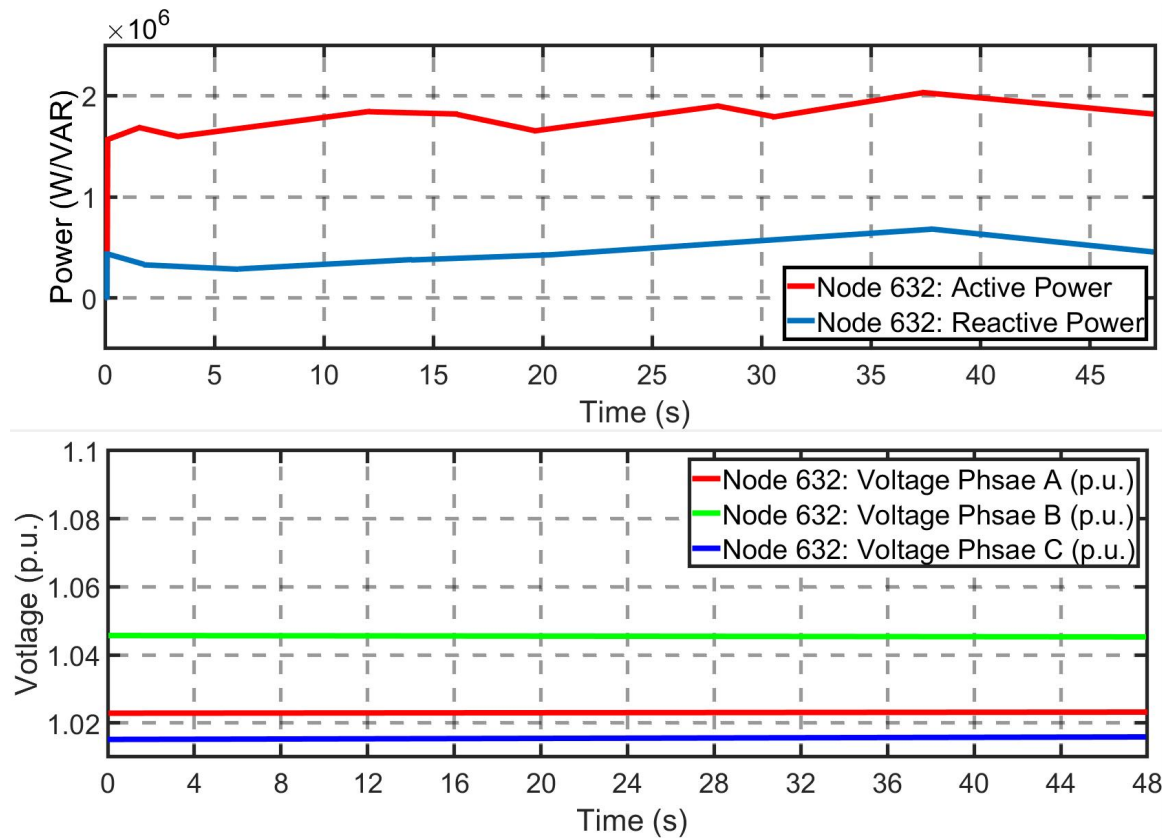


Figure 5.3: Dynamic Power and Voltage profile at node 632; Lack of variation in voltage suggests that node 632 is a strong bus

The voltage and dynamic load profile of the load connected to the node no. 632 shows that the voltage is quite stable for the changes in the active and reactive power demand. The steadiness in the voltage could also be due to the fact that node 632 is adjacent to the substation. Hence, the substation is capable of handling any local changes to the load profile. Figure 5.3 shows the load profile and voltage profile at a strong bus. The reason for the stable voltage in this particular node is since the node is connected directly to the substation. The substation is capable of maintaining the voltage constant for dynamic load changed in the local area. Perhaps a load change downstream from the substation would reveal a weak bus.

The next node to be studied would be the node numbered as 634. This node has a step down transformer, that converts the 4.16 kV to 230V (rms). The load in this bus is replaced by a dynamic load as well, a multiplication factor scales the power demand down to the operating range of the 13 bus system. The voltage profile of the node 634 shows that this is a weak bus, because the voltage change is quite significant in this node. The presence of a step down transformer is also convenient as it can act as an interface between the medium voltage and low voltage line.

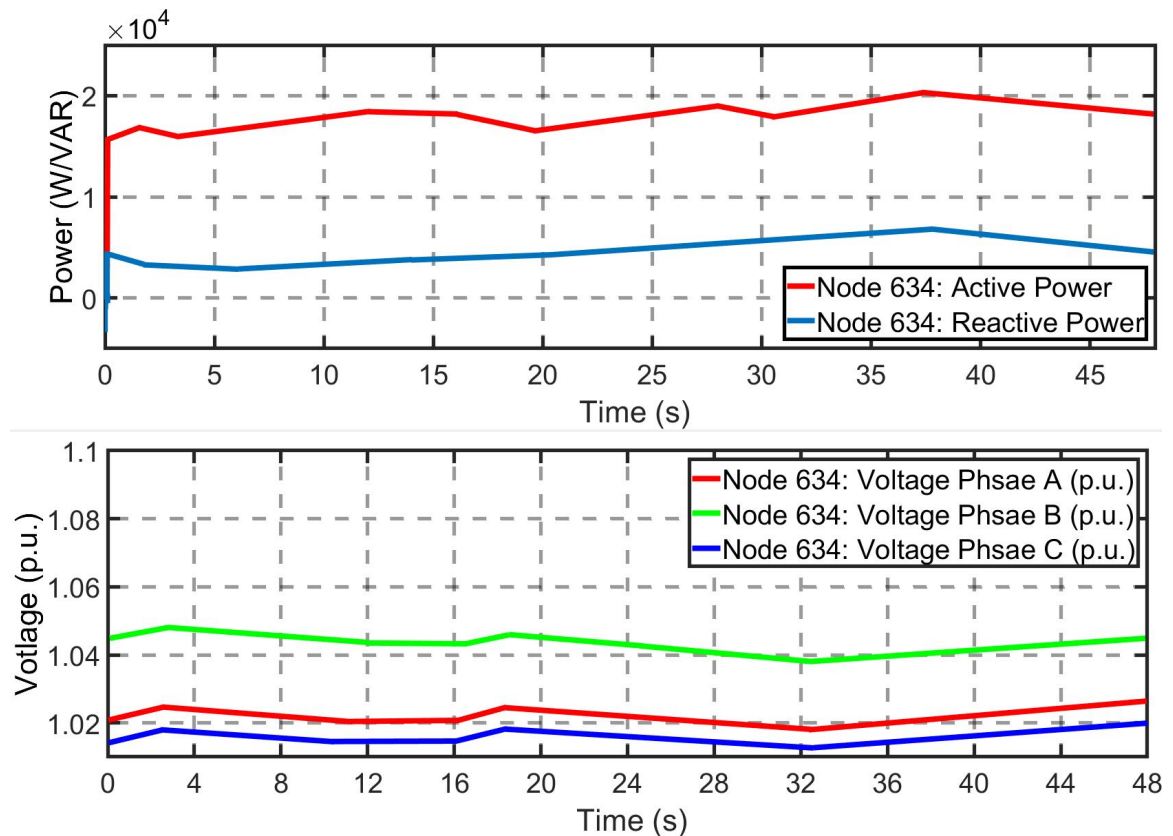


Figure 5.4: Dynamic Power and Voltage profile at node 634; Significant variation in voltage suggests that node 634 is a weak bus

Traditionally capacitors are connected to the system to control the node voltage. This however might not be possible in all the neighborhoods as the supply and demand varies and the control needs to be done by the power system, which is not welcomed in residential areas. Nodes 675 and 611 have capacitor banks that stabilize the voltage

in this system.

This theory is known as voltage support. This is a critical aspect of power systems today. In conventional systems, the voltage support is provided by large capacitor banks. These generally are placed in transmission systems, but they are present in distribution substations to increase the voltage to the rating of that particular bus. It is much rarer to see capacitor banks way down stream from the source, as the power engineers cannot support voltage from the customer's house. This could be averted by using the single phase inverter systems as the active and reactive power support capability will be capable of supporting the grid at the PCC.

5.1.2 Integration of PV-Energy storage system with the grid

The next step in the d-q control inverter's study would need to include the application of the d-q control inverter in the grid. The main ways to use the d-q control inverter would be to perform 2 unique tasks. The first being active power and reactive power management[61]. The other being frequency and voltage management.

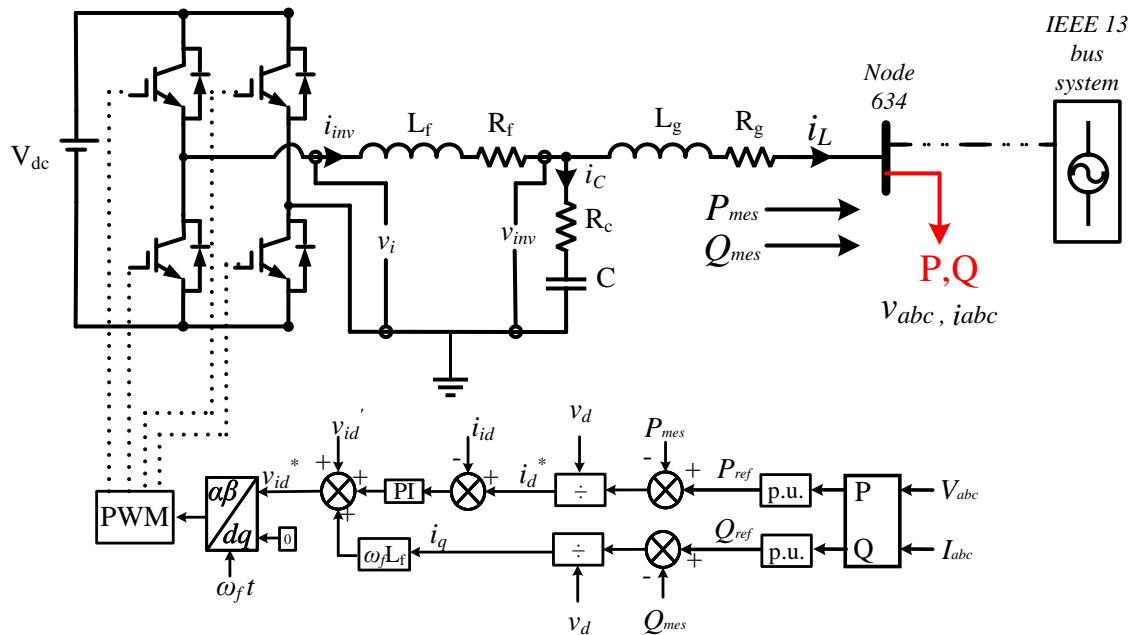


Figure 5.5: Inverter control methodology for interconnection with 13 bus system

The V_{dc} part represents the PV and Battery system. The red P and Q represents the dynamic load connected to Node 634, the the control methodology is also highlighted in figure 5.5. The v_d and v_q transformation terms are generated from v_{inv} and i_{inv} measured value. The subscript f and g represent the filter and grid quantities.

For active and reactive power management. The active and reactive power references are to be acquired from the load connected to the PCC. The active and reactive power references must be filtered, such that the inverter is capable of supplying active and reactive power only to the value it is capable of. Connecting a single inverter in one phase would have the capacity of 350W. But when multiple inverters are connected to the grid, in different phases, the power capacity of the system increases. For the story performed in the thesis, there are nine inverters connected to the grid, three in each phase. This would mean that each phase is capable of supplying about 1050 W of power, with the total power supplied, to be in the range of 3kW.

The inverter's inputs can be varied, such that the simulations are performed, such that the PV system has a variable reference, and the load can also be varied, such that active and reactive power demanded from the inverter is increased. This will be a part of the simulations that deal with the active and reactive power management of the inverter.

5.2 Active Power Management with Single Phase Inverter

For the first case, the active and reactive power management is simulated for a constant load and the performance of the inverter is evaluated. A large 3 phase load is switched on at 2 time intervals, once at $t=10$ seconds, functioning in the ON state for 10 seconds and again at $t= 30$ seconds, for another 10 seconds. With this analysis, we will be able to study the effect of PCC voltage and active power control of the local load. Using this analysis, we can perform the same task with the reactive power. The active power being drawn from the load is as follows. Two cases need to be studied. When the active power demand is greater than 2kW, the inverter is designed to assist

the grid when there is a sudden increase in active power demand. This would be beneficial for the weak bus.

5.2.1 Case 1: Study done for a constant 2 kilowatt Load at Node 634

The function of this test is to understand if the active power support from the inverter functions as theorized. For this particular case, the load at the node numbered 634, a constant load is created, such that the active power drawn from the grid is 2kW. The reactive power drawn by the load is zero, in this case.

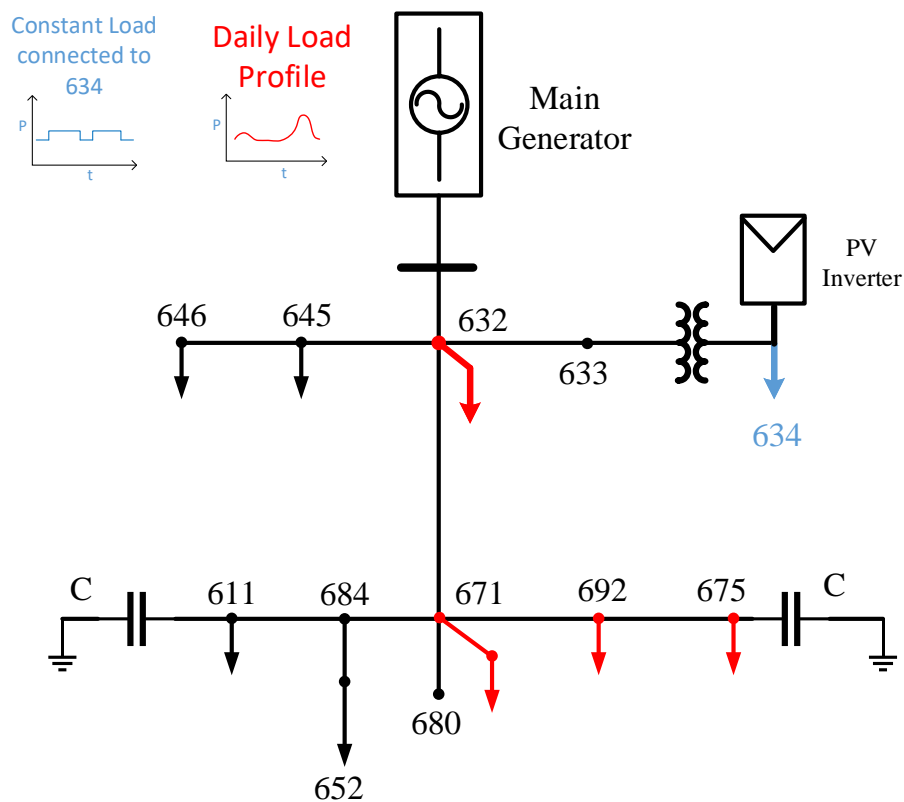


Figure 5.6: Modified 13 bus system; With constant active power load connected to Node 634

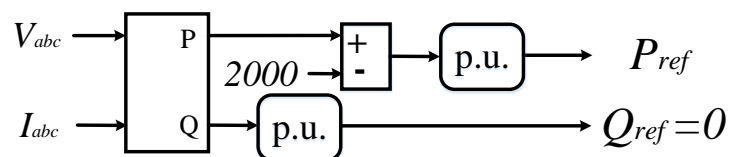


Figure 5.7: Active Power Reference Generated for the Inverter

The inverter is fed with the active power demand from the load, such that the inverter only supplies when the change in demand rises over the 2kW threshold. This is to simulate the effect of active power support when the demand is higher than 2kW and to get a preliminary understanding of how the active power change affects the voltage. This simulation would also assist in understanding how the inverter's support of active power would be able to reduce large changes in PCC voltage.

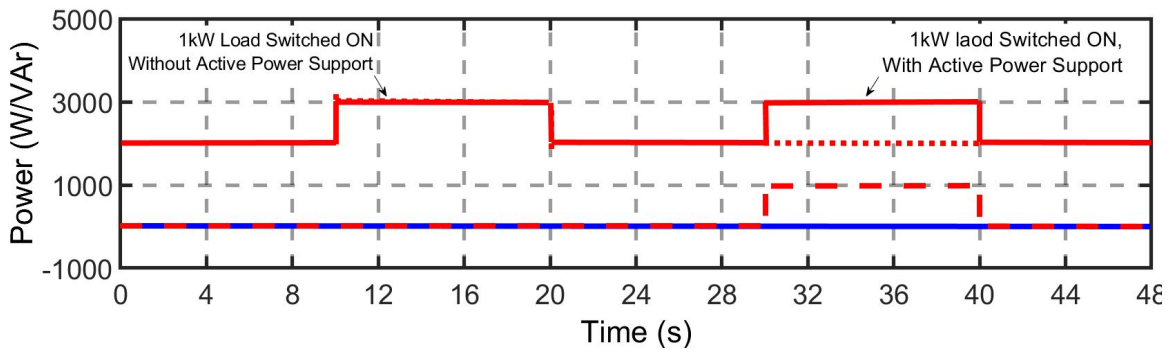


Figure 5.8: Comparison of power supplied by the inverter and the grid

Figure 5.8 shows the active power demand from the load, as the red solid line, the inverter's supply is shown by the dashed line and the grid supply is shown by the dotted red line. The reactive power drawn by the load is zero, which is shown with the blue line. The inverter supplies the 1kW demand, when the load demand rises. When the demand rises the first time, the inverter is disconnected and the grid supplies the power demanded by the load. When the load demand rises for a second time, the inverter is connected and it starts to supply the excess power demand.

It is the utility company's key task to maintain the power quality throughout the electrical system. This is to prevent large losses associated with variations in voltage and its effect on the insulation and the electrical equipment connected to the power grid. Although the utility company is responsible to maintain quality of power, it is also the energy consumers duty to support the grid. This role may be accomplished by the use of the grid tie inverter that can supply power to large local loads, to avoid adding undue electrical stress on the weak buses.

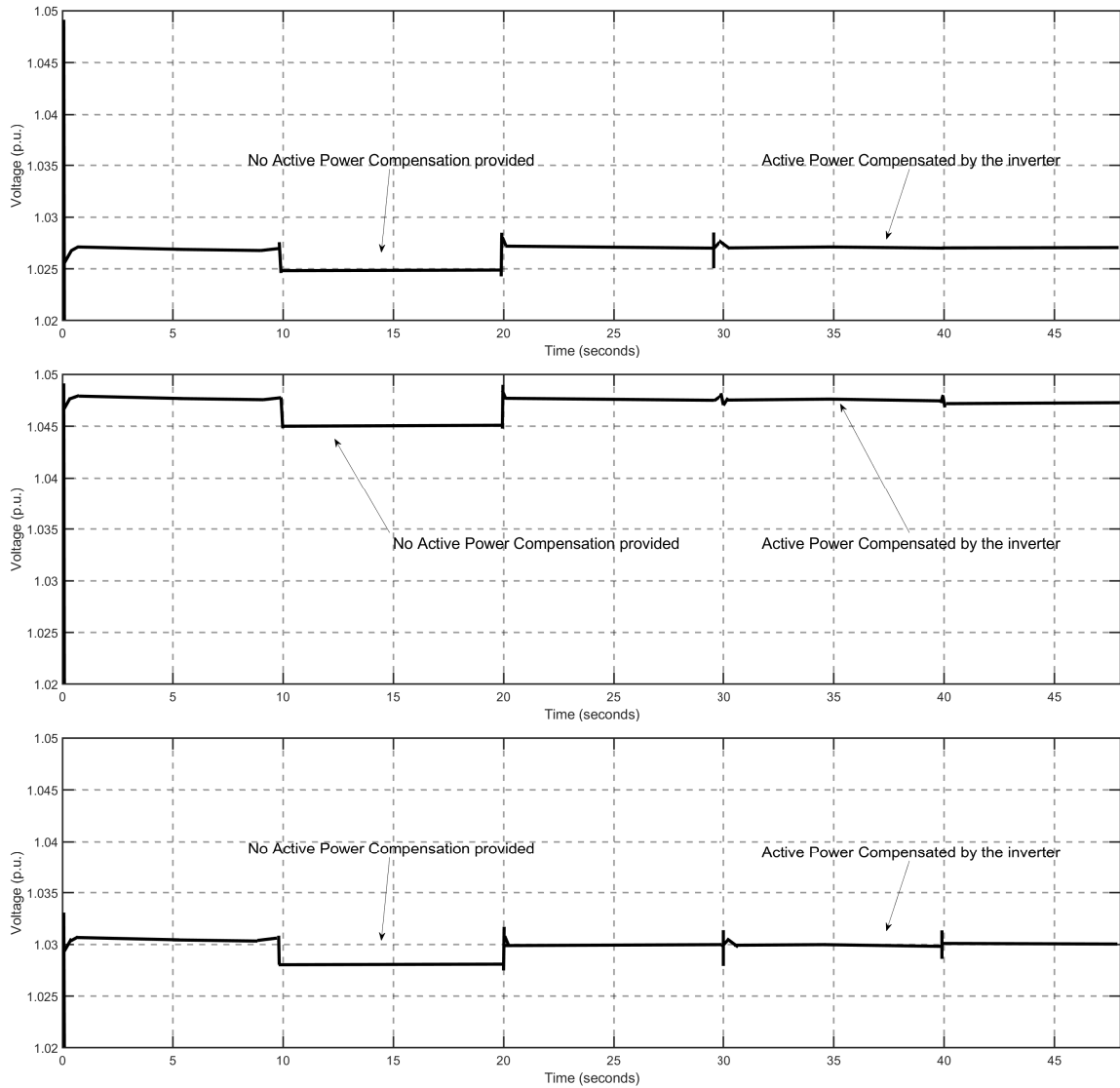


Figure 5.9: Effect of active power compensation on the PCC Voltage For Phase A, B and C

Figure 5.9 shows the effect of active power support of the single phase inverter in each phase. The inverter is able to stabilize the voltage. When the first step change occurs, the voltage drops considerably. This is mitigated when the inverter supplies the change in demand. The effect of the inverter is profound in this system and further studies need to be performed when there is a dynamic load at the PCC. The ability of the inverter to supply the load reduces the effect of a step change on the bus voltage.

5.2.2 Case 2: Study done for Varying Active Power Load at Node 634

In this case, the IEEE 13 bus system is modified to contain multiple dynamic loads connected throughout the system. The red arrows represent the location of the dynamic loads.

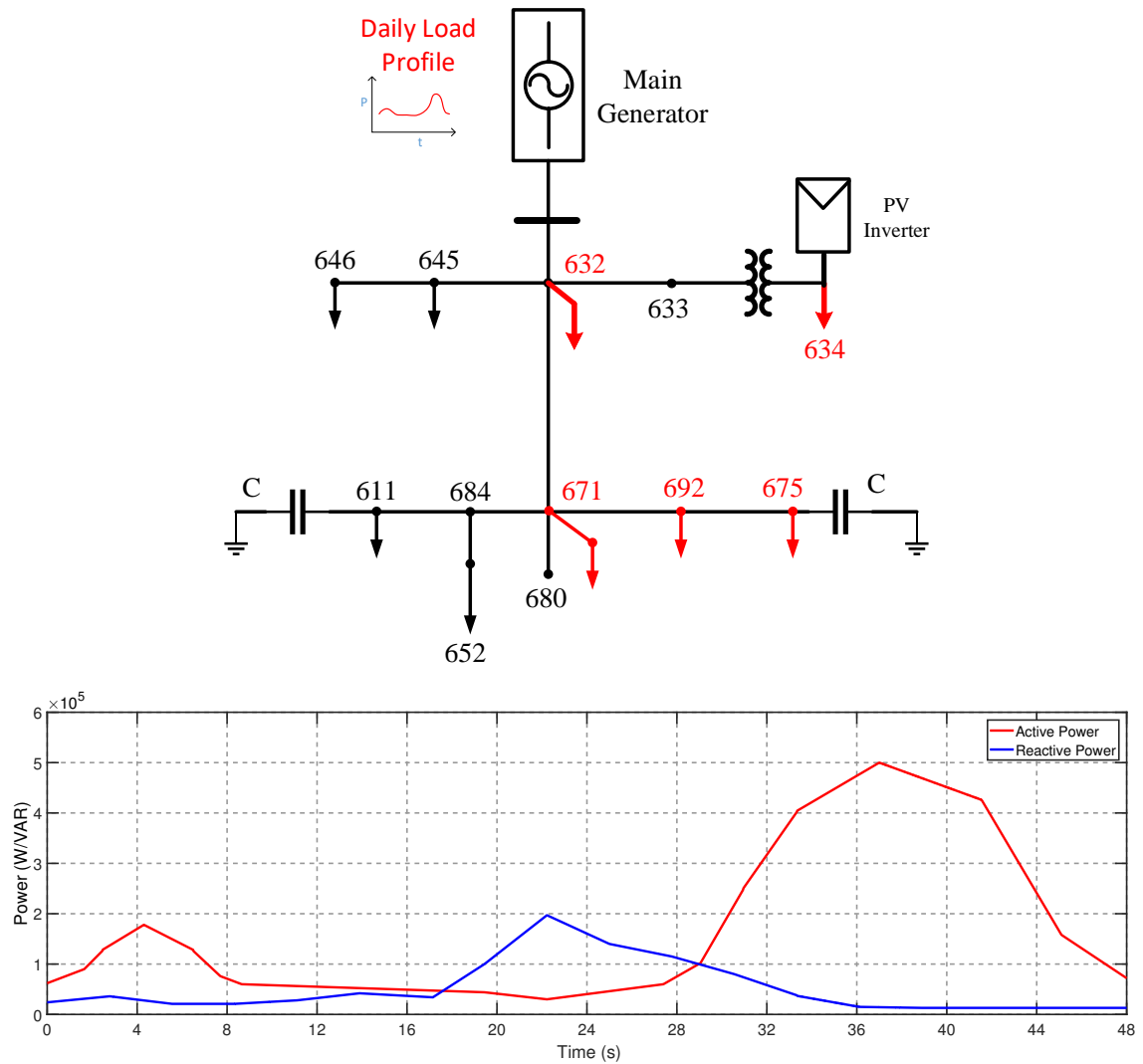


Figure 5.10: Modified 13 bus system; Load Profile for Dynamic Load

The grid supports the voltage as it does not have to supply the load. Case two deals with the introduction of a variable load connected to the PCC, with maximum power demand of 2kW, along with a step change of different values at different phases. Figure 5.10 shows the active and reactive power demand from the variable loads. A

multiplication factor helps us to scale the load to a similar value as the maximum loads in the actual 13 bus system. When the inverter starts to deliver the power to the load, the power supplied by the grid drops. The voltage at the Node 634 is balanced to study the effect of the active power support on a balanced node. Its effectiveness when the system becomes unbalanced is studied and the inverter's ability to balance the system by supplying active and reactive power at each phase is also studied.

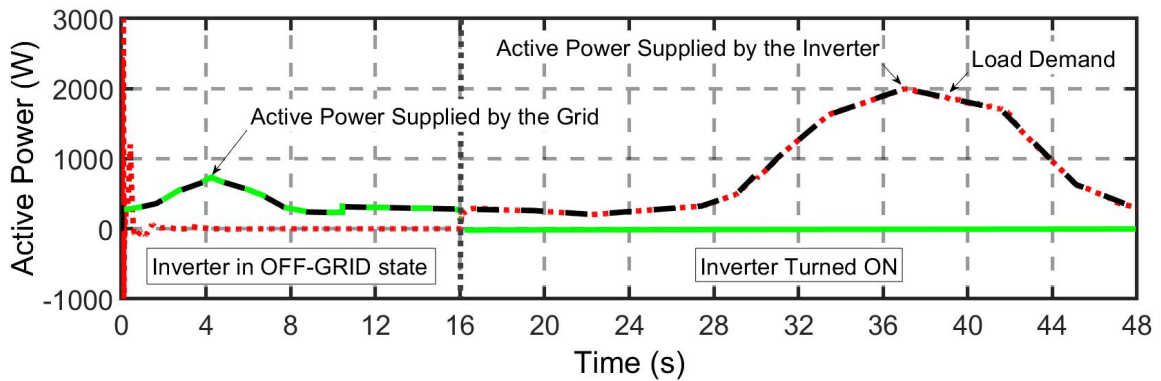


Figure 5.11: Load Demand shared between the inverter and the grid

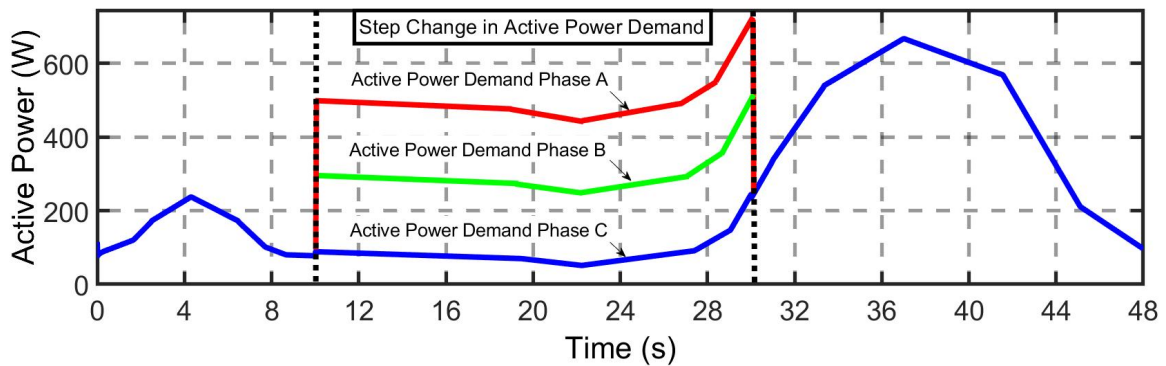


Figure 5.12: Active Power demand of the load in each phase increases to a different value, contributing to unbalanced voltage at PCC

Phase A has a step change of purely active power demand of 400W, while Phase B has a step change of 200W and Phase C has a step change of 25W. This step change is supplied between 10 to 30 seconds of the simulation. Figure 5.11 shows the active power sharing performed between the inverter and the grid. For the first 16 seconds, the inverter is disconnected from the grid. When the inverter is online, the grid does

not supply any power and the inverter is in-charge of supplying the load. Figure 5.12 shows the change in demand in each phase. Figure 5.13 shows the effect of the unbalanced nature of the load on a balanced network, and the inverter's ability to balance the network, by supplying the active power step change.

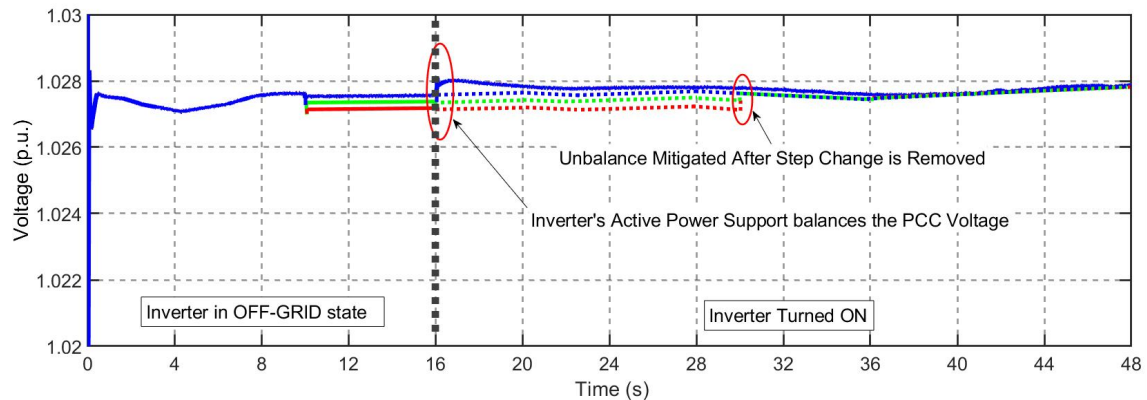


Figure 5.13: Effect of Active Power Support on balancing the voltage at the PCC

The voltage profile reveals that the difference in load demand affects each phase individually. So, the system changes from a balanced branch to an unbalanced branch. The dotted line in Figure 5.11, is the effect of active power of each phase on the PCC voltage, without the effects of the inverter. This was plotted by running the load flow and plotting the values of the voltage, based on the power demand in each phase at that instant. The introduction of the step change in active power affects the system and the voltage becomes unbalanced. When the inverter starts supplying the change in demand, the branch voltages become balanced. Between 10 seconds and 16 seconds of the simulation it can be seen that the voltage is unbalanced by a small amount. But when the inverter supplies the active power required by the load, the voltage becomes balanced.

5.3 Reactive Power Management with Single Phase Inverter

Reactive power support is performed by the inverter, in the following section. The Inverter is provided with the load's reactive power demand as the reference. This has

a similar effect to the active power support of the load, seen the previous section. Again two cases need to be studied. For constant and variable load change. The study is done to understand the effect of reactive power support on the voltage and the need for supplying reactive power to the grid, at the consumer end.

5.3.1 Case 1: Study Done for Constant 2 kiloVAr Load at Node 634

The function of this test is to understand if the reactive power support from the inverter is able to stabilize the voltage profile in a similar manner as the active power support.

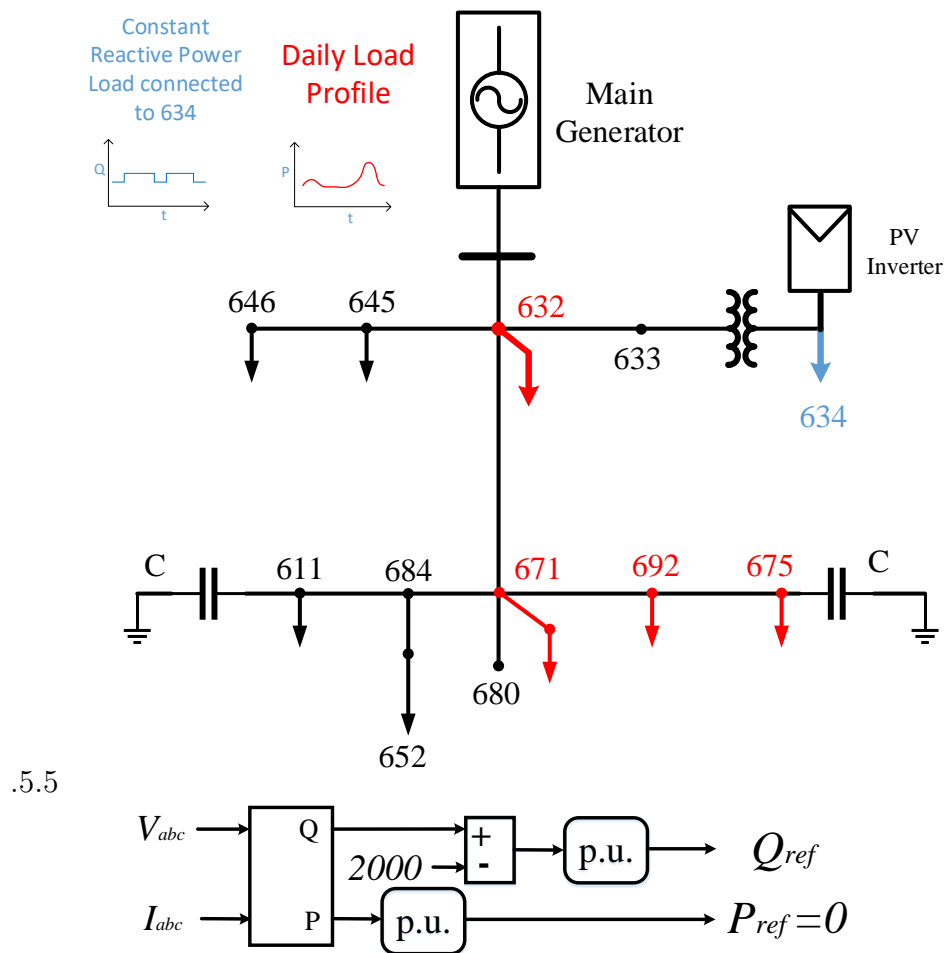


Figure 5.14: Modified 13 bus system with constant 2kVAr load at Node 634; the power references provided to the inverter is also shown

For this particular case, the load at the node numbered 634, is replaced by a

constant 2kVAr load. The inverter is initially disconnected from the grid. A step change in the reactive power is introduced such that the reactive power demand of the load increases, the inverter senses the increased reactive power demand and supplies the reactive power needed. In this particular condition, the load demands constant 2kVAr of reactive power. This is the threshold set for the inverter to start supplying the load. The inverter senses that the demand is lower than the threshold and does not supply any power. When the reactive power demand goes above the threshold, it begins to supply the reactive power.

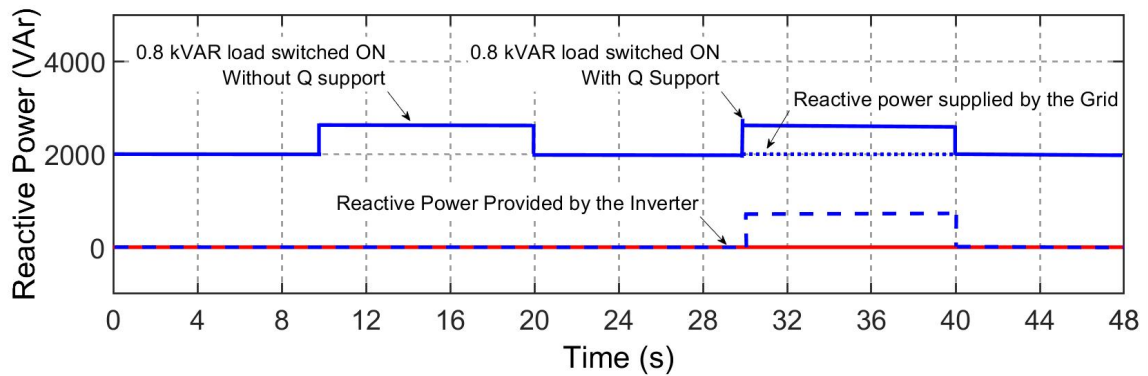


Figure 5.15: Reactive power support provided by the inverter for constant load of 2kVAr.

The step change in reactive power demand was created by connecting another constant load, such that the load is switched on at 2 time intervals. The first time the reactive power step change happens, the inverter is disconnected from the grid, to see the effects of the reactive power change on the voltage. When the reactive power step change happens for a second time, the inverter is connected and senses the change in demand and begins to support the grid, in supplying the increased demand.

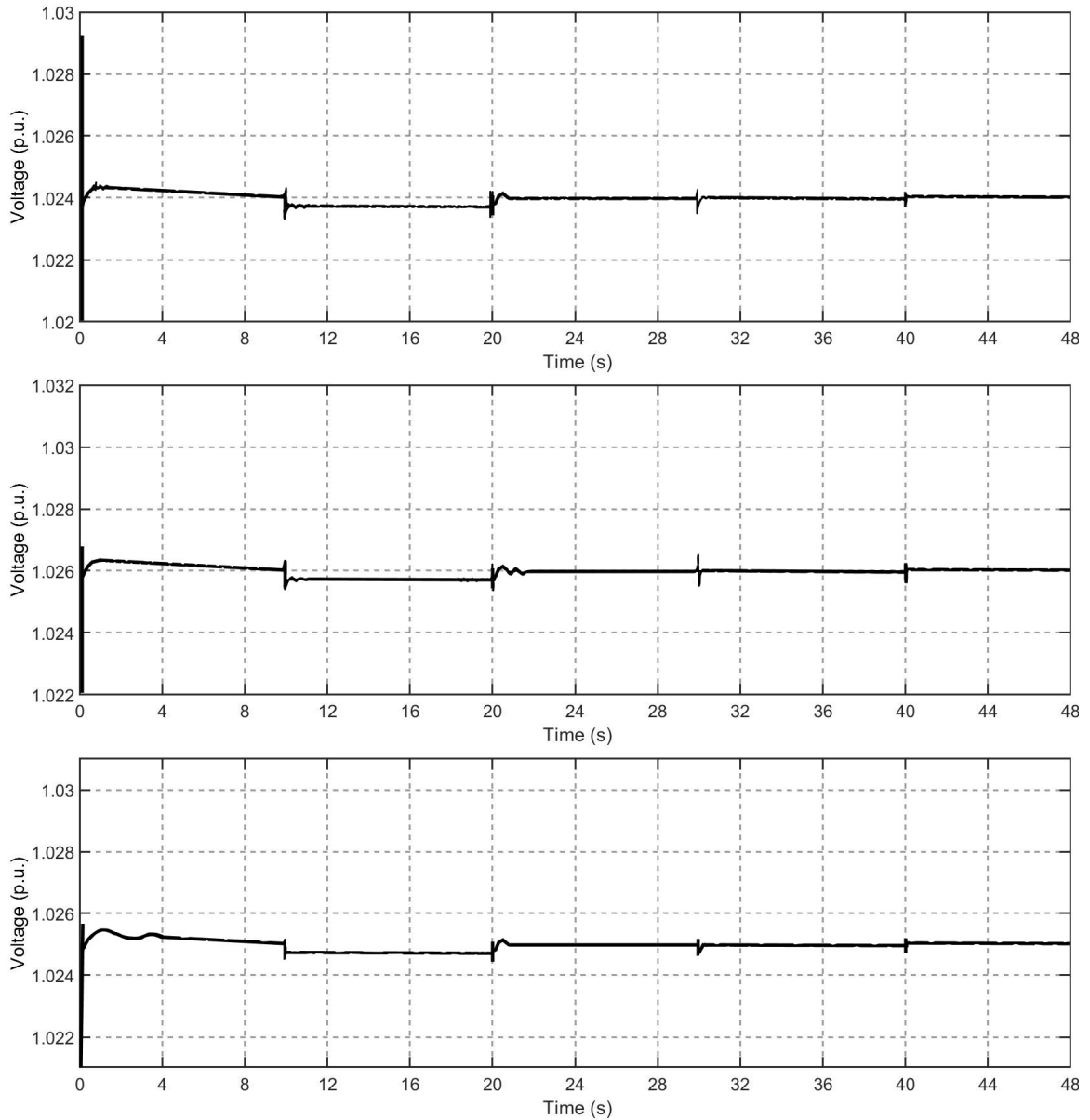


Figure 5.16: Effect of reactive power support on the PCC Voltage for Phase A, B and C

Figure 5.16 shows the voltage profile of the node. The effects on the voltage are similar to the study performed when a constant active power was provided to the load. The inverter's ability to supply the load in both the cases show that the tracking for active and reactive power is achieved in a large 13 bus distribution network, despite the unbalanced nature of the system. The voltage at the PCC is stabilized by the action of the inverter.

In this way, the grid voltage is maintained constant. If a load change happens beyond the capability of the inverter, the inverter will go on to supply the maximum possible value of the reactive power. This makes the inverter very robust and also reduces the demand placed on the grid to supply the power. This kind of operation will be useful in places where the grid is weak and needs active and reactive power support near the load.

5.3.2 Case 2: Study for a Varying Reactive Power Load at Node 634

This simulation deals with a dynamic profile of the reactive power. A step change is performed such that the reactive power demand in each phase is different. The purpose of the simulation is to show that the reactive power support provided by the inverter is capable of detecting an unbalanced load change and balanced the voltage.

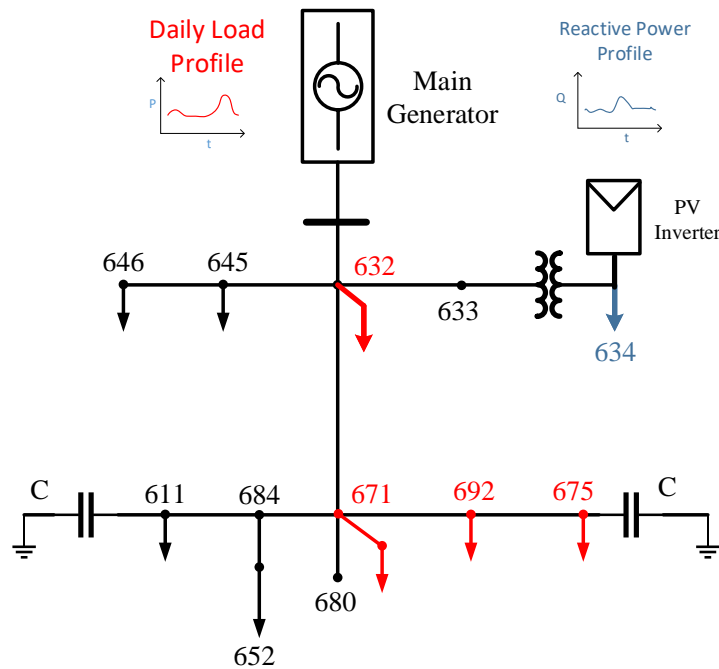


Figure 5.17: Modified 13 bus system with variable reactive power load connected at Node 634

Here, the inverter is disconnected from the grid for the first 16 seconds. When the inverter is turned on at the 16 second mark, the reactive power is supplied by the

inverter. The grid only tries to provide voltage regulation. The effect of the inverter, supplying the unbalanced load, can be seen when the bus voltage is observed.

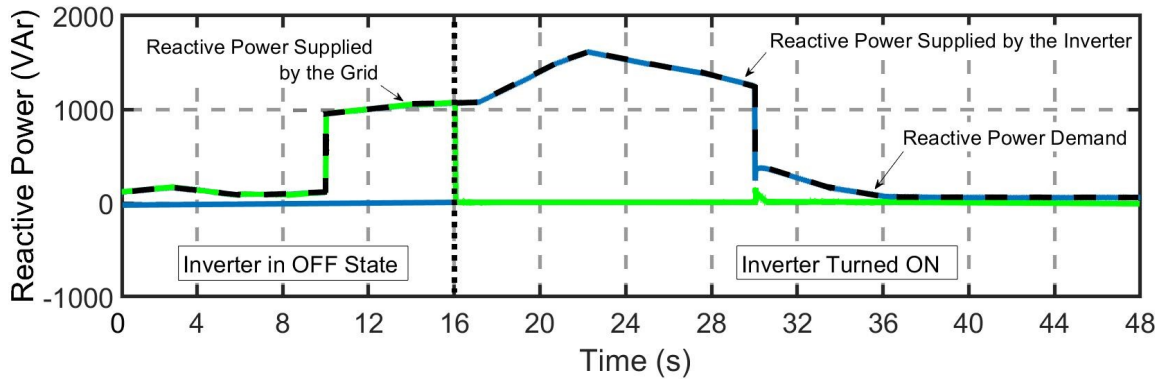


Figure 5.18: Reactive Power Demand shared between the inverter and the grid

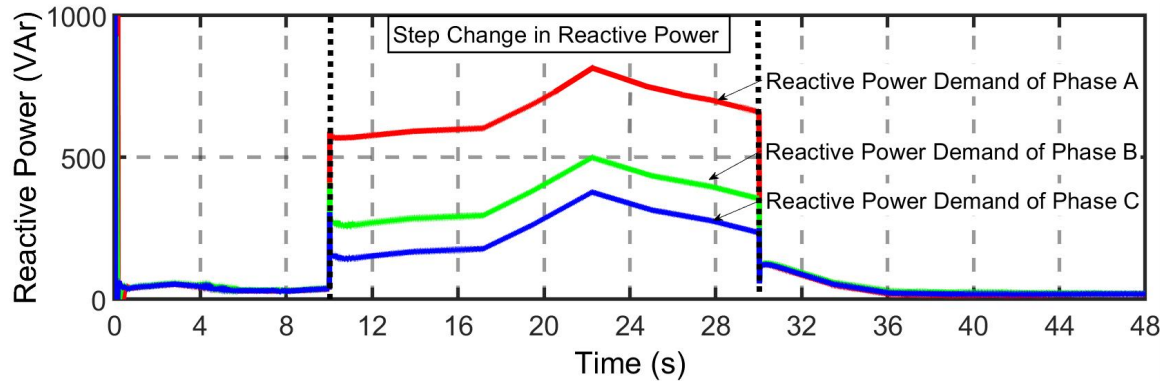


Figure 5.19: Reactive Power demand in Each Phase

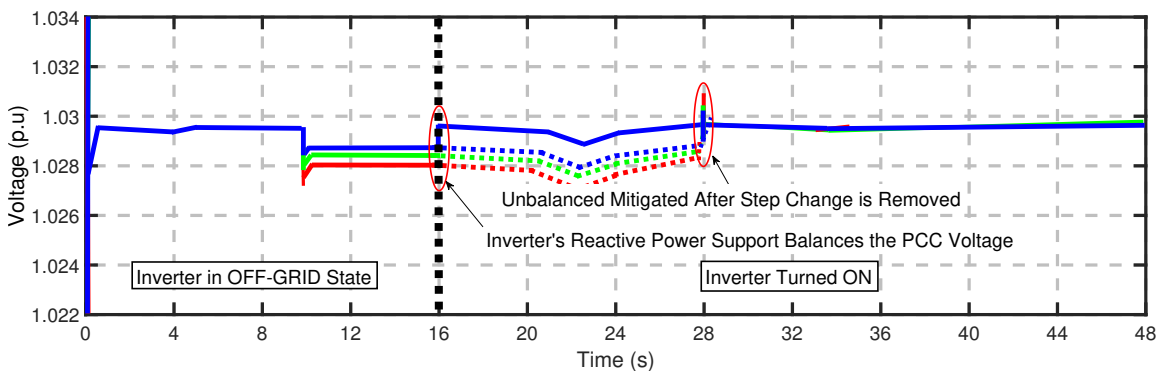


Figure 5.20: Effect of Reactive Power Support on the PCC Voltage

Figure 5.18 shows the reactive power demand shared between the grid and the inverter. The reactive power demand of the inverter rises between 10 seconds and 30

seconds. The inverter is disconnected from the grid between 0 and 16 seconds. After it is turned on, the light blue line shows that the reactive power demand is supplied completely by the inverter. Figure 5.19 shows the unbalanced reactive power demand in each phase. Finally, figure 5.20 reveals the effect of reactive power support in stabilizing the bus voltage.

Phase A has a step change of purely reactive power demand of 500 VAr, while Phase B has a step change of 200 VAr and Phase C has a step change of 25 VAr. This step change is supplied between 10 and 30 seconds of the simulation. The dotted lines in Figure 5.18 is the expected value of Voltage at the PCC, when the inverter does not supply the step change in power. This is plotted by using the Load flow results from the MATLAB code mentioned in Appendix A at every 1 second time-step. Although this is just an approximation, it shows the benefit of the inverter when performing reactive power support.

5.4 Active and Reactive Power Support Simultaneously

Now that the effects of the active and reactive power support of the inverter has been understood, the natural next step would be to perform active and reactive power support simultaneously. While the PV Arrays are fed with the irradiance profile of a sunny day.

The active and reactive power profile is similar to the shape in figure 5.10. The inverter again measures the active and reactive power demand from the load, to generate the power reference. The active and reactive power supplied by the inverter is limited by the apparent power limiter. The maximum power that can be transferred by the inverter is equal to the apparent power, which is given by the equation below:

$$S = \sqrt{P^2 + Q^2} \quad (5.1)$$

The Load's active and reactive power demand is shown in figure 5.21. There is a

step demand change between ten seconds and it falls back down at thirty seconds. The cumulative three phase demand is shown in Figure 5.23. The demand in each phase is different, and the three phase active power demand can be determined by the summation of the active and reactive power demand in each phase.

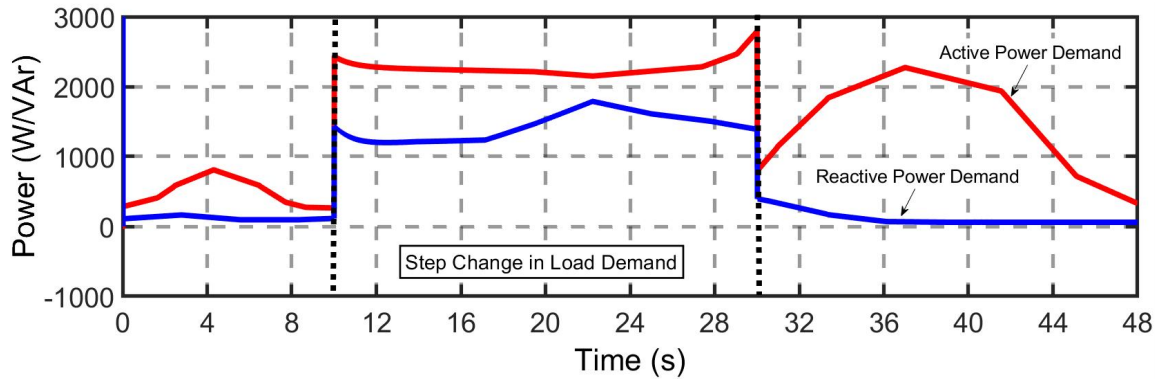


Figure 5.21: Three Phase Active and Reactive Power Demand

At 10 seconds the active and reactive power step change follows the following table:

Active and Reactive Power Demand In Each Phase		
Phase	Power	Value
Phase A	Active Power	100W
Phase B	Active Power	800W
Phase C	Active Power	900W
Phase A	Reactive Power	500 VAR
Phase B	Reactive Power	200 VAR
Phase C	Reactive Power	100 VAR

In this study the inverters is constantly connected to the grid. The inverter senses the load demand and just supplies that amount of power. If the load demand is higher than the capacity of the inverter, the grid supplies the excess power needed.

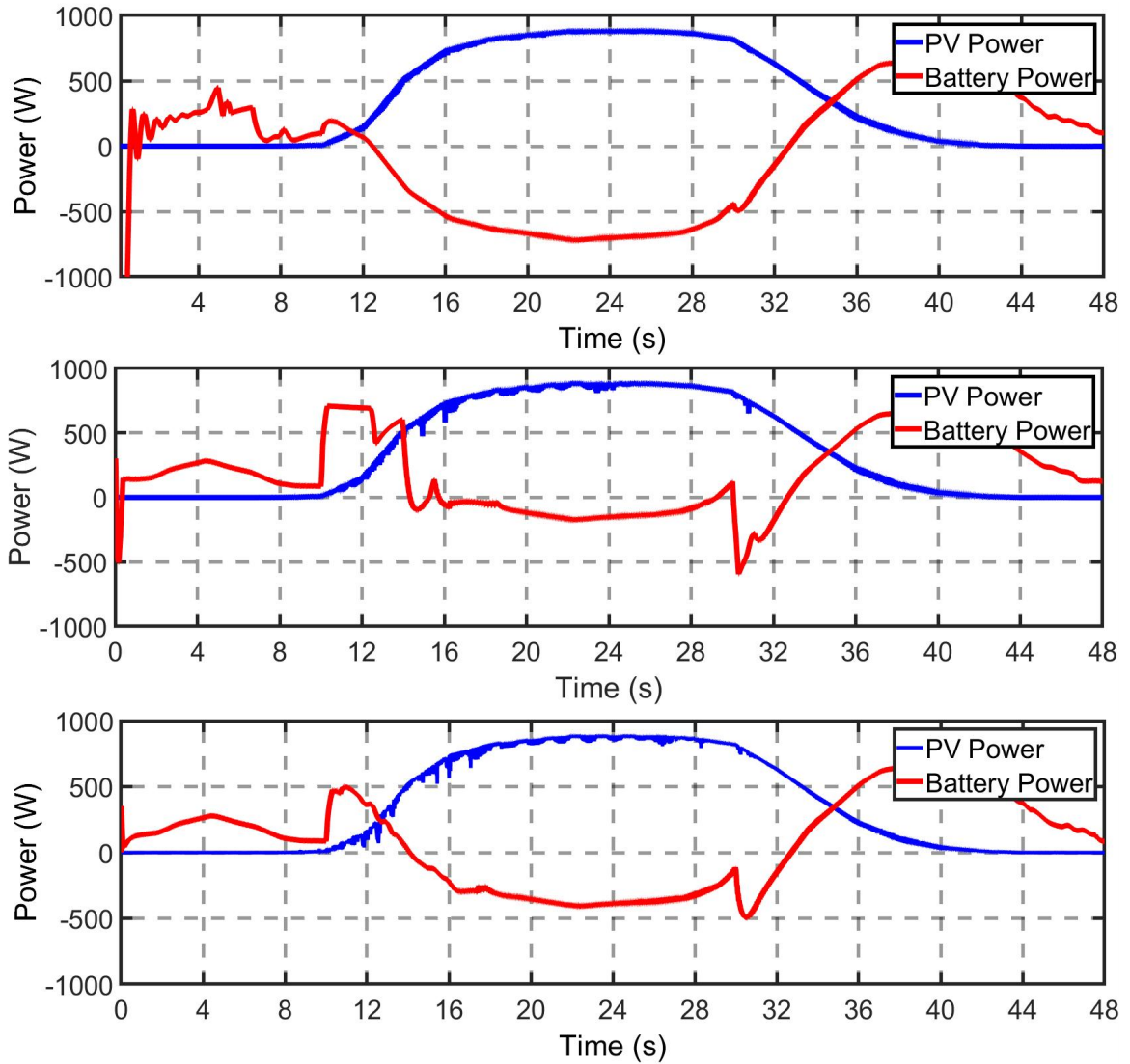


Figure 5.22: Power profile of the PV and the Battery

The PV and battery power is shown in figure 5.22, the power sharing between the PV and the battery when the PV irradiance profile varies is observed. The power shared between the battery and the PV, shows that it is stable. The inverter is also able to maintain the output voltage constant and perform normally, due to the constant DC bus voltage. This simulation shows that the elements of the DC bus works perfectly and that the power is being fed to the AC side.

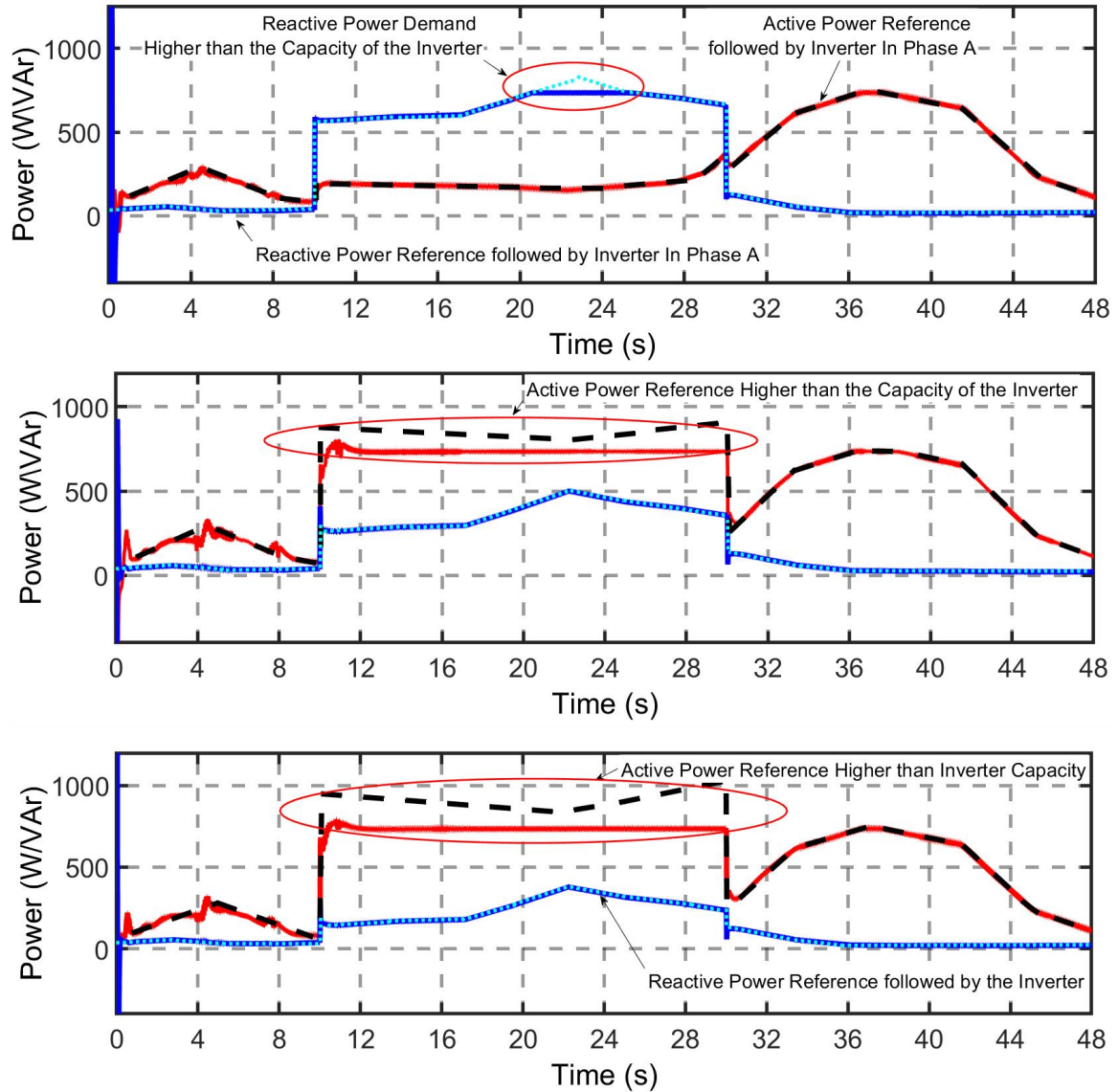


Figure 5.23: Inverter's Supply of Active and Reactive Power in each Phase

When the active and reactive power demand is higher than the capacity of the inverter, the grid supports the inverter in supplying the local load. But the effects of the voltage support provided by the inverter diminishes, as the load draws more power. The grid begins to provide the power to the load, if the inverter cannot supply power to the local load. The maximum power that the inverter can supply is about 350W, which is the apparent power. When the inverter supplies both active and reactive power, the amount of power supplied by the inverter is limited by equation

(5.1). The active and reactive power supplied by the inverter is shown with the red and blue solid line while the reference is shown by black and cyan dotted line. The plot shows the active power and the reactive power reference being followed by the inverter. In the Phase B and C, the active power demand is higher than the inverter's capacity, this excess power demand has an effect on the voltage at the PCC. This can be seen as a part of the voltage curve in each phase. When the inverter cannot supply the load, the grid provides the power to the local load. This kind of cutoff was designed using a saturation block that limits the active and reactive power reference based on the apparent power capacity of the inverter.

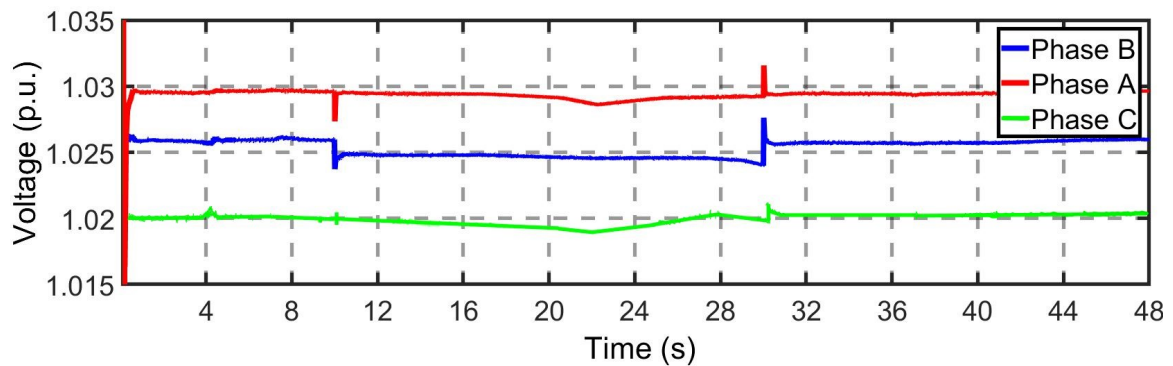


Figure 5.24: Voltage profile for all three phases at Node 634

The voltage in each phase, is maintained constant with the help of the active and reactive power following capability of the inverter. The voltage are unbalanced because of the unbalanced loads in other branches. The main takeaway from the voltage graph is that the active power and reactive power injected by the inverter greatly helps in maintaining the voltage constant. If the inverter is not able to supply the reactive power, then the deviation caused in the voltage is quite high.

5.5 Summary

- Method of control of power distribution grid with grid connected inverter is designed and tested on the IEEE 13 bus system.
- An approach to design the best location to place the inverter is proposed.

- A modified IEEE 13 bus system with grid connected inverter is designed.
- Three single phase inverters one on each phase of the power grid node is designed and connected to evaluate the active and reactive power support capabilities.
- Active power support is performed for a dynamic load connected to PCC. The effects of an unbalanced load change and the ability to stabilize the output voltage was also studied.
- Reactive power support was performed for a dynamic load connected to the PCC. the effects of an unbalanced load change and the ability of the inverter to stabilize the output voltage was also studied.
- A methodology for simultaneous active and reactive power support was performed with various PV farm output such as sunny day's PV profile, while maintaining the power when there is an unbalanced load change.

CHAPTER 6: DROOP CONTROL OF SINGLE PHASE INVERTER

The inverter's ability to supply the PCC with active and reactive power can manage the voltage and the frequency with reference to the point of common coupling. It would be useful if the inverters connected to a common bus could share active and reactive power such that the voltage and frequency are maintained constant if such a framework based on communication between inverters can be managed without the need for complex networks[62].

This chapter discusses a method of droop control between inverters connected to each phase of the power grid at the PCC. The architecture and simulation results are presented in this chapter.

6.1 Droop Control Introduction

Decentralized power management concept is how to generate a given amount of power distributed over smaller generators, rather than having a large generation system [63]. This concept is beneficial for security point of view, as a single attack cannot cripple the grid. It also leads the energy generation to occur closer to the loads. This means that there is lesser amount of power loss in transmission. The most valuable idea is that the power can be supplied even when the main power generators fail[64].

The biggest issue with this approach is the fact that a complex communication network must also be established such that the haywire generation does not cause havoc to the grid [65, 66]. This concept of DER has come into fruition with the increase in inverters and wind energy devices in the distribution system [67]. The future may consist of a large number of these inverter systems capable of supplying the loads and sharing power in the distribution system [68]. To avoid the problem

associated with the complex communication network, engineers have been hard at work trying to develop a method such that the power reference is dictated by the grid and the inverter supplies the required power [69].

In recent years, for the grid-tied mode, load sharing based on droop methodology has been widely utilized for active and reactive power control of electronically coupled three-phase distributed generator units. Single phase units have been neglected in this case [70]. This thesis will explore this topic in single phase grid tie inverters[71]. Since the control in this paper is based on d-q control which was derived from Clarke Transformation [72]. Droop control can be effective when used with such a system in grid-tied mode, subject to some means of communication between the converters being available [73].

Work has also been done on developing a Robust droop control such that power sharing is performed by limiting the current of the individual inverters. However there is a trade-off between droop based power sharing and voltage and frequency regulation. To perform droop control in a well regulated network, a method of introducing dynamic output impedance has been suggested. However there are drawbacks associated with that as well, as quite a large amount of power would be wasted while running in no-load condition [74].

The droop control presented in the thesis involves active power sharing between inverters using the droop equations to create the necessary active and reactive power reference. Although the droop control setup in the thesis is quite rudimentary, it provides a profound understanding of how droop control works and how it may be developed in the future to perform droop in both the active and reactive power domain.

6.1.1 Droop Methodology

The apparent power flowing into a network is described in the figure 6.1.

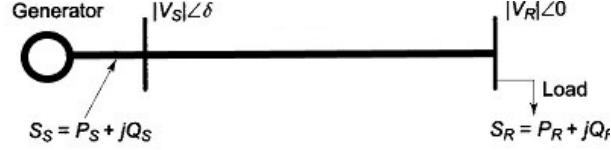


Figure 6.1: Flow of Apparent power

$$S = P + jQ = E.I^* = E.(E - V_g)/Z \quad (6.1)$$

Where S, P and Q are the apparent power, active and reactive power respectively, injected into the grid [75]. The E and V components are the voltage at the sending end and receiving end. ϕ is the phase angle between the distributed generators and the grid [76]. Then,

$$P = \frac{E^2}{Z} \cos \theta - \frac{EV_g}{Z} \cos \theta + \phi \quad (6.2)$$

$$Q = \frac{E^2}{Z} \sin \theta - \frac{EV_g}{Z} \sin \theta + \phi \quad (6.3)$$

$$Ze^{j\theta} = R + jX \quad (6.4)$$

The above equations can be rewritten as

$$P = \frac{E}{R^2 + X^2} [R(E - V_g \cos \phi) + XV_g \sin \phi] \quad (6.5)$$

$$Q = \frac{E}{R^2 + X^2} [R(V_g \sin \phi) + X(E - V_g \cos \phi)] \quad (6.6)$$

Since the system is connected to the distribution network, the resistance cannot be neglected in this above equation. Also, the power angle is small so, the assumption can be made that the cos terms are equal to 0. Then we get the following relationship.

$$\Delta P \propto (\omega_0 - \omega) \quad (6.7)$$

$$\Delta Q \propto (E_0 - E) \quad (6.8)$$

Where the ΔP and ΔQ terms represent the slope of the active and reactive terms. ω_0 and V_0 are the generator frequency and voltage amplitude. These equations represent 2 curves, known as the droop curves.

$$\omega = \omega_0 - m(\Delta P) \quad (6.9)$$

$$E = E_0 - n(\Delta Q) \quad (6.10)$$

Here, the m and n values are the droop coefficients and this relates to the amount of P and Q will be supplied based on the frequency and voltage of the system[77]. Here, the droop control is chosen as the control option when the inverter is in the grid-connected mode. In off-grid mode, the active and reactive power is supplied based on the requirement of the grid. This is true for rotating machines, this does not work for solid state devices like inverter. In order to obtain correct load sharing between the inverter and the network, it should be determined how the controller controls the inverter output. Analysis of the system reveals that the controller controls the voltage and frequency based on d-q control and this controls the current output[78].

It is critical for the difference in voltage to be zero for this droop controller to work. This is satisfied if the ratio of the active power droop coefficient is proportional to the output impedance. Also, to share real power effectively, the output impedance must satisfy

$$R_{o1} * S_1 = R_{o2} * S_2 \quad (6.11)$$

The equation above tells us that if the power capacity of the inverters are equal, then the output impedance must also be equal. If these conditions are not met, significant errors may occur in the real power sharing.

6.1.2 Droop in distribution systems

Unlike the transmission systems, where the droop equation is derived from, the X/R ratio is very different in the distribution side. The value of X/R in distribution

is dominated by both X and R. So, the droop equation must be rewritten with the variation in the effects of each of the components. The low voltage lines have a very high resistive effect as compared to an inductive effect present in the transmission systems. A proposed transformation that is popular today is to perform orthogonal linear rotation to create the new active and reactive power setpoints P' and Q' [79]. Hence, the equation for this is represented as follows.

$$\begin{bmatrix} P' \\ Q' \end{bmatrix} = T \begin{bmatrix} P \\ Q \end{bmatrix} = \begin{bmatrix} \sin \theta & -\cos \theta \\ \cos \theta & -\sin \theta \end{bmatrix} \begin{bmatrix} P \\ Q \end{bmatrix} = \begin{bmatrix} \frac{X}{Z} & -\frac{R}{Z} \\ \frac{R}{Z} & \frac{X}{Z} \end{bmatrix} \begin{bmatrix} P \\ Q \end{bmatrix} \quad (6.12)$$

This results in the following equation

$$\sin \delta \cong \frac{ZP'}{V_1 V_2} \quad (6.13)$$

$$V_1 - V_2 \cos \delta \cong \frac{ZQ'}{V_1} \quad (6.14)$$

So, by regulating P' , the frequency can be controlled, and by varying Q' , the voltage can be controlled. When the resistance of the line rises, the dominant term is $P' \cong -Q$ and $Q' \cong P$.

$$f = f_0 - k_p \frac{X}{Z} P - P_0 + k_p \frac{R}{Z} Q - Q_0 \quad (6.15)$$

$$V = V_0 - k_q \frac{R}{Z} P - P_0 + k_q \frac{X}{Z} Q - Q_0 \quad (6.16)$$

The new equations show that the frequency will be dependant on the real and reactive power as well as the ratio of the impedance in the line. It is sufficient that the ratio of the impedance is known, so the actual values of the resistance and reactance is not required[80].

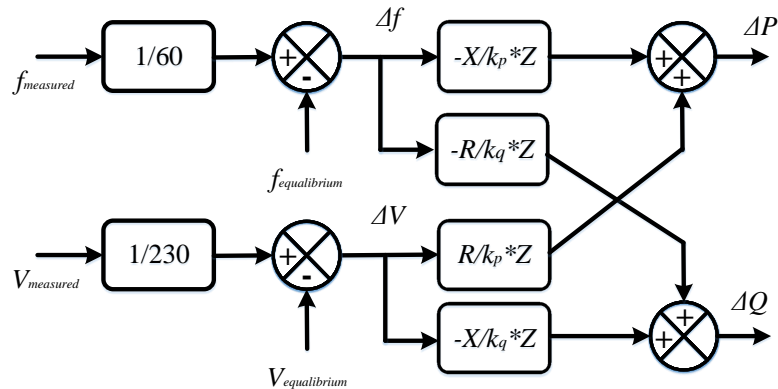


Figure 6.2: Implementation of conventional droop control

This is a simple form of droop control. This form of droop control may not work in a network with good voltage regulation. However it is possible to attain a simple active power sharing network with this form of droop control. The quantity $f_{equilibrium}$ and $V_{equilibrium}$ are the steady state quantity of the frequency and voltage at the current operating point. This value is taken from the filter inductance, as it is the best way to retrieve the operating parameters of the inverter. Else, the voltage regulation on the grid side would stabilize the voltage, which would adversely affect the droop control. The ΔP and ΔQ terms are then added to the P_{ref} and Q_{ref} reference provided to the inverters.

Since there is no voltage regulation present in this network, only active power droop is enabled. The reactive power loop is designed such that the output is zero.

6.2 Simulation overview

The 13 bus distribution system consists of 13 buses with 9 different loads connected to a three phase voltage source. The voltage source acts as an infinite bus and the point of contact to the transmission side[81]. This system, however the 13 bus system is a distribution network, with unbalanced loads. This turns out to be a good base point to start working on the inverter to grid connection.

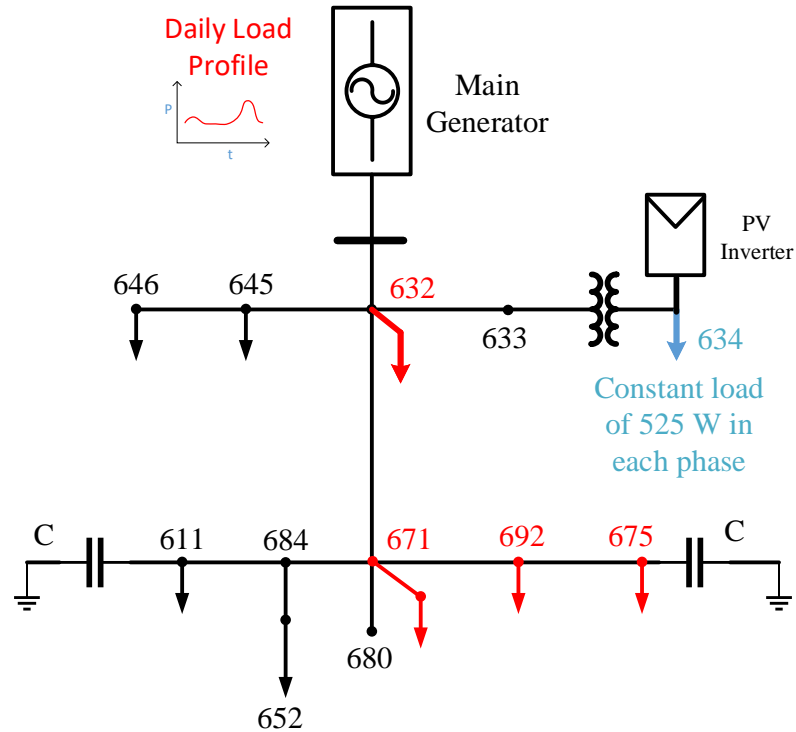


Figure 6.3: Modified 13 bus system to perform active power sharing; there are multiple PV inverters connected to each phase

The inverter model in this case cannot go off grid as it was in the previous chapter. That would be the next stage in the project. But this chapter goes to prove one important concept. The chapter uses the inverter to make the grid more balanced. The inverter performs this by supplying or absorbing a particular amount of reactive power so as to reduce the rms voltage to a consistent value.

The model had to be adjusted to work under the discrete mode of operation, as the original model was working in the phasor mode. Hence, the model's transmission lines were converted from the ti-line model to the pi-model. Now, the inverter is capable of connecting with the grid, as a part of the 13 bus system.

The load profile was provided to various three phase loads in the system, multiplied by a small factor to provide an output that was consistent with the capacity of the load. The PV was provided with the daily irradiance profile and the battery was supporting the voltage. There are 3 inverters in each phase, making the total number

of inverter to 9. Hence the capacity of the inverter system at the the PCC per phase will be 3 time 350W. Which is 1050W.

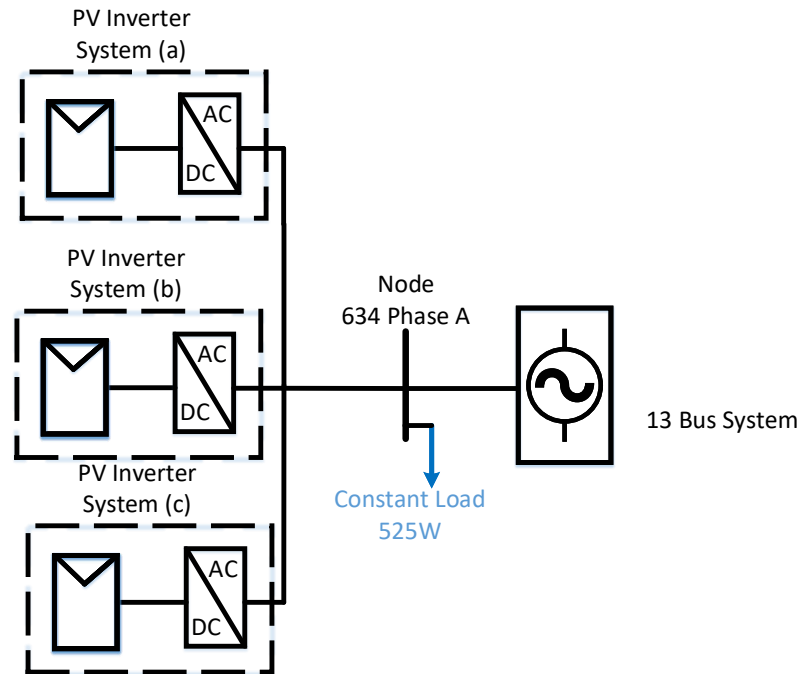


Figure 6.4: Inverter configuration in each phase, in Node 634

The test for active and reactive power droop control can be performed by limiting the capacity of each generator, while having a constant load. The active and reactive power reference for each inverter is initially 0.5 p.u. The multiple inverters connected to each phase share the power based on the droop coefficient calculations. When one of the inverter's output is limited, the other inverters supply the load and try to maintain the voltage constant.

6.3 Simulation results for Droop Control

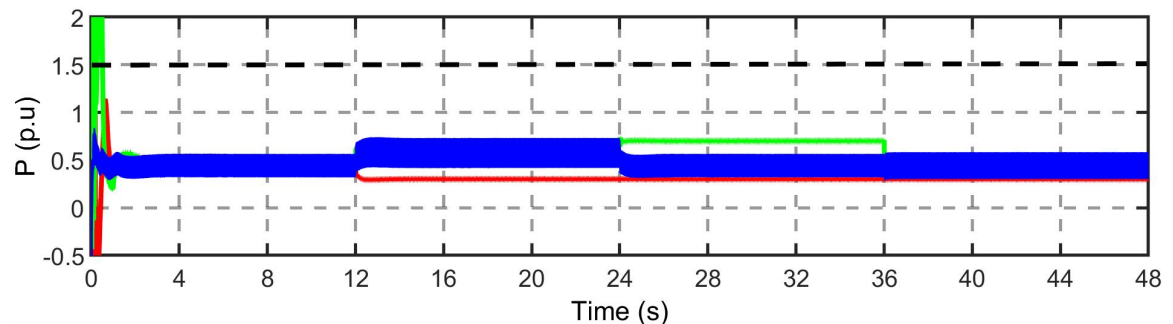
The simulation is performed to realize active power sharing among the multiple inverters connected to the point of common coupling in each phase. A constant active power demand is generated by the load, with reactive power demand kept at zero, in each phase. The active power corresponds to 50% of the operating capacity of the three inverters connected to each phase. The objective is to have the inverters

supply equal amounts of active and reactive power to the load, when all the inverters operate. Meaning that the load demand is shared equally among the inverters.

When the active power supplied by an inverter decreases, the droop control should be able to change the active power reference such that, the load demand is sufficiently supplied. This test should be able to measure the variations in frequency and voltage, and vary the power reference. to reduce the power supplied at a particular inverter, the active power or reactive power reference is replaced by a constant value.

Active and Reactive Power Demand In Each Phase		
Phase	Power	Value
Phase A	Active Power Demand	525W
Phase B	Active Power Demand	525W
Phase C	Active Power Demand	525W

The cumulative voltage and frequency of the PCC should be constant. But the frequency and voltage at the output of the inverter will vary because of the active power and reactive power supplied.



Time	Active Power Reference at different Time-steps			
	0 to 12	12 to 24	24 to 36	36 to 48
Inverter (a)	0.5	0.3 (Forced)	0.3 (Forced)	0.3 (Forced)
Inverter (b)	0.5	0.6 (By droop)	0.75 (Forced)	0.5 (Forced)
Inverter (c)	0.5	0.6 (By droop)	0.45 (By droop)	0.5 (Forced)
Total	1.5	1.5	1.5	1.3

Figure 6.5: Droop control in Phase A between three inverters.

The black dotted line represents the active power demand of the load in each phase. The inverter needs to add up all the powers of the individual inverters to properly

sustain the power demand. If the inverter is unable to supply the active power, the grid will take over and supply the load.

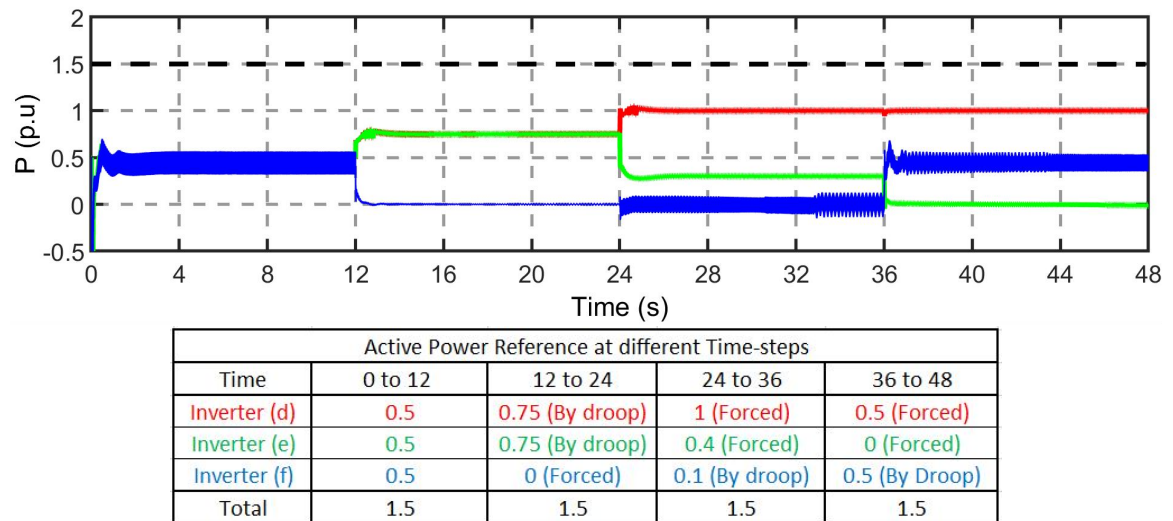


Figure 6.6: Droop control in Phase B between three inverters.

The oscillations created in the third inverter is probably due to the wobbling voltage and frequency.

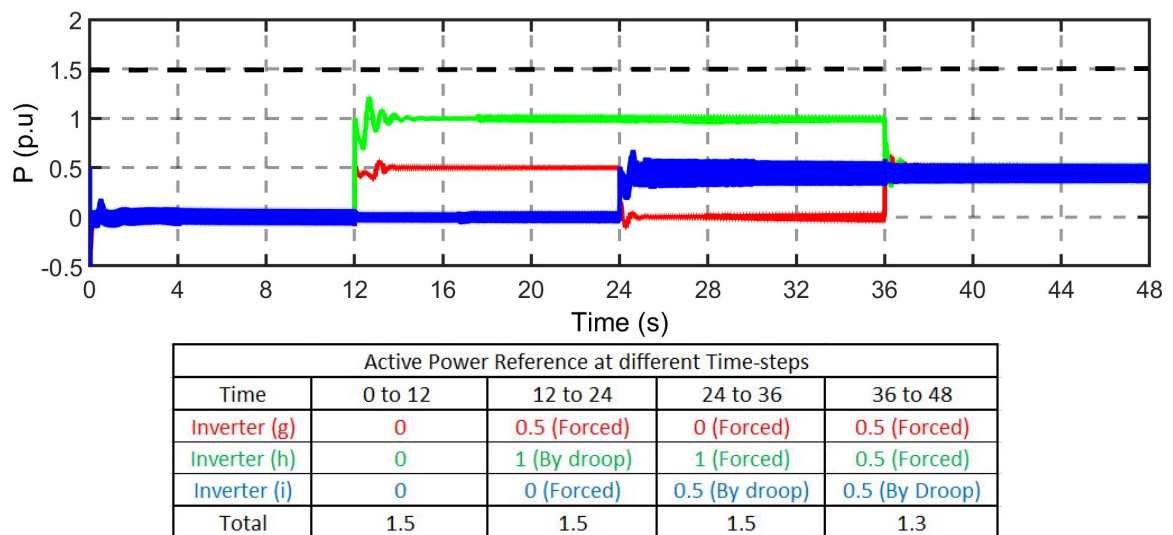


Figure 6.7: Droop control in Phase C between three inverters.

There are three inverters in each phase, which measure the voltage and frequency at the filter. The inverters also keep track of the active and reactive power demand.

Figures 6.5 to 6.7 show the active power sharing performed by each of the inverters in phase A, B and C.

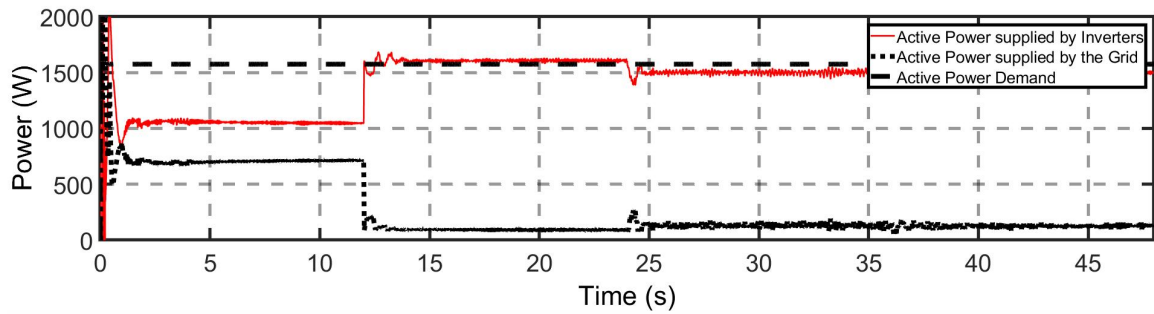


Figure 6.8: Active Power shared by the inverters and the grid

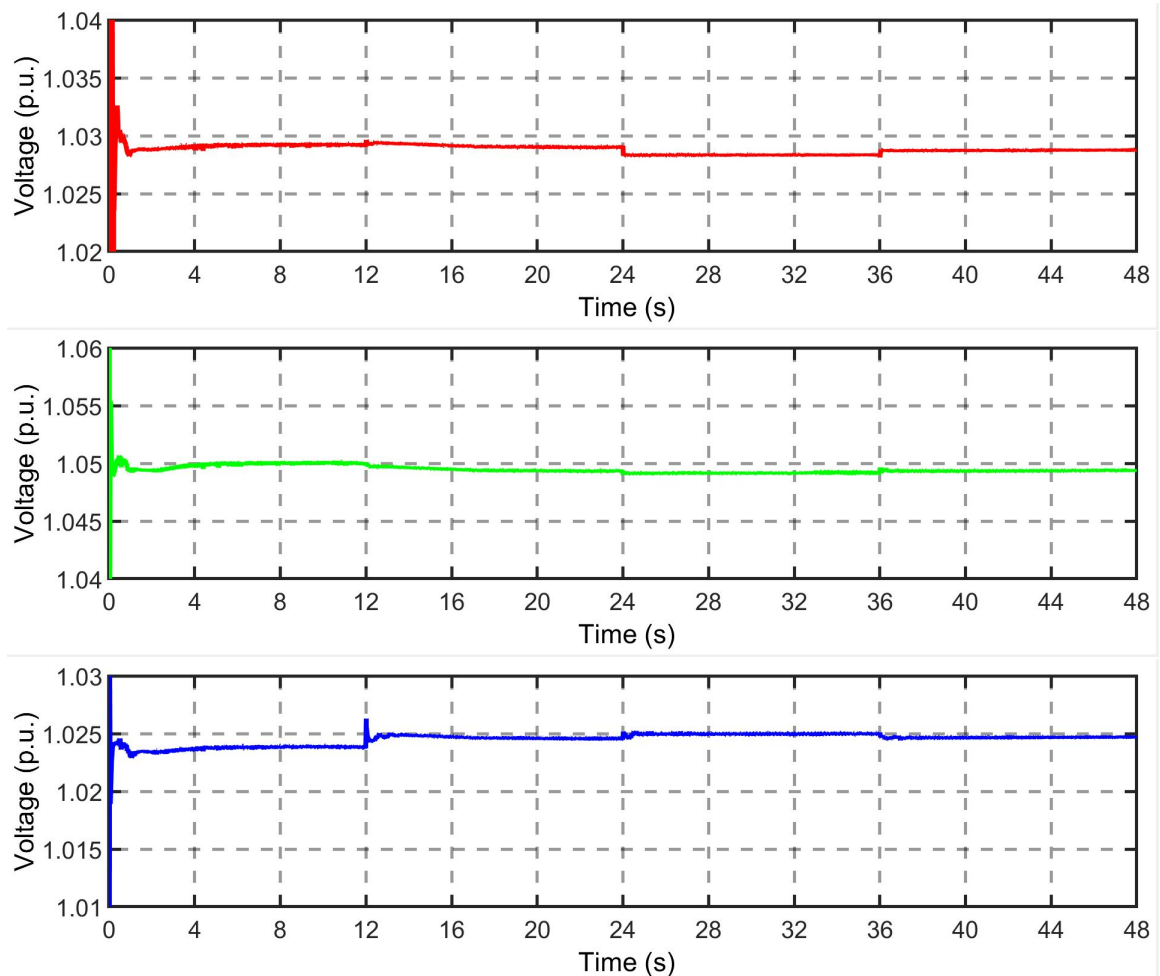


Figure 6.9: Voltage at Phase A, Phase B and Phase C, while performing Droop control

Figure 6.8 shows the active power shared between the inverters and the grid. The

grid supplies 50 % of the power in the beginning as the inverters in phase C are forced to deliver no active power to the load.

The voltage at the PCC was measured as shown in Figure 6.8. The change in active power supplied by the inverter affects the voltage slightly. This is probably due to the fact that the amount of power supplied by the inverters in each phase changes. The small change is due to the size of the inverters also, if the size of the inverters were large, then the effect of the changing power reference would greatly affect the voltage and frequency.

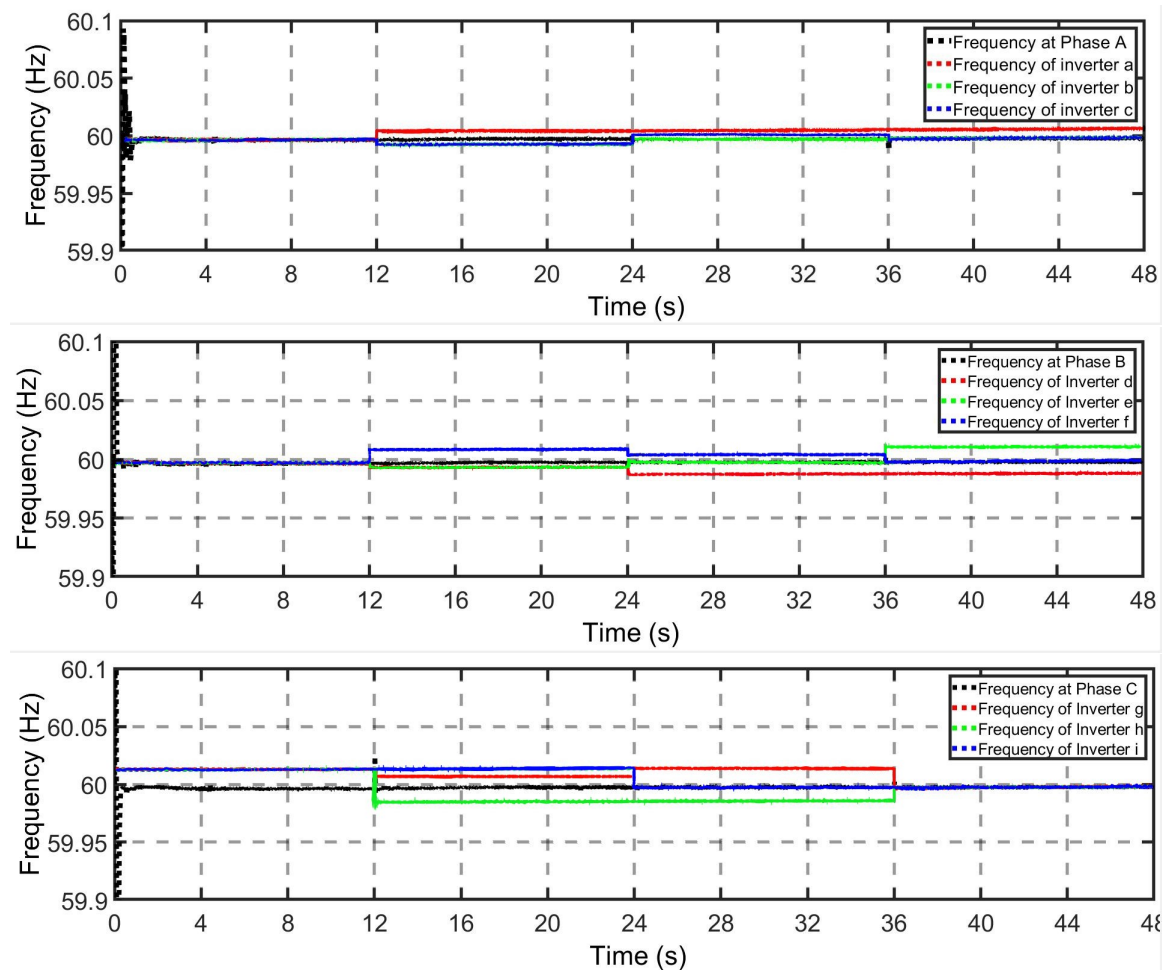


Figure 6.10: Frequency variation caused by the variation of the inverter Power output.

Since the network is modelled as a distribution system, the ratio of the reactance over the resistance is high and hence, causes a coupling to develop between the power

and voltage as well. This may also be the reason for the instability of the reactive power droop control. The coupling makes it difficult for the users to really determine the reactive power needed for stable operation of the droop reactive power control loop.

The frequency change is profound and enough to change the power set point of the inverter. The frequency change is inversely proportional to the change in active power. The reactive power output of the inverter is very wayward and needs better tuning to perform droop control in both the active and reactive power domain.

The droop control and active power sharing can be concluded as reasonable power sharing is achieved. This is the simplest form of droop control and is quite rudimentary. A more complex form would be the active and reactive power sharing between inverters in a network with good voltage regulation.

The variation in active power supplied by the grid in Figure 6.6, can be seen in the power delivered by the substation. This variation in the power at the substation end is another positive application for the inverter. As fewer power is demanded by the grid, the fewer losses in transmission will be present.

The applications of this type of droop control could be far more reliable and robust. This could be introduced in future scope of the thesis. In a well regulated network, the droop control is performed by changing the output impedance of the inverter. For this the cumulative impedance of the grid can be understood by running an impedance identifier. This type of droop control would be more useful in practical applications. Another key aspect to take into account is the presence of errors in measurements that can gravely affect the performance of the droop control and subsequently the inverter.

The effect of the droop change in power supplied is visible on the active power curve in the substation power profile. Once the inverters are all connected and supply the local load, the substation reduces its supply.

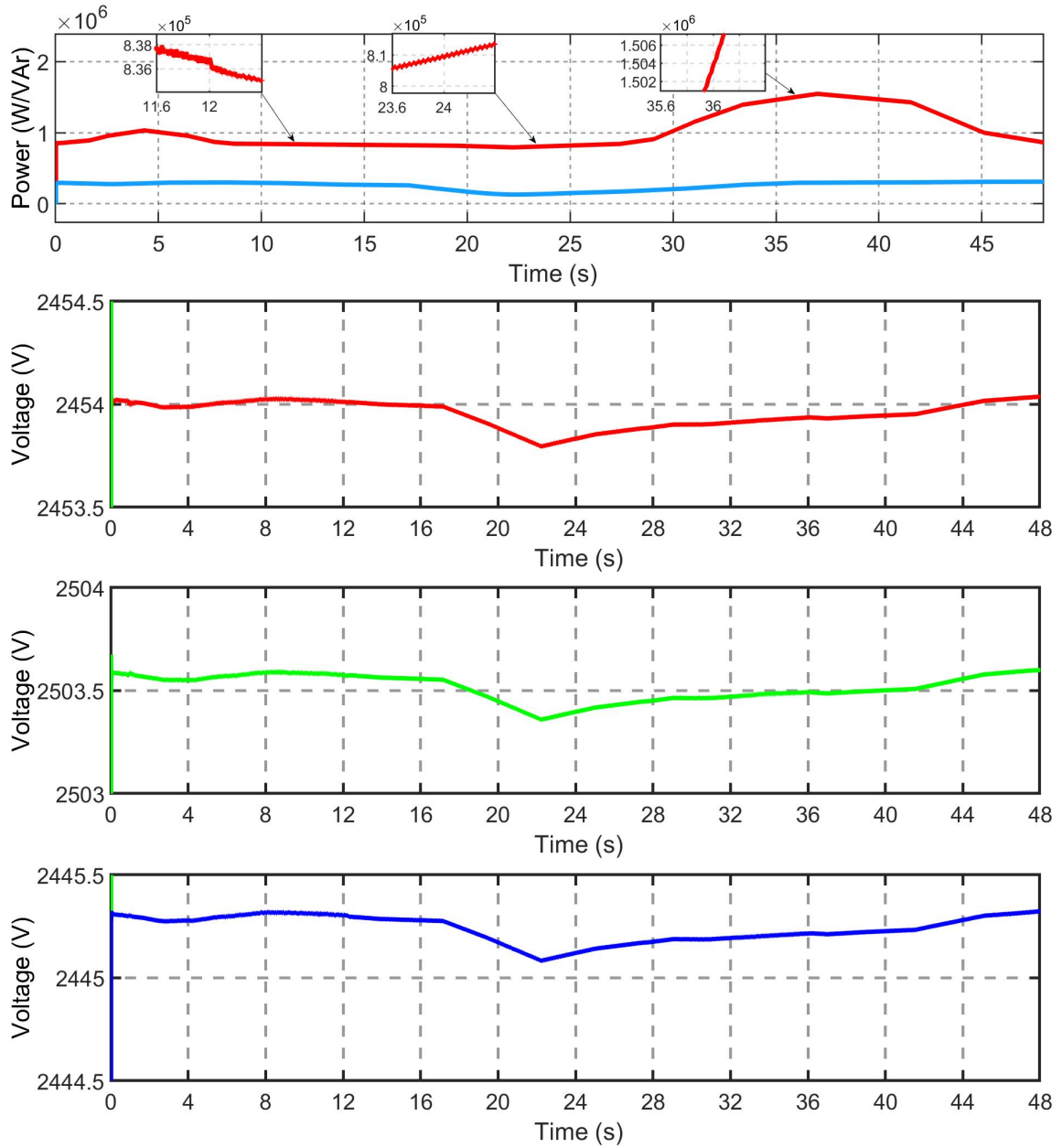


Figure 6.11: Substation Characteristics; Active and reactive power supplied by the substation and the voltages in each phase at the substation

6.3.1 Summary

- Active power sharing between multiple inverters has been realized, based on a proposed droop control methodology. The control logic is designed based on the the droop equations.
- The load demand is shared among three inverters connected to each phase. The

active power sharing occurs due to the variations in the inverter frequency and the voltage deviations.

CHAPTER 7: CONCLUSIONS AND FUTURE WORK

In this thesis, a single phase grid connected inverter has been designed and developed, using d-q based voltage and current control. The main scope of the work is to design an approach for active and reactive power control using d-q transformation. Then an application framework has been designed to use the grid connected single phase inverters with PV farm and energy storage for active and reactive power balance of the power distribution system. Further a droop control framework has been designed for power exchange between inverters. The main conclusions are as follows.

7.1 Conclusion

- A stable DC bus has been created that is able to support PV and Battery systems. The Battery is capable of maintaining the DC bus voltage constant at the operating capacity of 400V.
- The Battery is also able to share power to the load, when the PV input drops. At Maximum PV output, the battery resorts to charging itself.
- A single phase inverter is connected to the DC bus, such that the inverter is able to perform active and reactive power control, while maintaining the voltage and current within the operating limits.
- The inverter is also able to control the active and reactive power output by the modification of the d-q controller.
- The single phase inverter was developed to perform in on-grid and islanding modes, and seamlessly transition between the two modes of operation.
- The single phase grid-tie inverter was connected a large distribution network.

A number of studies were performed on the active and reactive power support by the inverter.

- The inverter's ability to balance an unbalanced load, while connected to the grid was also studied.
- Finally, Active Power sharing between multiple inverters, was performed, in the grid connected mode.

The inverter is capable of stable operation in both the grid-connected and off-grid modes. The inverter is also able to work in a large distribution network, with associated unbalance in the network.

7.2 Future Work

Using the inverter developed in the thesis, a whole host of applications may be developed.

- The droop control may be developed for reactive power as well. A robust droop control architecture that has been purposed as a part of recent publications may be implemented[74]. The robust droop control can be further modified to create the universal droop control that can also perform voltage and frequency stabilization.
- If the inverter can be developed to perform voltage and frequency stabilization, multiple inverter could be connected to create a micro-grid. This micro-grid setup can also perform seamless transfer from on-grid to off-grid, using the method created in the thesis.
- The inverter can be connected at different nodes of the system to replicate the effect of a system that has high penetration of DG.
- The single phase d-q control can be developed on a hardware setup. The active and reactive power supply of the system can be studied in a physical setup,

along with a study on power sharing among inverters.

- The DC- bus could be enlarged to create a DC micro-grid such that hybrid-EVs can be connected to DC bus for charging or discharging, while the inverter controls the power flow from the DC-bus to the grid.

REFERENCES

- [1] J. Hambrick, "Nrel smart grid projects," in *2012 IEEE PES Innovative Smart Grid Technologies (ISGT)*, pp. 1–1, Jan 2012.
- [2] T. Moriarty, "Simple, fast and effective correction for irradiance spatial nonuniformity in measurement of ivs of large area cells at nrel," in *2017 IEEE 44th Photovoltaic Specialist Conference (PVSC)*, pp. 1–5, June 2017.
- [3] S. Karmakar, T. Roy, P. K. Sadhu, and S. Mondal, "Analysis and simulation of a new topology of single phase multi-level inverter," in *2016 IEEE 1st International Conference on Power Electronics, Intelligent Control and Energy Systems (ICPEICES)*, pp. 1–6, July 2016.
- [4] A. Blorfan, P. Wira, D. Flieller, G. Sturtzer, and J. Merckl, "A three-phase hybrid active power filter with photovoltaic generation and hysteresis current control," 11 2011.
- [5] S. K. Sahoo, A. Ramulu, S. Batta, and S. Duggal, "Performance analysis and simulation of three phase voltage source inverter using basic pwm techniques," in *IET Chennai 3rd International on Sustainable Energy and Intelligent Systems (SEISCON 2012)*, pp. 1–7, Dec 2012.
- [6] ucsusa.org, "Renewable energy can provide 80 percent of u.s. electricity by 2050," https://www.ucsusa.org/clean_energy/smart_energy_solutions/increase_renewables/renewable_energy_80_percent_us_electricity.html, 2017.
- [7] iea.org, "Renewables 2017," <https://www.iea.org/publications/renewables2017/>, 2017.
- [8] instituteforenergyresearch.org, "Renewable energy," <https://instituteforenergyresearch.org/topics/encyclopedia/renewable-energy/>, 2016.
- [9] www.greentechmedia.com, "Us renewable energy generation now within striking distance of nuclear," <https://www.greentechmedia.com/articles/read/renewable-energy-generation-nuclear-bnef>, 2016.
- [10] wikipedia.org, "Renewable energy in the united states," https://en.wikipedia.org/wiki/Renewable_energy_in_the_united_states, 2015.
- [11] A. Thakallapelli, S. Ghosh, and S. Kamalasan, "Real-time reduced order model based adaptive pitch controller for grid connected wind turbines," in *Proc. IEEE Industry Applications Society Annual Meeting*, (Portland, USA), pp. 1–8, Oct. 2016.

- [12] K. B. stman and J. K. Jrvenhaara, "A rapid switch bridge selection method for fully integrated dc/dc buck converters," *IEEE Transactions on Power Electronics*, vol. 30, pp. 4048–4051, Aug 2015.
- [13] A. Filba-Martinez, S. Busquets-Monge, J. Nicolas-Apruzzese, and J. Bordonau, "Operating principle and performance optimization of a three-level npc dual-active-bridge dc x2013;dc converter," *IEEE Transactions on Industrial Electronics*, vol. 63, pp. 678–690, Feb 2016.
- [14] M. Mirhosseini, J. Pou, and V. G. Agelidis, "Single- and two-stage inverter-based grid-connected photovoltaic power plants with ride-through capability under grid faults," *IEEE Transactions on Sustainable Energy*, vol. 6, pp. 1150–1159, July 2015.
- [15] W. Huang and J. A. A. Qahouq, "Energy sharing control scheme for state-of-charge balancing of distributed battery energy storage system," *IEEE Transactions on Industrial Electronics*, vol. 62, pp. 2764–2776, May 2015.
- [16] M. Armstrong, D. J. Atkinson, C. M. Johnson, and T. D. Abeyasekera, "Auto-calibrating dc link current sensing technique for transformerless, grid connected, h-bridge inverter systems," *IEEE Transactions on Power Electronics*, vol. 21, pp. 1385–1393, Sept 2006.
- [17] P. G. Barbosa, H. A. C. Braga, M. D. C. B. Rodrigues, and E. C. Teixeira, "Boost current multilevel inverter and its application on single-phase grid-connected photovoltaic systems," *IEEE Transactions on Power Electronics*, vol. 21, pp. 1116–1124, July 2006.
- [18] S. Saha and V. P. Sundarsingh, "Novel grid-connected photovoltaic inverter," *IEE Proceedings - Generation, Transmission and Distribution*, vol. 143, pp. 219–224, Mar 1996.
- [19] Y. Chen and K. M. Smedley, "A cost-effective single-stage inverter with maximum power point tracking," *IEEE Transactions on Power Electronics*, vol. 19, pp. 1289–1294, Sept 2004.
- [20] A. M. Vijay and S. N. Saritha., "Pv-fed single phase single stage boost inverter," in *2012 International Conference on Computing, Electronics and Electrical Technologies (ICCEET)*, pp. 443–446, March 2012.
- [21] W. L. Yu, T. P. Lee, G. H. Wu, Q. S. Chen, H. J. Chiu, Y. K. Lo, and F. Shih, "A dsp-based single-stage maximum power point tracking pv inverter," in *2010 Twenty-Fifth Annual IEEE Applied Power Electronics Conference and Exposition (APEC)*, pp. 948–952, Feb 2010.
- [22] N. Kasa, T. Iida, and H. Iwamoto, "An inverter using buck-boost type chopper circuits for popular small-scale photovoltaic power system," in *Industrial Electronics Society, 1999. IECON '99 Proceedings. The 25th Annual Conference of the IEEE*, vol. 1, pp. 185–190 vol.1, 1999.

- [23] M. Shen, A. Joseph, J. Wang, F. Z. Peng, and D. J. Adams, "Comparison of traditional inverters and z-source inverter," in *2005 IEEE 36th Power Electronics Specialists Conference*, pp. 1692–1698, June 2005.
- [24] A. Ebrahimi, H. S. Fathi, and H. Gholamrezaei, "Novel switching pattern for single-stage current source inverter for grid-connected photovoltaics," *IET Power Electronics*, vol. 7, no. 10, pp. 2447–2454, 2014.
- [25] D. Cao, S. Jiang, X. Yu, and F. Z. Peng, "Low-cost semi-z-source inverter for single-phase photovoltaic systems," *IEEE Transactions on Power Electronics*, vol. 26, pp. 3514–3523, Dec 2011.
- [26] B. Farhangi and S. Farhangi, "Comparison of z-source and boost-buck inverter topologies as a single phase transformer-less photovoltaic grid-connected power conditioner," in *2006 37th IEEE Power Electronics Specialists Conference*, pp. 1–6, June 2006.
- [27] F. Ronilaya, I. Siradjuddin, and S. E. Wibowo, "An optimal power flow control method for pv systems with single phase shimizu inverter," in *2017 International Seminar on Intelligent Technology and Its Applications (ISITIA)*, pp. 75–80, Aug 2017.
- [28] R. Ortega, O. Carranza, V. H. Garc a, J. J. Rodr guez, and J. C. Sosa, "Control design for a single-phase inverter for operation in a microgrid using a dc-ac coordinate transformation method," in *IECON 2017 - 43rd Annual Conference of the IEEE Industrial Electronics Society*, pp. 4885–4890, Oct 2017.
- [29] R. Chan, J. c. Kim, J. Baek, N. Kim, and S. Kwak, "Model predictive current control method with constant switching frequency for single-phase voltage source inverters," in *2017 19th European Conference on Power Electronics and Applications (EPE'17 ECCE Europe)*, pp. P.1–P.5, Sept 2017.
- [30] W. Wang, L. Yan, X. Zeng, X. Zhao, B. Wei, and J. M. Guerrero, "Control method of single-phase inverter based grounding system in distribution networks," in *2016 IEEE Energy Conversion Congress and Exposition (ECCE)*, pp. 1–5, Sept 2016.
- [31] A. Chub, D. Vinnikov, F. Blaabjerg, and F. Z. Peng, "A review of galvanically isolated impedance-source dc x2013;dc converters," *IEEE Transactions on Power Electronics*, vol. 31, pp. 2808–2828, April 2016.
- [32] A. Thakallapelli, S. Ghosh, and S. Kamalasan, "Real-time frequency based reduced order modeling of large power grid," in *2016 IEEE Power and Energy Society General Meeting (PESGM)*, pp. 1–5, July 2016.
- [33] B. Ge, Y. Liu, H. Abu-Rub, and F. Z. Peng, "State-of-charge balancing control for a battery-energy-stored quasi-z-source cascaded-multilevel-inverter-based photovoltaic power system," *IEEE Transactions on Industrial Electronics*, vol. 65, pp. 2268–2279, March 2018.

- [34] I. S. Stoyanov, T. B. Iliev, G. Y. Mihaylov, and B. I. Evstatiev, "Modelling of power inverters used in pv systems," in *2017 IEEE 23rd International Symposium for Design and Technology in Electronic Packaging (SIITME)*, pp. 263–266, Oct 2017.
- [35] W. D. P. Vallejos, "Standalone photovoltaic system, using a single stage boost dc/ac power inverter controlled by a double loop control," in *2017 IEEE PES Innovative Smart Grid Technologies Conference - Latin America (ISGT Latin America)*, pp. 1–6, Sept 2017.
- [36] V. M. Iyer and V. John, "Low-frequency dc bus ripple cancellation in single phase pulse-width modulation inverters," *IET Power Electronics*, vol. 8, no. 4, pp. 497–506, 2015.
- [37] D. Roy and M. Singh, "A simplified space vector pulse width modulation for three phase three-level diode clamped inverter," in *2017 International Conference on Smart grids, Power and Advanced Control Engineering (ICSPACE)*, pp. 226–230, Aug 2017.
- [38] J. Guo, P. Yue, J. Si, Y. Sun, and Q. Chen, "Modeling and simulation of phase-locked loop for grid voltage based on the improved synchronous reference frame," in *2018 Chinese Control And Decision Conference (CCDC)*, pp. 5694–5700, June 2018.
- [39] S. Zhou, J. Liu, and Y. Zhang, "A decoupling method based on reference current feedforward for dq-frame pi current control of grid-connected voltage source converters," in *2015 IEEE 2nd IFEEC Conference*, pp. 1–6, Nov 2015.
- [40] K. Andanapalli and B. R. K. Varma, "Park's transformation based symmetrical fault detection during power swing," in *2014 Eighteenth National Power Systems Conference (NPSC)*, pp. 1–5, Dec 2014.
- [41] D. Reid, "Dq rotating frame pi control algorithm for power inverter voltage regulation modelling and simulation using the openmodelica platform," in *South-eastCon 2015*, pp. 1–4, April 2015.
- [42] E. Makovenko, O. Husev, C. Roncero-Clemente, E. Romero-Cadaval, and D. Vinnikov, "Modified dq control approach for three-phase inverter," in *2017 IEEE 58th International Scientific Conference on Power and Electrical Engineering of Riga Technical University (RTUCON)*, pp. 1–3, Oct 2017.
- [43] A. M. Mnider, D. J. Atkinson, M. Dahidah, and M. Armstrong, "A simplified dq controller for single-phase grid-connected pv inverters," in *2016 7th International Renewable Energy Congress (IREC)*, pp. 1–6, March 2016.
- [44] M. Mehra, M. Rezanejad, E. Pouresmaeil, J. P. S. Catalão, and S. Zabihi, "Analysis and control of single-phase converters for integration of small-scaled renewable energy sources into the power grid," in *2016 7th Power Electronics and Drive Systems Technologies Conference (PEDSTC)*, pp. 384–389, Feb 2016.

- [45] R. Bhattarai, N. Gurung, and S. Kamalasadana, "Dual mode control of a three-phase inverter using minimum variance adaptive architecture," *IEEE Transactions on Industry Applications*, vol. 54, pp. 3868–3880, July 2018.
- [46] M. Ahmed, R. Bhattarai, S. J. Hossain, S. Abdelrazek, and S. Kamalasadana, "Coordinated voltage control strategy for voltage regulators and voltage source converters integrated distribution system," in *2017 IEEE Industry Applications Society Annual Meeting*, pp. 1–8, Oct 2017.
- [47] R. Bisht, S. Subramaniam, R. Bhattarai, and S. Kamalasadana, "Active and reactive power control of single phase inverter with seamless transfer between grid-connected and islanded mode," in *2018 IEEE Power and Energy Conference at Illinois (PECI)*, pp. 1–8, Feb 2018.
- [48] D. Pan, X. Ruan, X. Wang, F. Blaabjerg, X. Wang, and Q. Zhou, "A highly robust single-loop current control scheme for grid-connected inverter with an improved lcl filter configuration," *IEEE Transactions on Power Electronics*, vol. 33, pp. 8474–8487, Oct 2018.
- [49] J. Farhang, M. Eydi, B. Asaei, and B. Farhangi, "Flexible strategy for active and reactive power control in grid connected inverter under unbalanced grid fault," in *2015 23rd Iranian Conference on Electrical Engineering*, pp. 1618–1623, May 2015.
- [50] A. Thakallapelli and S. Kamalasadana, "An online reduced order modeling based frequency regulation adaptive control architecture for wind integrated power grid," in *Proc. Industry Applications Society Annual Meeting (IAS), IEEE*, Sep 2018.
- [51] S. J. Hossain, T. G. Paul, R. Bisht, A. Suresh, and S. Kamalasadana, "An integrated battery optimal power dispatch architecture for end-user-driven microgrid in islanded and grid-connected mode of operation," *IEEE Transactions on Industry Applications*, vol. 54, pp. 3806–3819, July 2018.
- [52] R. Bhattarai, N. Gurung, and S. Kamalasadana, "Control of grid connected inverters using minimum variance adaptive architecture," in *2016 IEEE International Conference on Power Electronics, Drives and Energy Systems (PEDES)*, pp. 1–6, Dec 2016.
- [53] F. Shaikh and B. Joseph, "Simulation of synchronous reference frame pll for grid synchronization using simulink," in *2017 International Conference on Advances in Computing, Communication and Control (ICAC3)*, pp. 1–6, Dec 2017.
- [54] M. Cirrincione, F. R. Islam, P. Nogara, and G. Vitale, "Impedance estimation of fea's grid in fiji islands by v-i measurement by using the synchronous reference frame-pll," in *2017 IEEE International Conference on Environment and Electrical Engineering and 2017 IEEE Industrial and Commercial Power Systems Europe (EEEIC / I CPS Europe)*, pp. 1–6, June 2017.

- [55] P. Rodriguez, J. Pou, J. Bergas, J. I. Candela, R. P. Burgos, and D. Boroyevich, "Correction to "decoupled double synchronous reference frame pll for power converters control" [mar 07 584-592]," *IEEE Transactions on Power Electronics*, vol. 22, pp. 1078–1078, May 2007.
- [56] C. Subramanian and R. Kanagaraaj, "Rapid tracking of grid variables using pre-filtered synchronous reference frame pll," *IEEE Transactions on Instrumentation and Measurement*, vol. 64, pp. 1826–1836, July 2015.
- [57] S. Golestan, M. Monfared, F. D. Freijedo, and J. M. Guerrero, "Performance improvement of a prefiltered synchronous-reference-frame pll by using a pid-type loop filter," *IEEE Transactions on Industrial Electronics*, vol. 61, pp. 3469–3479, July 2014.
- [58] S. H. Hwang, L. Liu, H. Li, and J. M. Kim, "Dc offset error compensation for synchronous reference frame pll in single-phase grid-connected converters," *IEEE Transactions on Power Electronics*, vol. 27, pp. 3467–3471, Aug 2012.
- [59] C. H. da Silva, R. R. Pereira, L. E. B. da Silva, G. Lambert-Torres, B. K. Bose, and S. U. Ahn, "A digital pll scheme for three-phase system using modified synchronous reference frame," *IEEE Transactions on Industrial Electronics*, vol. 57, pp. 3814–3821, Nov 2010.
- [60] A. Thakallapelli and S. Kamalasan, "Optimization based real-time frequency dependent reduced order modeling of power grid," in *2017 IEEE Power Energy Society General Meeting*, pp. 1–5, July 2017.
- [61] A. Thakallapelli and S. Kamalasan, "Alternating direction method of multipliers (admm) based distributed approach for wide-area control," in *2017 IEEE Industry Applications Society Annual Meeting*, pp. 1–7, Oct 2017.
- [62] R. Bhattarai, N. Gurung, A. Thakallapelli, and S. Kamalasan, "Reduced-order state observer-based feedback control methodologies for doubly fed induction machine," *IEEE Transactions on Industry Applications*, vol. 54, pp. 2845–2856, May 2018.
- [63] L. Rolim, M. Alves, T. M. L. Assis, P. O. L. Gatta, and G. N. Taranto, "Virtual inertia impact on microgrid voltage and frequency control," in *2018 Simposio Brasileiro de Sistemas Eletricos (SBSE)*, pp. 1–6, May 2018.
- [64] T. Wu, Z. Liu, J. Liu, B. Liu, and R. An, "A decoupled current droop control method for parallel inverters in microgrids," in *2017 IEEE 3rd International Future Energy Electronics Conference and ECCE Asia (IFEEC 2017 - ECCE Asia)*, pp. 2117–2122, June 2017.
- [65] L. Hongpeng, Z. Jiajie, L. Pengfei, and W. Wang, "An improved droop control strategy of three-phase inverter for grid voltage unbalance compensation," in *2017 IEEE 3rd International Future Energy Electronics Conference and ECCE Asia (IFEEC 2017 - ECCE Asia)*, pp. 110–115, June 2017.

- [66] A. Thakallapelli and S. Kamalasadana, "Alternating direction method of multipliers (ADMM) based distributed approach for wide-area control," in *Proc. Industry Applications Society Annual Meeting (IAS), IEEE*, Oct 2017.
- [67] M. Mao, C. Qian, and Y. Ding, "Decentralized coordination power control for islanding microgrid based on pv/bes-vsg," *CPSS Transactions on Power Electronics and Applications*, vol. 3, pp. 14–24, March 2018.
- [68] S. Nowak, M. S. Metcalfe, W. Eberle, and L. Wang, "Comparison of voltage control methods in distribution systems using q-v based pi and droop controls of solar inverters," in *2017 IEEE Power Energy Society General Meeting*, pp. 1–5, July 2017.
- [69] A. Bolzoni, G. M. Foglia, L. Frosio, M. F. Iacchetti, and R. Perini, "Impact of line and control parameters on droop stability in inverters for distributed generation," *IEEE Transactions on Smart Grid*, pp. 1–1, 2017.
- [70] S. Bayhan and H. Abu-Rub, "Model predictive droop control of distributed generation inverters in islanded ac microgrid," in *2017 11th IEEE International Conference on Compatibility, Power Electronics and Power Engineering (CPE-POWERENG)*, pp. 247–252, April 2017.
- [71] H. Dong, S. Yuan, Z. Han, X. Ding, S. Ma, and X. Han, "A comprehensive strategy for power quality improvement of multi-inverter-based microgrid with mixed loads," *IEEE Access*, vol. 6, pp. 30903–30916, 2018.
- [72] C. Hu, Y. Wang, S. Luo, and F. Zhang, "State-space model of an inverter-based micro-grid," in *2018 3rd International Conference on Intelligent Green Building and Smart Grid (IGBSG)*, pp. 1–7, April 2018.
- [73] T. D. Cardoso, G. M. S. Azevedo, M. C. Cavalcanti, F. A. S. Neves, and L. R. Limongi, "Implementation of droop control with enhanced power calculator for power sharing on a single-phase microgrid," in *2017 Brazilian Power Electronics Conference (COBEP)*, pp. 1–6, Nov 2017.
- [74] F. Alam, M. Ashfaq, S. S. Zaidi, and A. Y. Memon, "Robust droop control design for a hybrid ac/dc microgrid," in *2016 UKACC 11th International Conference on Control (CONTROL)*, pp. 1–6, Aug 2016.
- [75] S. Singh and S. P. Singh, "Energy saving estimation in distribution network with smart grid-enabled cvr and solar pv inverter," *IET Generation, Transmission Distribution*, vol. 12, no. 6, pp. 1346–1358, 2018.
- [76] I. Ziouani, D. Boukhetala, A. M. Darcherif, B. Amghar, and I. E. Abbassi, "A hierarchical control for flexible single-phase microgrid based on parallel vsis," in *2017 6th International Conference on Systems and Control (ICSC)*, pp. 178–182, May 2017.

- [77] A. Thakallapelli, S. J. Hossain, and S. Kamalasadán, “Coherency and online signal selection based wide area control of wind integrated power grid,” *IEEE Transactions on Industry Applications*, vol. 54, pp. 3712–3722, July 2018.
- [78] F. Saggin, D. Coutinho, and M. L. Heldwein, “Parallel operation of single-phase voltage source inverters: Modeling and control based on lmi constraints,” in *IECON 2016 - 42nd Annual Conference of the IEEE Industrial Electronics Society*, pp. 270–275, Oct 2016.
- [79] S. K. Hosseini, M. Mehrasa, S. Taheri, M. Rezanejad, E. Pouresmaeil, and J. P. S. Catalao, “A control technique for operation of single-phase converters in stand-alone operating mode,” in *2016 IEEE Electrical Power and Energy Conference (EPEC)*, pp. 1–6, Oct 2016.
- [80] A. Micallef, M. Apap, C. Spiteri-Staines, J. M. Guerrero, and J. C. Vasquez, “Reactive power sharing and voltage harmonic distortion compensation of droop controlled single phase islanded microgrids,” *IEEE Transactions on Smart Grid*, vol. 5, pp. 1149–1158, May 2014.
- [81] S. A. A. Fallahzadeh, N. R. Abjadi, and A. Kargar, “Direct active and reactive power control of inverter-based dgs using adaptive input-output feedback linearization,” in *2016 21st Conference on Electrical Power Distribution Networks Conference (EPDC)*, pp. 19–25, April 2016.

APPENDIX : MATLAB CODES AND LOAD FLOW DATA FOR TOPICS
PRESENTED IN THE THESIS

The appendix includes the calculations performed to design the DC-DC converter and the passive components of the converter. The MATLAB code used to design the boost converter is mentioned below.

The calculations for the buck converter is mentioned below.

```

clc
clear
Vin=200;
Vout=400;
Dprime=Vin/Vout;
D=1-Dprime;
Pout=350;
Pin=Pout;
Iin=Pin/Vin;
Iind=Iin;
Fsw=1e3;
T=1/Fsw;
Iout=Pout/Vout;
R=Vout^2/Pout;
ripple=0.01; %considering 1% ripple
I_ripple=ripple*Iin;
V_ripple=ripple*Vout;
I_ripple_buck = ripple*Iout;
V_ripple_buck = ripple*Vin;
ESR = 0.06;
%Element design
Ldesign= D*T*Vin/(2*I_ripple);
Ldesign=1.25*Ldesign;
Cdesign=Vout*D*T/(2*R*V_ripple);
Cdesign=1.25*Cdesign;
H=1; %unity gain feedback
Cbuck= I_ripple_buck*(Dprime/Fsw)/(V_ripple_buck-(I_ripple_buck*ESR));
Cbuck=1.25*Cbuck;

```

The calculations for the boost converter is mentioned in the image below.

```
Win=200;
Vout=400;
Dprime=1-Vin/Vout;
D=1-Dprime;
Pout=350;
Pin=Pout;
Iin=Pin/Vin;
Iind=Iin;
Fsw=1e3;
T=1/Fsw;
Iout=Pout/Vout;
R=Vout^2/Pout;
ripple=0.01; %considering 1% ripple
I_ripple=ripple*Iin;
V_ripple=ripple*Vout;
I_ripple_buck = ripple*Iout;
V_ripple_buck = ripple*Vin;
ESR = 0.06;
%Element design
Ldesign= D*T*Vin/(2*I_ripple);
Ldesign=1.25*Ldesign;
Cdesign=Vout*D*T/(2*R*V_ripple);
Cdesign=1.25*Cdesign;
H=1; %unity gain feedback
Cbuck= I_ripple_buck*(Dprime/Fsw)/(V_ripple_buck-(I_ripple_buck*ESR));
Cbuck=1.25*Cbuck;
```

The MATLAB code for the load flow is found here in the figure below. The MATLAB code retrieves the values of the 13 bus system from an excel file. The MATLAB code is useful to determine the voltage and phase value in each phase for different active and reactive power values.

```

% Load Flow Calculation
clc
clear all
% Acquire data from EXCEL
Feeder = LoadFeeder('FEEDER IEEE13_SINREGULADOR.xlsx');
% Plotting the feeder
figure(1)
PlotFeeder(Feeder);
% Load Flow Transfer
Res = ThreePhase_LoadFlow(Feeder);
ShowResults(Res,Feeder);
% Linear Load Flow
disp('Linear Load Flow');
ResL = Linear_Load_Flow_Unbalanced(Feeder);
ShowResults(ResL,Feeder);

if Feeder.Options.DeltaLoadFlow
    Error = abs(Res.Vpu_line-ResL.Vpu_line);
else
    Error = abs(Res.Vpu_phase-ResL.Vpu_phase);
end
figure(2)
bar(Error)
title('Error in Percentage')
grid on

```

These are the parameters of the slack bus and the parameters of the source connected to the thirteen bus system.

General Data	
Slack	632
Vnom (kV)	4.16
InternationalSystem	0
DeltaLF	0
V_slack_ph_A	1.0217
V_slack_ph_B	1.0424
V_slack_ph_C	1.01813
Ang_slack_ph_A	-2.19
Ang_slack_ph_B	-121.673
Ang_slack_ph_C	117.896

Line reactances in each phase is shown below. These values are unaltered in all the simulations.

Config	Lin=1, Trafo=0	R11	R12	R13	R22	R23	R33
1	1	0.3465	0.1560	0.1580	0.3375	0.1535	0.3414
2	1	0.7526	0.1580	0.1560	0.7475	0.1535	0.7436
3	1	0.0000	0.0000	0.0000	1.3294	0.2066	1.3238
4	1	1.3238	0.0000	0.2066	0.0000	0.0000	1.3294
5	1	0.0000	0.0000	0.0000	0.0000	0.0000	1.3292
6	1	0.7982	0.3192	0.2849	0.7891	0.3192	0.7982
7	1	1.3425	0.0000	0.0000	0.0000	0.0000	0.0000

X11	X12	X13	X22	X23	X33
1.0179	0.5017	0.4236	1.0478	0.3849	1.0348
1.1814	0.4236	0.5017	1.1983	0.3849	1.2112
0.0000	0.0000	0.0000	1.3471	0.4591	1.3569
1.3569	0.0000	0.4591	0.0000	0.0000	1.3471
0.0000	0.0000	0.0000	0.0000	0.0000	1.3475
0.4463	0.0328	-0.0143	0.4041	0.0328	0.4463
0.5124	0.0000	0.0000	0.0000	0.0000	0.0000

B11	B12	B13	B22	B23	B33
6.2998	-1.9958	-1.2595	5.9597	-0.7417	5.6386
5.6990	-1.0817	-1.6905	5.1795	-0.6588	5.4246
0.0000	0.0000	0.0000	4.7097	-0.8999	4.6658
4.6658	0.0000	-0.8999	0.0000	0.0000	4.7097
0.0000	0.0000	0.0000	0.0000	0.0000	4.5193
96.8897	0.0000	0.0000	96.8897	0.0000	96.8897
88.9912	0.0000	0.0000	0.0000	0.0000	0.0000

Node	Alfa							
	Y=1, D=0	(PQ=0, I=1, Z=2)	Ph-1 (kW)	Ph-1 (kVAr)	Ph-2 (kW)	Ph-2 (kVAr)	Ph-3 (KW)	Ph-3 (kVAr)
633	1	0	160	110	120	90	120	90
645	1	0	0	0	170	125	0	0
646	0	2	0	0	230	132	0	0
652	1	2	128	86	0	0	0	0
671	1	0	402	230	451	258	672	439
675	1	0	485	-10	68	-140	290	12
611	1	1	0	0	0	0	170	-20
692	1	1	0	0	0	0	0	0
634	1	1	525	0	525	0	525	0

Load-Flow results of unmodified 13 bus system:

Node	Ph-1	Ph-1	Ph-2	Ph-2	Ph-3	Ph-3
	V(p.u.)	Angle(deg)	V(p.u.)	Angle(deg)	V(p.u.)	Angle(deg)
611	0.9588	115.2676
632	1.021	-2.49	1.042	-121.72	1.0174	117.83
633	1.0181	-2.55	1.0401	-121.765	1.0148	117.8243
634	1.011	-3.2	1.0399	-121.842	1.012	117.842
645	.	.	1.0328	-121.8999	1.0154	117.8573
646	.	.	1.0311	-121.9755	1.0134	117.9026
652	0.9952	-5.4099
671	1.0029	-5.4636	1.0509	-121.9105	0.9625	115.531
675	0.9966	-5.7161	1.0531	-122.0685	0.9605	115.531
680	1.0029	-5.4636	1.0509	-121.911	0.9625	115.531
684	1.0009	-5.4844	.	.	0.9606	115.422
692	1.0276	-3.01	1.0538	-121.83	1.0251	117.21

Figure 1: Load flow results of IEEE 13 bus system

Load flow result of modified IEEE 13 bus system for the lowest set-point of active and reactive power. Note that the lowest point of the active and reactive power is at the beginning of the simulation, where the signal provided to the dynamic load is at its lowest.

Node	Ph-1	Ph-1	Ph-2	Ph-2	Ph-3	Ph-3
	V(p.u.)	Angle(deg)	V(p.u.)	Angle(deg)	V(p.u.)	Angle(deg)
611	0.973	117.2419
632	1.029	-2.49	1.0301	-121.72	1.0289	117.83
633	1.0282	-2.49	1.0287	-121.8033	1.0283	117.789
634	1.0274	-2.5685	1.0274	-121.82	1.0275	117.7533
645	.	.	1.0328	-121.899	1.0154	117.8573
646	.	.	1.0311	-121.9755	1.0134	117.9026
652	0.9637	-5.7846
671	0.9887	-5.3186	1.0549	-122.7159	0.9778	117.4052
675	0.9886	-5.3171	1.0549	-122.8365	0.977	117.4227
680	0.9887	-5.3186	1.0549	-122.716	0.9784	117.405
684	0.982	-5.6	.	.	0.9778	117.39
692	0.99	-5.8	1.055	-122.72	0.9749	117.4

Figure 2: Load flow results of the modified IEEE 13 bus system

Load flow result of modified IEEE 13 bus system for the highest set-point of active and reactive power. Note that the highest point of the active and reactive power is at the peak value of the simulation, where the signal provided to the dynamic load is at its lowest.

Node	Ph-1	Ph-1	Ph-2	Ph-2	Ph-3	Ph-3
	V(p.u.)	Angle(deg)	V(p.u.)	Angle(deg)	V(p.u.)	Angle(deg)
611	0.973	117.2419
632	1.021	-2.49	1.042	-121.72	1.0174	117.83
633	1.0191	-2.49	1.04	-121.8033	1.015	117.789
634	1.0001	-2.5685	1.0398	-121.82	1.0149	117.7533
645	.	.	1.0328	-121.899	1.0154	117.8573
646	.	.	1.0311	-121.9755	1.0134	117.9026
652	0.9637	-5.7846
671	0.9887	-5.3186	1.0549	-122.7159	0.9778	117.4052
675	0.9886	-5.3171	1.0549	-122.8365	0.977	117.4227
680	0.9887	-5.3186	1.0549	-122.716	0.9784	117.405
684	0.982	-5.6	.	.	0.9778	117.39
692	0.99	-5.8	1.055	-122.72	0.9749	117.4

Time domain based load flow results for Node 634, for simulation in section 5.1.2.

Load Flow results for Node 634 at different time intervals						
Time	Phase A		Phase B		Phase C	
	Voltage	Angle	Voltage	Angle	Voltage	Angle
10	1.0273	-1.01	1.0275	118.99	1.0277	-121.01
12	1.0273	-1.02	1.0275	118.98	1.0277	-121.02
14	1.0273	-1.08	1.0275	118.92	1.0277	-121.08
16	1.0273	-1.08	1.0275	118.92	1.0277	-121.08
18	1.0272	-1.08	1.0274	118.92	1.0276	-121.08
20	1.0273	-1.08	1.0275	118.92	1.0277	-121.08
22	1.0271	-1.08	1.0273	118.92	1.0275	-121.08
24	1.0272	-1.08	1.0274	118.92	1.0276	-121.08
26	1.0272	-1.07	1.0274	118.93	1.0276	-121.07
28	1.0273	-1.06	1.0275	118.94	1.0277	-121.06
30	1.0274	-1.05	1.0276	118.95	1.0278	-121.05
32	1.0278	-1.04	1.028	118.96	1.0282	-121.04
34	1.0278	-1.03	1.0278	118.97	1.0278	-121.03
36	1.0278	-1.04	1.0278	118.96	1.0279	-121.04

Time domain based load flow results for Node 634, for simulation in section 5.2.2.

Load Flow results for Node 634 at different time intervals						
Time	Phase A		Phase B		Phase C	
	Voltage	Angle	Voltage	Angle	Voltage	Angle
10	1.0277	-4.01	1.0287	115.99	1.0291	-124.01
12	1.0279	-4.02	1.0287	115.98	1.0291	-124.02
14	1.028	-4.05	1.0286	115.95	1.029	-124.05
16	1.028	-4.08	1.0286	115.92	1.0288	-124.08
18	1.0277	-4.08	1.0284	115.92	1.0285	-124.08
20	1.0274	-4.09	1.0281	115.91	1.0282	-124.09
22	1.0267	-4.1	1.0271	115.9	1.0278	-124.1
24	1.0272	-4.09	1.0278	115.91	1.0282	-124.09
26	1.0275	-4.1	1.0281	115.9	1.0284	-124.1
28	1.0275	-4.09	1.0285	115.91	1.0286	-124.09
30	1.0315	-4.15	1.0305	115.85	1.0308	-124.15
32	1.0294	-4.01	1.0294	115.99	1.0294	-124.01
34	1.0294	-4.02	1.0295	115.98	1.0293	-124.02
36	1.0294	-4.02	1.0294	115.98	1.0294	-124.02